University of Massachusetts Medical School
eScholarship@UMMS

GSBS Dissertations and Theses | Graduate School of Biomedical Sciences

2015-06-22

The Role of Medial Habenula-Interpeduncular Nucleus Pathway in Anxiety: A Dissertation

Xueyan Pang
University of Massachusetts Medical School

Let us know how access to this document benefits you.
Follow this and additional works at: https://escholarship.umassmed.edu/gsbs_diss

 Part of the Behavioral Neurobiology Commons, and the Molecular and Cellular Neuroscience Commons

Repository Citation
Pang X. (2015). The Role of Medial Habenula-Interpeduncular Nucleus Pathway in Anxiety: A Dissertation. GSBS Dissertations and Theses. https://doi.org/10.13028/M2VP49. Retrieved from https://escholarship.umassmed.edu/gsbs_diss/811

This material is brought to you by eScholarship@UMMS. It has been accepted for inclusion in GSBS Dissertations and Theses by an authorized administrator of eScholarship@UMMS. For more information, please contact Lisa.Palmer@umassmed.edu.

THE ROLE OF MEDIAL HABENULA-INTERPEDUNCULAR NUCLEUS PATHWAY IN ANXIETY

A Dissertation Presented

By

XUEYAN PANG

Submitted to the Faculty of the University of Massachusetts

Graduate School of Biomedical Sciences, Worcester

in partial fulfillment of the requirements for the degree of

DOCTOR OF PHILOSOPHY

June 22, 2015

PROGRAM IN NEUROSCIENCE

THE ROLE OF MEDIAL HABENULA-INTERPEDUNCULAR NUCLEUS

PATHWAY IN ANXIETY

A Dissertation Presented By

XUEYAN PANG

The signatures of the Dissertation Defense Committee signify completion and approval as to style and content of the Dissertation

Andrew R. Tapper, Ph.D., Thesis Advisor

Paul D. Gardner, Ph.D., Thesis Advisor

Joel Richter, Ph.D., Member of Committee

Haley E. Melikian, Ph.D., Member of Committee

Fen-Biao Gao, Ph.D., Member of Committee

Darlene H. Brunzell, Ph.D., Member of Committee

The signature of the Chair of the Committee signifies that the written dissertation meets the requirements of the Dissertation Committee

David R. Weaver, Ph.D., Chair of Committee

The signature of the Dean of the Graduate School of Biomedical Sciences signifies that the student has met all graduation requirements of the school.

Anthony Carruthers, Ph.D.,
Dean of the Graduate School of Biomedical Sciences

Program in Neuroscience
June 22, 2015

This dissertation is dedicated to my beloved husband-Yong, my lovely children-Sophia and Eric and my parents. I give my deepest expression of love and appreciation for the encouragement that you gave and the sacrifices you made during this graduate program. Thank you for the support and company during late nights of typing.

ACKNOWLEDGEMENTS

First of all, I want to thank my graduate advisors, Dr. Andrew R. Tapper and Dr. Paul D. Gardner. I first worked with Andrew as a research associate for one year from 2009. That time I just came from China and had some problem to communicate with people because of the language barrier. But I could feel Andrew"s enthusiasm and determination toward learning, teaching and researching. Instead of letting me focus on the routine lab maintenance, he encouraged me to take part in an interesting research project. Andrew has an ability to explain a topic in depth and yet simplify it with an interdisciplinary point of view. And we talked about the project progress every week. From that on, I started to enjoy the boring research and decided to become a graduate student and study for the PhD degree.

In 2010, I enrolled in UMass Medical School and joined the Program in Neuroscience. After several rotations in the first year, I decided to join in Dr. Tapper"s lab and Dr. Gardner"s lab (Tardner lab), as I really like the training and guidance I can get from the mentors. It is very nice that Andrew and Paul both have “open door policy” in their office and we have “two on one” meeting almost every week. Therefore, in the past five years, whenever there is any problem about my project, I can talk with them and they always encourage me and try to figure it out together. With their help, I went through the ups and downs for the projects, which make me grow up to be a more independent researcher. And finally now I am close to get my PhD degree.

Not only for the research project, I also got many help for my life. As an international student who lives in a totally different culture, it is very stressful. But like the lab parents, whenever there is frustration and happiness in life, decision to make for the career planning, they are always there to listen, to support and to give advice. Thanks, Andrew and Paul.

I am also sincerely grateful to my thesis committee members –Dr. David Weaver, Dr. Fen-Biao Gao, Dr. Joel Richter, Dr. Haley Melikian, and Dr. Darlene Brunzell. Thank you for all the insightful comments for my research presented in the thesis here. Special thanks to Dr. David Weaver, who is the chair of the Program in Neuroscience and also the chair of my QE, TRAC and dissertation exam. Thank you for always taking the time to listen, to support, and to encourage.

I would like to thank everyone in the Tardner lab: Rubing Zhao-Shea, Liwang Liu, Jennifer Ngolab, Melissa Guilford, Steven Degroot, Alison Casserly, Susanna Casacuberta, Ciearra Smith, Anthony Sacino; as well as the former Tadner lab members: Linzy Hendrickson, Lindsey Soll, Ma Reina Improgo, Eric Hogan, Michael Scofield. Thank you so much for all the generous help and support, and also thank you so much for providing fun and happy atmosphere for the past five years. Special thanks to Rubing, who has been a sister, a friend and a teacher in this chapter of my life. Thank you so all the help in academics as well as in everyday life.

Finally, I would like to thank my family and friends in China who are always there providing non-stop support and encouragement. Thank you.

ABSTRACT

Recently, the medial habenula-interpeduncular (MHb-IPN) axis has been hypothesized to modulate anxiety although neuronal populations and molecular mechanisms regulating affective behaviors in this circuit are unknown. Here we show that MHb cholinergic neuron activity directly regulates anxiety-like behavior. Optogenetic silencing of MHb cholinergic IPN inputs reduced anxiety-like behavior in mice. MHb cholinergic neurons are unique in that they robustly express neuronal nicotinic acetylcholine receptors (nAChRs), although their role as autoreceptors in these neurons has not been described. nAChRs are ligand-gated cation channels that are activated by the excitatory neurotransmitter, acetylcholine (ACh), as well as nicotine, the addictive component of tobacco smoke. We expressed novel nAChR subunits that render nAChRs hypersensitive to ACh, ACh detectors, selectively in MHb cholinergic neurons of adult mice. Mice expressing these ACh detectors exhibited increased baseline anxiety-like behavior that was alleviated by blocking the mutant receptors. Under stressful conditions, such as during nicotine withdrawal, nAChRs were functionally upregulated in MHb cholinergic neurons mediating an increase in anxiety-like behavior. Together, these data indicate that MHb cholinergic neurons regulate anxiety via signaling through nicotinic autoreceptors and point toward nAChRs in MHb as molecular targets for novel anxiolytic therapeutics.

Table of Contents

List of Tables

List of Figures

List of Abbreviations

5-HT	serotonin
ACh	acetylcholine
AChR	acetylcholine receptor
ACSF	artificial cerebrospinal fluid
ARC	arcuate nucleus
BAC	bed nucleus of the anterior commissure
BLA	basolateral amygdala
BNST	bed nucleus of the stria terminalis
BZD	benzodiazepine
CAMKII	calmodulin kinase II
CeA	central nucleus of the amygdala
CeL	central lateral nucleus of the amygdala
CeM	central medial nucleus of the amygdala
ChAT	choline acetyltransferase
ChR	channelrhodopsin
CP	caudate putamen
CPA	conditioned place aversion
Cys	cysteine
Cys-loop	cysteine-loop
DA	dopamine
DAergic	dopaminergic
DAT	dopamine transporter
DDC	dorsal diencephalic conduction
DHβE	Dihydro-β-erythroidine hydrobromide
DIO	double-inverted open
DMT	dorsomedial thalamus
DR	dorsal raphe
DSt	dorsal striatum
DTR	dorsal tegmental region
EGFP	enhanced green fluorescent protein
EPM	elevated plus maze
fMRI	functional magnetic resonance imaging
fr	fasciculus retroflexus
GABA	gamma-aminobutyric acid
GAD	generalized anxiety disorder
GAPDH	glyceraldehyde-3-phosphate dehydrogenase
GFP	green fluorescent protein
Glu	glutamate
Hb	habenula
Hb-IPN	habenulo-interpeduncular nucleus

IC	inferior colliculus
IL-18	interleukin 18
IPA	apical sub-nucleus of IPN
IPC	central sub-nucleus of IPN
IPDL	dorsolateral sub-nucleus of IPN
IPDM	dorsomedial sub-nucleus of IPN
IPI	intermediate sub-nucleus of IPN
IPL	lateral sub-nucleus of IPN
IPN	interpeduncular nucleus
IPR	rostral sub-nucleus of IPN
ISH	in situ hybridization
KO	knock-out
L9'A	Leu9'Ala
LC	locus ceruleus
LCM	laser capture micro-dissection
LH	lateral hypothalamus
LHb	lateral habenula
mAChR	muscarinic acetylcholine receptor
MBT	marble burying test
MHb	medial habenula
MHbD	the dorsal region of MHb
MHbS	the superior region of MHb
MHbV	the ventral region of MHb
MHbVc	the ventrocentral region of MHb
MHbVl	the ventro-lateral region of MHb
MHbVm	the verntro-medial region of MHb
miRNA	microRNA
MRE	miRNA-recognition elements
MS	medial septum
NAc	nucleus accumbens
nAChR	nicotinic acetylcholine receptor
NDB	nucleus of diagonal band
NpHR	halorhodopsin
OCD	obsessive-compulsive disorder
Oprm	m-opioid receptor
PAG	periaqueductal gray
PET	positron emission tomography
PFC	prefrontal cortex
PTSD	post-traumatic stress disorder
qRT-PCR	quantitative reverse transcription-PCR
RN	raphe nuclei
SACSF	sucrose artificial cerebrospinal fluid
SAD	social anxiety disorder

SC	superior colliculus
SDS-PAGE	SDS–polyacrylamide gel electrophoresis
SFi	septofimbrial nucleus
sm	stria medullaris
SNpc	substantia nigra pars compacta
SNr	substantia nigra
SP	substance P
SSRI	selective serotonin re-uptake inhibitor
TH	tyrosine hydroxylase
TM	transmembrane domain
TSN	triangular septal nucleus
UTR	untranslated region
VP	ventral pallidum
VTA	ventral tegmental area
WT	wild type
YFP	yellow fluorescent protein
α4*	α4 subunit containing nAChR
α4KO	α4 knock out mouse
α-Bgtx	α-Bungarotoxin

Copyright Page

Some of the chapters of this dissertation have appeared in separate publications:

Appendix 2:

Pang, X., E. M. Hogan, A. Casserly, G. Gao, P. D. Gardner and A. R. Tapper (2014). Dicer expression is essential for adult midbrain dopaminergic neuron maintenance and survival. Mol Cell Neurosci 58: 22-28.

Contributions of authors are addressed at the beginning of each chapter.

CHAPTER I

Introduction

I.A. Anxiety disorder and current therapeutics

What is anxiety disorder?

Anxiety disorders are the major mental illness in the U.S., affecting 18% of the U.S. population (around 40 million adults in the United States) (Kessler, Chiu et al. 2005). It costs the United States economy more than $42 billion per year, which is almost one-third of the $148 billion total mental health bill of the country (Kessler, Chiu et al. 2005).

Anxiety is the normal unpleasant feelings of dread in response to stress and can actually be beneficial in some situations. However, anxiety disorders are different from anxiety. Patients with anxiety disorder feel extremely fearful and unsure most of the time every day for at least 6 months (Morrison and Ressler 2014). They may also have difficulty controlling it and it may negatively affect their daily life. If the anxiety disorder is not treated, patients can get even worse.

There are a wide variety of anxiety disorders, including generalized anxiety disorder (GAD), social anxiety disorder (SAD), obsessive-compulsive disorder (OCD) and post-traumatic stress disorder (PTSD) (Farb and Ratner 2014). Anxiety disorders commonly occur along with other mental or physical illnesses, such as alcohol or substance abuse, which make the anxiety symptoms even worse (Grant, Stinson et al. 2004). Interestingly, women are more likely than men to experience an anxiety disorder over their lifetime (Farb and Ratner 2014).

Current therapeutics

To date, there are two main approaches to treat anxiety disorders.

The first-line treatment is selective serotonin re-uptake inhibitors (SSRIs) (Masand and Gupta 2003). SSRI are a class of compounds inhibiting serotonin reuptake into the presynaptic cell, and increase the extracellular level of the neurotransmitter serotonin (Barlow 2009). Although these compounds have been shown to be beneficial for the treatment of certain anxiety disorders, in many patients they showed delays in producing the desired clinical effect or even potential worsening of anxiety (Farb and Ratner 2014).

Another class of drugs are benzodiazepines (BZDs), which work by increasing the efficiency of inhibitory neurotransmitter, gamma-aminobutyric acid (GABA), decreasing the excitability of neurons in the brain (Page C 2002). BZDs has played a central role in the pharmacologic management of anxiety disorders for about 50 years, but it has many side effects such as drowsiness, ataxia, drug dependence and impairment of cognition (Farb and Ratner 2014).

Therefore, it is important to better understand the neural circuitry underlying anxiety as well as to develop a more effective approach to treat anxiety disorders.

I.B. The brain circuitry of anxiety disorders

Anxiety is a complicated emotional response that involves multiple neurotransmitters within several different brain regions, such as amygdala, the

bed nucleus of the stria terminalis (BNST), prefrontal cortex (PFC), nucleus accumbens (NAc) and hippocampus (Farb and Ratner 2014) (Fig I-1). In this thesis, the involvement of amygdala and the BNST in anxiety will be discussed in detail.

The role of amygdala in anxiety

The amygdala is one brain region in the limbic system, and it receives afferent input from the sensory cortex and sends projections to the hypothalamus, periaqueductal gray matter, locus ceruleus (LC), raphe nuclei (RN) and ventral tegmental area (VTA) (Sah, Faber et al. 2003).

There are several sub-regions in the amygdala: the basolateral amygdala (BLA) and the central nucleus of the amygdala (for short, CeA, can be divided into the central lateral and central medial portion, CeL and CeM, respectively). The BLA mainly sends the excitatory glutamatergic projection to the CeA (Tye, Prakash et al. 2011), whereas the CeL sends the inhibitory input to the CeM, which is the main output of the amygdala (LeDoux 2000).

In humans, several imaging studies have shown that amygdala is involved in anxiety. For example, people who have more anxiety showed higher amygdala volume, and patients with anxiety disorder showed increased amygdala activation (Boehme, Ritter et al. 2014, Machado-de-Sousa, Osorio Fde et al. 2014, Qin, Young et al. 2014). In rodents, after exposure to anxiogenic stimulation, the immediate early gene was activated in the amygdala, and

pharmacological inactivation of the CeA, but not into the BLA, by GABAA receptor agonist, muscimol, is anxiolytic in the elevated plus maze (EPM) (Silveira, Sandner et al. 1993, Butler, White et al. 2012). These lines of evidence suggest that the amygdala is critical for the anxiety in both humans and rodents.

Lesion studies and local drug infusion studies indicate that the CeA, but not the BLA is required for avoidance of open spaces (Moller, Wiklund et al. 1997, Moreira, Masson et al. 2007, Carvalho, Moreira et al. 2012). However, these pharmacological studies and lesion studies might provide the inaccurate information because of methodological limitations (Adhikari 2014). Recently, optogenetic techniques allow researchers to overcome these limitations (Adhikari 2014). Optogenetics is the combination of genetics and optics to control the firing rate of specific type of neurons quickly and reversibly by light (Tye, Prakash et al. 2011). It was shown that optogenetic activation of the entire glutamatergic BLA somata increased anxiety, while selective activation of the projection from the BLA to CeA decreased anxiety, suggesting that multiple subpopulations or projections of BLA neurons can act in opposition in anxiety-like behavior (Tye, Prakash et al. 2011).

The role of BNST in anxiety

Bed nucleus of the stria terminalis (BNST) receives a major output from the amygdala, and has been shown to be involved in anxiety in both human and rodents (Adhikari 2014) (Fig I-1).

In human imaging studies, it has been shown that the BNST of generalized anxiety disorder patients was activated when they participate in high uncertainty task (Yassa, Hazlett et al. 2012). Moreover, the BNST showed greater recruitment in individuals with greater anxiety (Somerville, Whalen et al. 2010). In rodents, it also has been shown that BNST lesion had an anxiogenic effect on the plus maze test (Duvarci, Bauer et al. 2009), and infusion of glutamate antagonists in the BNST was anxiolytic in the light potentiated startle paradigm (Walker and Davis 1997).

Like the amygdala, BNST also has several sub-nuclei which have different anatomical and neurochemical features. Optogenetic studies have shown that inactivation of the oval nucleus of the BNST is anxiolytic, while decreasing the activity of the anterodorsal BNST is anxiogenic (Kim, Adhikari et al. 2013). It also has been shown that three distinct anterodorsal BNST efferent projections implemented independent features of anxiolysis: the lateral hypothalamus reduced risk-avoidance, the parabrachial nucleus reduced respiratory rate, and the VTA increased positive valence, respectively (Kim, Adhikari et al. 2013). Another optogenetic study showed that when mice were presented with aversive stimuli, the firing rate of BNST glutamatergic neurons increased, whereas the firing rate of BNST GABAergic neurons decreased (Jennings, Sparta et al. 2013). Moreover, activation of BNST glutamatergic projections by optogenetics resulted in aversive and anxiogenic phenotypes, whereas activation of BNST GABAergic

projections produced rewarding and anxiolytic phenotypes (Jennings, Sparta et al. 2013).

Taken together, BNST is involved in anxiety and different subregions of BNST have specific functions.

Conclusion:

In conclusion, there has been an explosion of research into the biological mechanism, especially the brain circuitry, underlying anxiety disorders. There are many brain regions that work together to modulate the anxiety state in humans and rodents. The development of new technologies might facilitate the search for new brain regions that are involved in anxiety disorders, and provide new therapeutic targets.

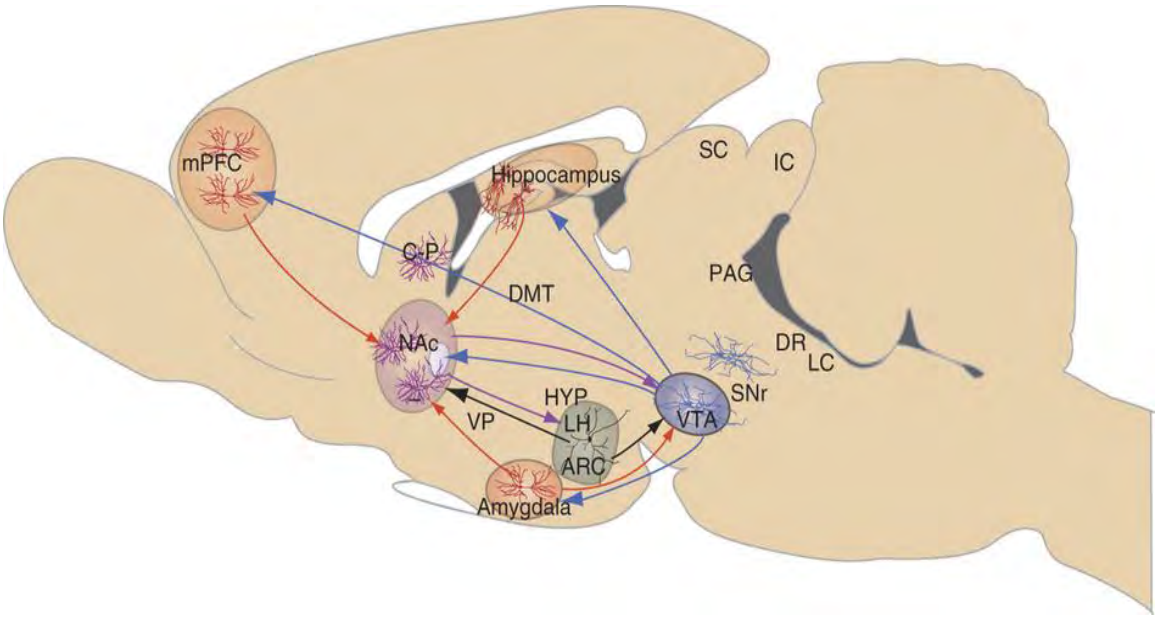

Figure I-1. Brain circuitry implicated in anxiety disorders

The red solid lines represent excitatory glutamatergic afferents to NAc from mPFC, amygdala, and hippocampus, and glutamatergic innervation of VTA by amygdala. The purple solid lines are GABAergic inhibitory circuits including connections from NAc to VTA and hypothalamus. Green solid lines are dopamine neurons projecting from VTA to a range of limbic targets, including NAc, mPFC, amygdala, and hippocampus. Peptidergic pathways though which the hypothalamus (e.g., ARC, arcuate nucleus, and LH, lateral hypothalamus) alters neurotransmission in NAc and VTA are shown in solid black lines. Each structure contains specialized neuronal cell types thought to regulate anxiety disorders. These cell types, color–coded to reflect the transmitter signal they convey, include amygdala, PFC and hippocampal glutamatergic neurons (red), GABAergic NAc medium spiny neurons (purple), hypothalamic peptidergic

neurons (black), and VTA dopaminergic neurons (blue). CP, caudate-putamen; DMT, dorsomedial thalamus; SC, superior colliculus; IC, inferior colliculus; VP, ventral pallidum; SNr, substantia nigra; PAG, periaqueductal gray; DR, dorsal raphe; and LC, locus ceruleus. Figure modified with permission from (Russo, Murrough et al. 2012)

I.C. The anatomy of medial habenula and interpeduncular nucleus pathway

Habenula

The habenula (meaning “little rein” in Latin) is a bilateral small, complex and well-conserved structure, which located by the third ventricle (Klemm 2004). It can be divided into medial habenula and lateral habenula (MHb and LHb, respectively) based on their anatomical and functional differences (Klemm 2004, Lecourtier and Kelly 2007). The habenula is part of the dorsal diencephalic conduction (DDC) system, which connects the limbic forebrain with the midbrain and hindbrain (Lecourtier and Kelly 2007). Interestingly, a recent study of human fetuses showed that the habenulo-interpeduncular (Hb-IPN) tract is one of the first major fiber tracts to form in the developing brain, being present as early as eight weeks gestation (Antolin-Fontes, Ables et al. 2014).

It has been shown that habenula plays an important role in many behaviors including sleep (Haun, Eckenrode et al. 1992, Valjakka, Vartiainen et al. 1998), circadian rhythm (Zhao and Rusak 2005), stress response (Carboni, Carletti et al. 1998, Sugama, Cho et al. 2002, Lecourtier, Neijt et al. 2004, Mathuru and Jesuthasan 2013), pain (Michl, Jocic et al. 2001, Plenge, Mellerup et al. 2002), feeding (Sandyk 1991), depression (Shumake, Edwards et al. 2003), memory (Kobayashi, Sano et al. 2013) as well as nicotine withdrawal (Salas, Sturm et al. 2009, Fowler, Lu et al. 2011, Frahm, Slimak et al. 2011).

In the past ten years, many studies have focused on the function of the lateral habenula, whereas the medial habenula remains largely understudied. Therefore, the medial habenula anatomy and histochemical characters will be discussed here.

Medial habenula afferents and efferents

Afferents

The medial habenula receives major inputs via a white matter bundle called stria medullaris (sm) (Herkenham and Nauta 1977, Qin and Luo 2009). The most prominent input is from the two nuclei in the posterior septum: the triangular septal nucleus (TSN) and septofimbrial nucleus (SFi), which release glutamate and ATP to the MHb (Herkenham and Nauta 1977, Qin and Luo 2009). Interestingly, the MHb contains the highest expression level of $GABA_B$ receptors in the brain, suggesting the presence of strong inhibitory inputs (Bischoff, Leonhard et al. 1999, Durkin, Gunwaldsen et al. 1999, Charles, Evans et al. 2001, Wang, Gong et al. 2006). It has been shown that the GABAergic inputs to the MHb are from the Nucleus of Diagonal band (NDB) and the medial septum (MS) (Qin and Luo 2009). Moreover, it also has been reported that MHb received monoaminergic inputs, including the dopaminergic inputs from the interfascicular nucleus of VTA (Phillipson and Pycock 1982, Viswanath, Carter et al. 2013) and noradrenergic inputs from the locus coeruleus and superior cervical ganglion (Gottesfeld 1983). In addition, physiological and neurochemical studies have

shown that the MHb also has the highest expression of nicotinic acetylcholine receptors (nAChRs) (Sheffield, Quick et al. 2000). Evidence from lesion studies showed that the NDB or posterior septum might send the cholinergic input to the MHb, but more precise research still needs to be done (Contestabile and Fonnum 1983).

Efferents

The MHb has several subregions, in which the neurotransmitter expression pattern is highly localized: the superior MHb (MHbS) have vesicular glutamate transporters and therefore are glutamatergic; the dorsal region of the MHb (MHbD) expresses substance (SP) and glutamate (Glu); and the ventral region MHb (MHbV) (can be divided into the ventro-medial (MHbVm), the ventrocentral (MHbVc) and the ventro-lateral (MHbVl) subnuclei) expresses acetylcholine (ACh) and Glu (Contestabile, Villani et al. 1987, Aizawa, Kobayashi et al. 2012). In addition to the highly localized expression of neurotransmitters, expression pattern of other markers has also been shown to be subnuclei specific. For instance, the mu-opioid receptor (Oprm) is only expressed in the MHbVl part, and interleukin 18 (IL-18) is only expressed in the MHbS and MHbD parts (Aizawa, Kobayashi et al. 2012, Antolin-Fontes, Ables et al. 2014).

The medial habenula sends major inputs to the interpeduncular nucleus (IPN) via the internal portion of an axon bundle called fasciculus retroflexus (fr) (Herkenham and Nauta 1977, Carlson, Noguchi et al. 2001). It is interesting that

habenular fibers traverse the entire width of the IPN several times to make various synaptic connections with the IPN neurons (Lenn 1976). MHb projects to distinct subnuclei of the IPN, and releases three distinct neurotransmitters: ACh, Glu, and SP (Ren, Qin et al. 2011, Aizawa, Kobayashi et al. 2012). The dorsal MHb innervate the lateral IPN (IPL and IPR, described below) in a cluster pattern and release the SP; the Choline acetyltransferase (ChAT) positive neurons in the ventral MHb innervate the ventral IPN (IPC and IPI, described below) (Contestabile, Villani et al. 1987) and the MHbVl part only innervates the dorsal IPN (IPR, described below) (Shih, Engle et al. 2014), and they release ACh and Glu at different transmission modes (Herkenham and Nauta 1979, Contestabile and Flumerfelt 1981, Ren, Qin et al. 2011). This highly restricted neurotransmitter expression and projection pattern suggest that the subnuclei might have specific functions in the brain.

It also has been reported that the MHb might project to the pineal gland (Ronnekleiv and Moller 1979). In addition, there are two observations suggesting that the intrinsic habenular circuitry exist and the direction is from medial to lateral. One of the evidence is that boutons en passant were found from MHb to the LHb, but not from the LHb to the MHb (Kim and Chang 2005). The other evidence is that the sectioning of the MHb efferent axons reduced SP levels in the LHb (Sutherland 1982). These evidence suggest that MHb may regulate LHb activity, while the LHb probably does not directly influence activity in the MHb.

Interpeduncular nucleus afferents and efferents

The Interpeduncular nucleus (IPN) is an unpaired midline structure in the posterior part of the midbrain (Klemm 2004). In rodents, it lies just above the pituitary gland. IPN is surrounded dorsally by the ventral tegmental area (VTA) and median raphe, anteriorly by the mammillary bodies of the hypothalamus, posteriorly by the pontine nuclei (Klemm 2004). Based on anatomical features and neurotransmitter expression pattern, at least seven subnuclei were identified. They were divided into two groups: unpaired and paired subnuclei. There are three unpaired subnuclei: Apical sub-nucleus (IPA), Central sub-nucleus (IPC), Rostral sub-nucleus (IPR); and four paired subnuclei: Dorsolateral sub-nucleus (IPDL), Dorsomedial sub-nucleus (IPDM), Intermediate sub-nucleus (IPI) and Lateral sub-nucleus (IPL) (Hamill and Lenn 1984).

Afferents

As discussed above, the IPN receives major input from the MHb via the fasciculus retroflexus, and this connection is highly conserved throughout the vertebrate lineage (Shibata, Suzuki et al. 1986, Viswanath, Carter et al. 2013). It also receives the input from several other brain regions in the limbic forebrain, including the medial frontal cortex, the nucleus of the diagonal band, substantia innominata, preoptic and hypothalamic nuclei and the supramammillary nucleus (Hamill and Fass 1984, Woolf and Butcher 1985, Shibata, Suzuki et al. 1986, Dinopoulos, Papadopoulos et al. 1989). In addition, several brain regions in the

brain stem also project to the IPN, including the raphe nucleus (RN), locus coeruleus (LC) and dorsal tegmental region (DTR) (Contestabile and Flumerfelt 1981, Hamill and Jacobowitz 1984, Shibata, Suzuki et al. 1986, Vertes and Fass 1988, Takagishi and Chiba 1991).

Biochemical studies have shown extremely high levels of acetylcholine, choline acetyltransferase, acetylcholine esterase and high-affinity choline uptake within the IPN, suggesting that the IPN received very strong cholinergic input (Contestabile and Fonnum 1983). MHb is the major cholinergic input to the IPN, and dorsal tegmental region and mediobasal forebrain area might also send the cholinergic projection to the IPN (Contestabile and Fonnum 1983, Woolf and Butcher 1985). Other neurotransmitters present in the IPN, include GABA, substance P, and various monoamines (noradrenaline, dopamine and serotonin) Morley (1986).

Efferents

The IPN is well known for its widespread projections. The dorsal tegmental region and the raphe nucleus are the major projection targets of IPN (Hamill and Lenn 1984). It also has been reported that IPN sends the output to the hippocampus, entorhinal cortex, hypothalamus, thalamus and the septum (Hamill and Lenn 1984).

Conclusion:

The anatomical studies show that the MHb-IPN tract is the key connection that links these forebrain and midbrain structures. Habenula and IPN both have multiple sub-nuclei, but not much is known about the specific input and output of each sub-nucleus and their interaction or function.

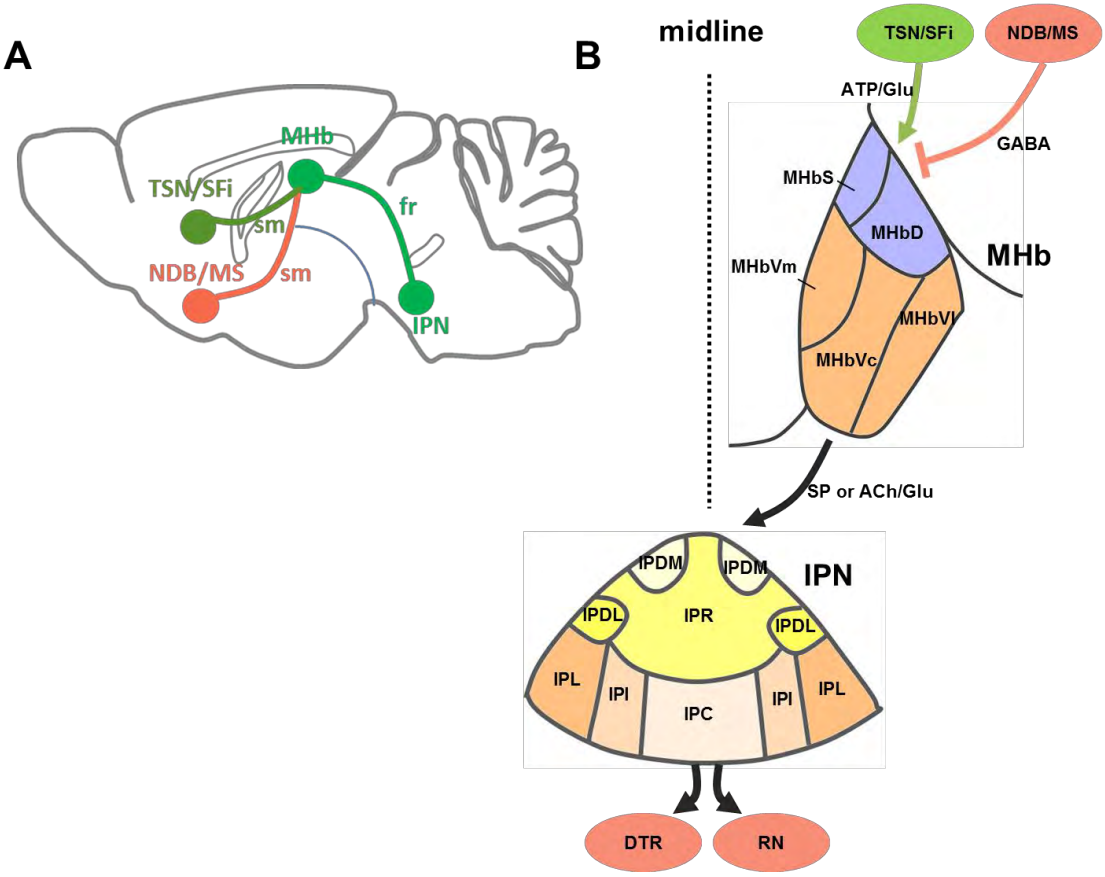

Figure I-2. The neuroanatomy of MHb-IPN pathway.

A. Schematic sagittal view of rodent brain showing known MHb and IPN connectivity. The MHb receives input mainly from the limbic system through stria medullaris (sm) and sends output through fasciculus retroflexus (fr) to the IPN, which projects to the raphe nuclei.

B. Afferent and efferent connections of the MHb and IPN. TSN and SFi send the excitatory projection to the MHb and release ATP/Glu, whereas the NDB and MS send the inhibitory projection to the MHb and release GABA. MHb can be divided into the MHbD, MHbS and MHbV (can be further divided into MHbVm, MHbVc

and MHbVl). The MHbD projects to the IPL to release SP, which is involved in fear. MHbV projects to the rest of the IPN to release ACh and Glu, which is involved in anxiety. The IPN can be divided into IPR, IPC, IPA, IPDM, IPDL, IPI and IPL.

Abbreviations for the brain regions indicated are: TSN, the triangular septal nucleus; SFi, the septofimbrial nucleus; NDB, the nucleus of diagonal band; MS, the medial septum; sm, stria medullaris; MHb, medial habenula; fr, fasciculus retroflexus; IPN, interpeduncular nucleus; MHbS, medial habenula superior; MHbD, the dorsal region of medial habenula; MHbVm, the ventro-medial region of medial habenula; MHbVc, the ventrocentral region of medial habenula; MHbVl, the ventro-lateral region of medial habenula; IPDM, dorsomedial sub-nucleus of IPN; IPDL, dorsolateral sub-nucleus of IPN; IPR, rostral sub-nucleus of IPN; IPL, Lateral sub-nucleus of IPN; IPI, intermediate sub-nucleus of IPN; IPC, Central sub-nucleus of IPN; DTR, Dorsal tegmental region; RN, raphe nucleus.

I.D. The role of MHb in anxiety, fear, and depression

The study of MHb had a first golden age in the 1970"s, when there were several high quality reports about the MHb anatomical connections and possible functions (Cuello, Emson et al. 1978, Herkenham and Nauta 1979, Herkenham 1981, Stern, Johnson et al. 1981, Hamill, Olschowka et al. 1984). However, the pace of MHb functional studies slowed down because of its small size, the complexity of its role and the lack of suitable pharmacological agents (Baldwin, Alanis et al. 2011). Recently, thanks to the emergence of new techniques that allow researchers to study the small brain regions specifically, such as high resolution functional magnetic resonance imaging (fMRI), immunotoxin-mediated cell targeting, as well as optogenetics, the habenula has attracted great attention again.

In a human positron emission tomography (PET) study, the habenula has been shown to be hyperactive in patients with major depression (Morris, Smith et al. 1999). Another fMRI study showed that self-detected errors or negative feedback in a dynamically adaptive motion prediction task activated the habenular complex, suggesting that the habenular complex might regulate the human reward system (Ullsperger and von Cramon 2003).

In 2010, the medial habenula was shown to regulate the expression of fear in zebrafish (Agetsuma, Aizawa et al. 2010). Following genetic silencing with tetanus toxin or lesion with nitroreductase, both adult and larval zebrafish

showed enhanced freezing in aversive conditioning paradigms compared to the control animals (Agetsuma, Aizawa et al. 2010, Lee, Mathuru et al. 2010). In detail, when first exposed to an electric shock paired with a red light, both control and lesioned fish froze. As more shocks were delivered, freezing decreased in control fish, but not in habenula-lesioned fish (Agetsuma, Aizawa et al. 2010). Similarly, in larval zebrafish, they learn to avoid a light that has been paired with a mild shock but fail to do so when pre-exposed to inescapable shock. In this test, freezing appeared gradually in lesioned fish in the latter half of the conditioning session, but never in control fish (Lee, Mathuru et al. 2010). These studies suggest that habenula is critical for stress, and its disruption could contribute to anxiety disorders.

However, in rodents, the role of habenula in depression is contradictory. One study showed that habenula lesions reduced avoidance deficits caused by inescapable shock (Amat, Sparks et al. 2001). In contrast, other studies conclude that habenula lesions cause avoidance deficits (Thornton and Bradbury 1989). These contradictory results may be caused by imprecise lesions induced by traditional methods, as the habenula is a small brain structure (Wilcox, Christoph et al. 1986). The new specific genetic lesion approaches overcome these limitations and provide more accurate information. MHb was selectively lesioned by genetic approaches, and the MHb lesions led to abnormalities in a wide range of behavioral tests, such as hyperlocomotion during the early night period, delay and effort aversion in a decision-making test, deficits in spatial memory, a subtle

increase in anxiety levels, and attenuated sensorimotor gating (Kobayashi, Sano et al. 2013). These findings demonstrate that the MHb is involved in inhibitory control and cognition-dependent executive functions.

Recently, the MHb has been shown to play an important role in anxiety and fear (Yamaguchi, Danjo et al. 2013). The posterior septum, consisting of the triangular septum (TS) and the bed nucleus of the anterior commissure (BAC), has been implicated in the control of anxiety and fear responses (Yamaguchi, Danjo et al. 2013). Interestingly, anatomical studies showed that TS projects to ventral MHb whereas the BAC projects to dorsal MHb (Yamaguchi, Danjo et al. 2013). By immunotoxin-mediated cell targeting, the projection from the TS to MHbV or from BAC to the MHbD was selectively eliminated, respectively (Yamaguchi, Danjo et al. 2013). The behavioral data showed that ablation of the projection from the TS to the MHbV reduced anxiety whereas ablation of the projection from the BAC to the MHbD showed enhancement of fear responses and fear learning (Yamaguchi, Danjo et al. 2013). These data suggest that the TS-MHbV and BAC-MHbD pathways have distinct roles in the regulation of anxiety and fear, respectively (Yamaguchi, Danjo et al. 2013).

Conclusion:

MHb is involved in anxiety, fear and depression. In addition, it seems that the different sub-region of MHb modulate different behaviors. However, the role of

different neuronal population and the molecular mechanisms underlying different behaviors still need to be studied.

I.E. nAChR: Structure, Function and the role in anxiety

Overview:

Acetylcholine (ACh) is one of the most important neurotransmitters in the central nervous system (Woolf and Butcher 1985). Acetylcholine receptor (AChR), as its name indicates, is an integral membrane protein that responds to the binding of ACh (Gotti and Clementi 2004). AChRs not only respond to endogenous neurotransmitter, ACh, they also respond to other exogenous molecules, like nicotine (the main addictive substance in tobacco) and muscarine (toxins from various mushrooms) (Rubio, Perez et al. 2006). According to their relative affinities and sensitivities to different molecules, AChR can be divided into two main classes: nicotinic acetylcholine receptors (nAChR) and muscarinic acetylcholine receptors (mAChR) (Bikadi and Simonyi 2003). Both of them are expressed by neuronal and non-neuronal cells throughout the body (Gotti and Clementi 2004, Dani and Bertrand 2007).

nAChR (also known as "ionotropic" acetylcholine receptors) are cation channels and they are particularly responsive to nicotine in micro- to submicro- second range (Bikadi and Simonyi 2003). In contrast, mAChR (also known as "metabotropic" acetylcholine receptors) are particularly responsive to muscarine, responding relatively slowly in the milliseconds to seconds range and they are G-

protein-coupled receptors that activate other ionic channels and other cellular processes via a second messenger cascade (Bikadi and Simonyi 2003).

nAChRs: Structure

nAChRs belong to the large superfamily of Cystine-loop ligand-gated ion channels, that also includes $GABA_{A/C}$, glycine and $5\text{-}HT_3$ ionotropic receptors (Romanelli, Gratteri et al. 2007). Like all of the other members of the Cystine-loop ligand-gated ion channel superfamily, all nAChR subunits have an approximately 200 amino acid long relatively hydrophilic extracellular amino terminal portion that carries the ACh binding site, followed by three hydrophobic transmembrane domains (TM1-TM3), a large intracellular domain which varies significantly from one subunit to the other, then a fourth hydrophobic transmembrane domain (TM4) and an extracellular carboxy terminal (Gorne-Tschelnokow, Strecker et al. 1994). Both the amino- and the carboxy- terminals are extracellular (Zoli, Pistillo et al. 2014).

In the first extracellular domain, there is a cysteine-loop (Cys-loop) defined by two cysteines (Cys) that are separated by 13 intervening amino acids, which is required for agonist binding (Kao and Karlin 1986, Karlin, Cox et al. 1986, Cockcroft, Osguthorpe et al. 1990, Lansdell and Millar 2000, Albuquerque, Pereira et al. 2009, Tsetlin, Kuzmin et al. 2011). Subunits are classified into α- and non-α subunits based on the presence of a Cys-Cys pair: α subunits has

Cys-Cys pair, whereas non-α subunits are lacking the Cys-Cys pair (Nef, Oneyser et al. 1988, Lukas, Changeux et al. 1999)

Each nAChR is composed of five subunits that combine to form a functional receptor and all five subunits contribute to channel kinetics, ion conductance and selectivity (Steinbach 1989, Albuquerque, Pereira et al. 2009). The agonist-binding site is a hydrophobic pocket at the interface formed between α subunits and adjacent subunits, where the Cys-Cys pair is required (Karlin, Cox et al. 1986). The TM2 segment of all five subunits forms the conducting pore of the channel, and the regions in the TM2 intracellular loop is critical for the ion selectivity, permeability and channel gating of the receptor (Kuryatov, Gerzanich et al. 1997, Lester, Fonck et al. 2003). When a ligand, such as nicotine or ACh, binds to the interface, it produces a rotational force in the β-barrel of the extracellular domain that produces torque on TM2 to rotate it from a hydrophobic-based, channel closed configuration to a more open hydrophilic channel that favors ion passage (Akabas, Kaufmann et al. 1994, Wilson and Karlin 1998). This conformational change happens within microseconds. The L9′S mutation in the TM2 pore forming region produces a partial relief of the gate and increase channel permeability nonspecifically (Tapper, McKinney et al. 2004).

Three functional states have been described in ACh receptors: the resting (closed) state (R), the open state (O), and the desensitized (closed) state (D) (Baenziger, Miller et al. 1992, Champtiaux, Gotti et al. 2003, Albuquerque,

Pereira et al. 2009). The resting state is the most stable state in the absence of agonists and the channel is closed; the open state is the transient metastable states when agonist occupies the ligand binding site and the channel is open to allow the cations to flow down their electrochemical gradient; the desensitized state is the most stable state in the presence of agonists and the receptor is not responsive to the ligand (Edelstein, Schaad et al. 1996). Recovery from the desensitization state will take seconds to minutes (Fenster, Rains et al. 1997).

nAChRs: The subunit diversity

In vertebrate species, 17 nAChR subunits have been identified (α1- α10, β1-β4, γ,δ and ε) (Dani and Bertrand 2007). Historically, nAChRs are subdivided into muscle or neuronal subtypes based on their major expression site. Muscle nAChRs are either $(\alpha1)_2\beta1\gamma\delta$ in the embryonic tissues or $(\alpha1)_2\beta1\varepsilon\delta$ in the adult tissues (Mishina, Takai et al. 1986), whereas neuronal nAChRs can be either homopentamers $(\alpha)_5$ or heteropentamers $(\alpha)_2(\beta)_3$ or $(\alpha)_3(\beta)_2$ (Dani and Bertrand 2007).

Of 17 nAChR subunits, there are 12 neuronal nAChR subunit genes in vertebrates and they are classified into two subfamilies: nine alpha subunits (α2–α10) and three beta subunits (β2– β4) (Le Novere and Changeux 1995).

For the homomeric nAChRs, they are preferentially formed by α7, α8, or α9 subunits (Couturier, Bertrand et al. 1990, Gerzanich, Anand et al. 1994) and overall they have high Ca^{2+} permeability (comparable to the NMDA receptors), a

rapid desensitization rate and can be blocked by nanomolar concentrations of α-Bungarotoxin (α-Bgtx) (Gotti and Clementi 2004) . Therefore they were called α-Bgtx sensitive nAChRs. Of which, α7 containing nAChRs are one of the most abundantly expressed subtypes in the brain (Gotti and Clementi 2004), α8 nAChRs have only been identified in the chick nervous system (Gotti, Hanke et al. 1994), whereas α9 can form homomeric nAChRs but more efficiently when co-expressed with α10 subunit (Elgoyhen, Vetter et al. 2001, Sgard, Charpantier et al. 2002).

For the heteromeric nAChRs, they are formed by α2-6 and β2-4 subunits, which have high affinity for nicotine, but are insensitive to α-Bgtx. Therefore they were called α-Bgtx insensitive nAChRs. In the brain, α4β2* nAChRs (an asterisk in nAChR nomenclature indicates that other nAChR subunits are also present and can be read as “α4β2-containing nAChRs”) are the most abundant and widely expressed subtype. But in different brain regions, the diversity of the nAChR subtype can be huge.

For instance, α3β4* subtype is highly expressed in the autonomic ganglia and MHb as well as the IPN (Zoli, Pistillo et al. 2014). The dopaminergic (DAergic) neurons of the VTA express not only α4 β2 subunit but also α6 β3 subunits, and they can form α4α6β2β4* nAChRs, which has totally different properties compared to α4β2* subtype (Grady, Salminen et al. 2007).

The vast diversity of nAChR subtype expression determines the specialized properties and functions of the mature receptors, like the receptor open time, the channel conductance as well as the pharmacological properties (Albuquerque, Pereira et al. 2009).

nAChRs: The expression location

Electrophysiological recording combined with pharmacological tools provided a wealth of knowledge regarding the localization of native nAChRs on discrete neuronal compartments and enhanced our understanding of the role of various nAChRs in mediating or modulating synaptic transmission (Albuquerque, Pereira et al. 2009). Multiple lines of evidence have shown that nAChRs are located at five primary locations: the cell soma, dendrites, pre-terminal axon regions, axon terminal and myelinated axons on the neurons (Wonnacott 1997, MacDermott, Role et al. 1999, Gotti, Clementi et al. 2009). The different location of unique nAChR subtype might have specific functional implications (Wonnacott 1997, MacDermott, Role et al. 1999, Albuquerque, Pereira et al. 2009). For instance, in the mesolimbic dopamine pathway, different subtypes of nAChRs are found to be expressed on DAergic neurons, GABAergic neurons and glutamatergic neurons: DAergic neurons in the VTA project to the NAc and α4β2* , α6β2*, α7 subtypes are expressed in the soma and the presynaptic terminals; GABAergic neurons are interneurons in the VTA and α4β2* and α7 subtypes are expressed; glutamatergic input to the VTA is from the prefrontal cortex, synapsing on

DAergic neurons that express α7 nAChRs on the pre-synaptic terminals (Champtiaux, Gotti et al. 2003). When people smoke, nicotine from the tobacco rapidly crosses the blood brain barrier within 5 seconds and binds to the nAChRs in the DAergic neurons of VTA, which will induce the increase of burst firing and increase the dopamine release in the NAc (Dani and Bertrand 2007). Similar activation of these pathways in mice will cause the nicotine reward behaviors. Interestingly, when nicotine binds to the nAChR, the α4β2* nAChRs on the DAergic neurons will transit to the desensitized state rapidly (Dani and Bertrand 2007), while the α7 nAChRs at the terminal of glutamate neurons will not significantly desensitize and will continue to increase the glutamatergic transmission onto the DAergic neurons (Mansvelder and McGehee 2000). Therefore, the net effect of decreased GABAergic transmission and increase glutamatergic transmission result in the overall excitation of the mesolimbic DA reward system (Mansvelder, Keath et al. 2002).

nAChRs: Long term nicotine treatment regulate the expression of nAChRs

Long term exposure of nicotine increase the density of nicotinic receptor binding sites in rodent and primates brains (Marks, Burch et al. 1983, Parker, Fu et al. 2004, McCallum, Parameswaran et al. 2006, Hong, Jhou et al. 2011). Similarly, in human, the tobacco smoker brains showed increased nAChR density compared to non-smokers brains by membrane binding studies, autoradiography studies and PET studies (Benwell, Balfour et al. 1988, Perry,

Davila-Garcia et al. 1999, Brody, Mandelkern et al. 2004, McClernon, Kozink et al. 2008, Mukhin, Kimes et al. 2008, Cosgrove 2010).

More specifically, when mice were chronically treated with nicotine by continuous intravenous infusion of 4.0 mg/kg/hr for 10 d, L-^{3}H-nicotine binding in cortex and midbrain increased, but there was no change in cerebellum (Marks, Pauly et al. 1992). Another study showed that chronic nicotine treatment (48 mg/kg/day administrated for 10 days by means of an osmotic minipump, MP) upregulates functional alpha 4* nAChRs in the cortex, midbrain and hypothalamus, but not in the thalamus or cerebellum (Nashmi, Xiao et al. 2007). Consistent with this study, by autoradiography, immunoprecipitation and western blotting studies, it has been shown that animals chronically treated with nicotine (6-48 mg/kg/day administrated for 14 days by means of an MP) increase in ^{3}H-epibatidine binding, suggesting that there is an increase in the number of α4β2 receptors (Mugnaini, Tessari et al. 2002, Marks, Rowell et al. 2004, Perry, Mao et al. 2007, Mao, Perry et al. 2008, Gotti, Guiducci et al. 2010). Interestingly, in the presence of α5 subunit, the α4β2 subtype did not up-regulated *in vivo* in rat hippocampus, striatum, cerebral cortex and thalamus (Mao, Perry et al. 2008, Gotti, Guiducci et al. 2010). In addition, the α3β4* subtype, which is highly expressed in the pineal gland, medial habenula, nucleus interpeduncularis and autonomic ganglia, seems to be resistant to up-regulation (Nguyen, Rasmussen et al. 2003).

It has been shown that α6* receptors play an important role in striatal dopamine release, locomotion and nicotine self-administration (Gotti, Clementi et al. 2009). Intravenous nicotine self-administration (approximately 1.5 mg free base/kg/day) increased α6* nAChRs expression in VTA/SN and nucleus accumbens (Parker, Fu et al. 2004). In contrast, chronic nicotine treatment by minipump (3–6 mg/kg/day administrated for 14 days by means of an MP) or by drinking water (50–300 μg/ml for up to 6 weeks) decreases the number of α6* receptors in midbrain dopaminergic neurons (Mugnaini, Tessari et al. 2002, Lai, Parameswaran et al. 2005, Perry, Mao et al. 2007, Gotti, Guiducci et al. 2010).

In contrast, α2, α3, α4, α5 or β2 mRNA levels in chronic nicotine (intravenous infusion of 4.0 mg/kg/hr for 10 d) treated mouse brain did not differ from control brains, suggesting that the increase of nAChR expression is due to post-transcriptional mechanisms (Marks, Pauly et al. 1992). In another study, when mice were treated with chronic nicotine for 10 days (1.5 and 30.0 mg/kg/day), levels of alpha7 subunit mRNA were significantly elevated in SNpc, SNpr and VTA, but were unchanged in cortex and hippocampus (Ryan and Loiacono 2001).

In conclusion, the regulation of nAChRs by long-term nicotine treatment in rodents may strongly depend on the dosage of nicotine, the method of nicotine delivery, the rodent strain and the brain region. Also, the change of mRNA level does not positively correlate with the change of protein level.

nAChRs: The genetic modified nAChR mice model

Because of the huge nAChR diversity and the lack of subunit specific pharmacological tools, genetically modified nAChR mouse model can provide considerable insights into the basic neurobiological mechanisms of disease, such as addiction (Fowler and Kenny 2012). Genetically modified nAChR mice in combination with nAChR pharmacology are even more powerful.

Conventional knockout mice

Conventional knockout mice are made by introducing site-specific genetic deletion into the genome of mouse embryonic stem cells and the target gene will not be expressed throughout their entire lifespan in the whole body (Fowler and Kenny 2012).

The first genetically modified nAChR mouse was made by deleting a region of DNA that encodes the β2 subunit gene, Chrnb2, termed “β2 knock-out” and abbreviated as β2 KO (Picciotto, Zoli et al. 1995). Importantly, these mice develop and breed normally and they were tested for many disease related behaviors (Picciotto, Zoli et al. 1995).

Since 1995, knock-out nAChR mice has been made for the α7, α4, α3, β4, α5, α6, and β3 nAChR subunits (Orr-Urtreger, Goldner et al. 1997, Xu, Gelber et al. 1999, Ross, Wong et al. 2000, Champtiaux and Changeux 2002, Champtiaux, Han et al. 2002).

In this thesis, the α4 knock out mouse (α4 KO) will be used. In the homozygous α4 KO mouse, a 750 bp fragment from the fifth exon of the Chrna4 gene was removed, which contains DNA encoding the first hydrophobic transmembrane domain through the second cytoplasmic loop, therefore the mice do not express functional α4* nAChRs (Ross, Wong et al. 2000). Homozygous knockout mice are born in normally expected ratios, are capable of reproduction and have no physical abnormalities (Ross, Wong et al. 2000). Importantly, there is no significant difference in the expression of other nAChR subunits such as α3, α5, or α6, indicating that deletion of the α4 gene does not induce compensatory changes in other nAChR subunit mRNAs or proteins (Marubio, del Mar Arroyo-Jimenez et al. 1999).

Conventional knockin mice

As opposed to knockout mice, knockin mice are made by expressing the protein product with altered function than the wildtype product from the endogenous locus.

Another mouse model used in this thesis is the Leu9'Ala α4 knock-in mouse (L9'A). This mouse line contains a single point mutation from Leucine to Alanine at the 9' position of the transmembrane 2 pore-forming domain, causing these receptors to be 50-fold more sensitive to nicotine and endogenous acetylcholine (Tapper, McKinney et al. 2004). This hypersensitive mutation allows for selective activation of α4* nAChRs with low doses of nicotine that have no effect in WT

mice. For example, mice with this mutation developed nicotine-induced locomotor sensitization and nicotine conditioned place preferences at very low doses of nicotine that have no effect in WT mice (Tapper, McKinney et al. 2004).

Other transgenic mice

Other than the conventional knockout and knockin mice, several different genetically modified mice have been generated. For instance, transgenic mice can be created by injecting the bacterial artificial chromosome vector into a fertilized egg which carries large DNA inserts and will produce the transgene, such as the hypersensitive α6 nAChR mice (Leu9'Ser α6 nAChR) (Drenan, Nashmi et al. 2008). In conditional knockout mice, the target gene can be disrupted in a spatially and temporally controlled manner. Florescent knockin mouse with green fluorescent protein (GFP) -tag infused to different nAChR subunits are very useful to study the subunit expression pattern in the brain (Shih, Engle et al. 2014). These lines are very useful to study the role of nAChRs in disease and the expression pattern of the nAChRs.

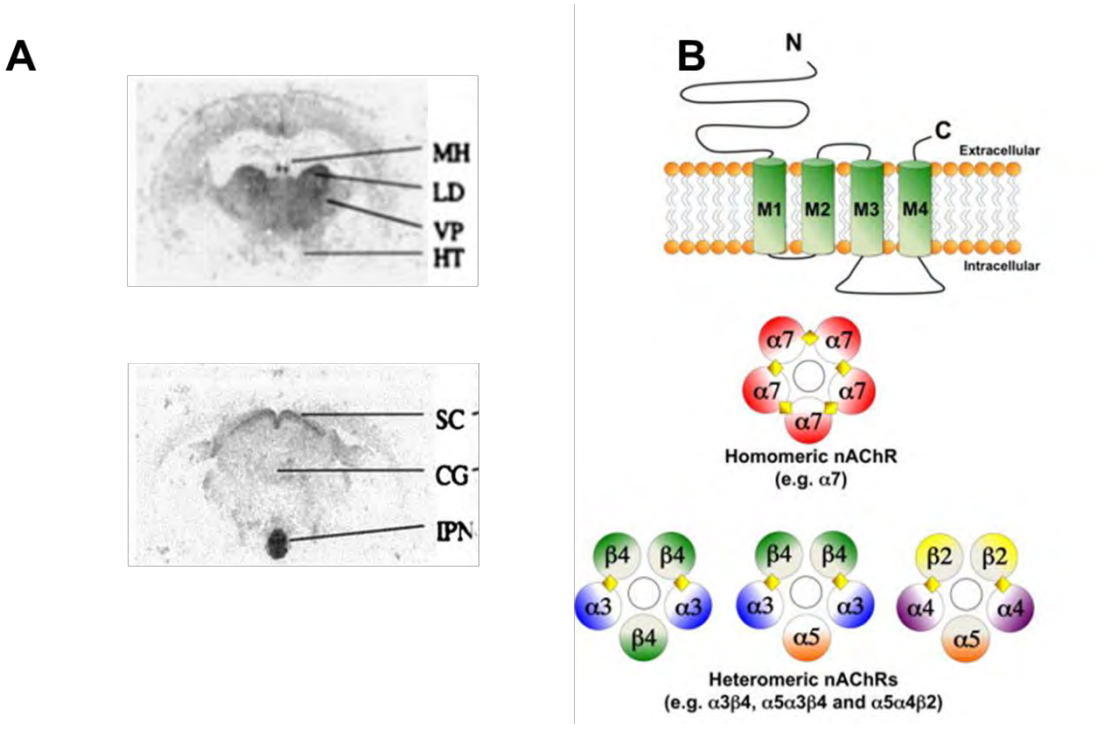

Figure I-3. Structure of nAChRs.

A. Coronal sections of the mice brain with [^{3}H] nicotine binding, showing that the nAChRs are highly expressed in the MHb (upper) and IPN (lower). Figure modified with permission from (Marks, Burch et al. 1983)

B. Schematic representation of an individual nAChR subunit. Each subunit consists of an extracellular amino (N) and carboxy (C) terminal, four transmembrane domains (M1-M4), and a large intracellular loop between M3 and M4 (upper). Five subunits co-assemble to form homomeric (middle) or heteromeric (lower) nAChR subtypes. White circles in the center of each pentamer represent the pore region. Diamonds represent ligand binding sites Figure modified with permission from (Improgo, Tapper et al. 2011).

nAChRs: The native subtypes in the IPN and MHb

It has been shown that there is strongest [^{3}H] nicotine binding in the mice MHb and IPN, which suggest that the nAChRs are highly expressed in the MHb-IPN tract (Marks, Smith et al. 1998). Then, several subunits are expressed in the MHb as shown by in situ hybridization (ISH) and single cell PCR, such as α3, α4, α5, α6, α7, β2, β3 and β4 subunit (Sheffield, Quick et al. 2000).

Notably, the MHb-IPN tract highly expresses the unique CHRNA5-A3-B4 gene cluster which encodes α5, α3 and β4 subunits (Antolin-Fontes, Ables et al. 2014). It has been shown that variants of this gene cluster are associated with higher levels of nicotine consumption and dependence in human genetics studies (Berrettini, Yuan et al. 2008, Ware, van den Bree et al. 2011).

Biochemical and immunoprecipitation studies have confirmed the heterogeneity of the nAChR subtypes expressed in the MHb-IPN tract. Basically, there are two major populations: β2* and β4* receptors. In the MHb, the β2* population mainly co-assemble with the α3 and α4 subunits, some of which also contain the accessory α5 or β3 subunits, whereas the β4* population mainly contains α3, α4 and β3 (Grady, Moretti et al. 2009). In the IPN, the β2* nAChRs consist of three populations of approximately equal size: α2β2*, α3β2* and α4β2*, whereas the β4* population mainly contains α3, α4 and β3, which is very similar to the MHb (Grady, Moretti et al. 2009).

Even though the immunoprecipitation studies provide evidence of the native nAChR subtypes, their spatial resolution is not high enough to map the subregion expression pattern in the brain circuitry (Zoli, Pistillo et al. 2014). Recently, the knockin mouse strains expressing GFP tagged α3, α4, α6, β2, β3, or β4 nAChR subunits have made it possible to determine the precise localization of the receptors (Fowler and Kenny 2012).

For the study of α4 subunit expression pattern in MHb, two knock-in mice lines were used: one mouse line expresses fluorescently tagged α4* nAChRs (α4YFP (Nashmi, Xiao et al. 2007), and the other one is the hypersensitive α4* nAChRs mice line, as mentioned above, where there is a single point mutation at the 9' position of the TM2 domain from Leucine to Alanine α4L9'A, (Tapper, McKinney et al. 2004, Fonck, Cohen et al. 2005). Combining electrophysiological and genetic approaches in these two mice lines, it has been demonstrated that nAChRs containing α4 subunits are mainly localized in the ventrolateral MHb and they contribute to the selective activation of these neurons in the ventrolateral MHb (Fonck, Nashmi et al. 2009). This result is consistent with previous in situ hybridization study (Le Novere, Zoli et al. 1996).

The high-resolution mapping of nAChR expression in the MHb-IPN pathway was extended by using many more GFP-tagged mice (Shih, Engle et al. 2014). It was shown that α3 and β4 nAChR subunits are highly expressed throughout the MHbV, which is consistent with the previous studies by western blot, in situ

hybridization and transgenic studies (Sheffield, Quick et al. 2000). In contrast, α6, β2, β3, and α4 subunits are selectively expressed in some, but not all, areas of MHbV and showed localization gradient across both MHb and IPN (Shih, Engle et al. 2014, Zoli, Pistillo et al. 2014). All subunits were found in both ChAT-positive and ChAT-negative cells in MHbV (Shih, Engle et al. 2014).

nAChRs: The function in the IPN and MHb

Several evidence showed that the nAChRs in MHb-IPN pathway regulate nicotine intake, mediate nicotine aversive properties as well as nicotine withdrawal related behaviors (Antolin-Fontes, Ables et al. 2014).

Withdrawal behaviors

Adverse health consequence caused by smoking kills approximately 6 million people annually, making tobacco use a major health problem worldwide (Picciotto and Kenny 2013). Upon cessation of tobacco use, unpleasant withdrawal syndromes occur in tobacco dependent individuals, which often drives relapse (Benowitz 2008).

Both humans and rodents with chronic nicotine consumption will show withdrawal symptoms if nicotine intake is suddenly stopped (spontaneous withdrawal) or a nicotinic antagonist, such as mecamylamine (non-specific nAChR antagonist), is administered (Antolin-Fontes, Ables et al. 2014). The nicotine withdrawal symptoms can be divided into affective and physical symptoms (Kenny and

Markou 2001). In humans, affective symptoms include anxiety, depressed mood, difficulty concentrating, disrupted cognition and nicotine craving; and physical symptoms include bradycardia, gastrointestinal discomfort and increased appetite accompanied by weight gain (Dani and De Biasi 2013). In rodents, physical signs (also called “somatic signs”) include increased scratching, rearing, jumping, head nods, and body shakes (Damaj, Kao et al. 2003, Grabus, Martin et al. 2005); whereas affective signs include anxiety-like behaviors and withdrawal-induced conditioned place aversion (CPA) (Jackson, Martin et al. 2008).

It has been shown that mecamylamine infusion into the habenula or the IPN, but not into the cortex, VTA or hippocampus, precipitated withdrawal symptoms in chronic nicotine treated mice, suggesting that the nAChRs in the MHb-IPN pathway are involved in nicotine withdrawal (Salas, Sturm et al. 2009). As the α2, α5, β2 and β4 subunits are highly expressed in the MHb-IPN tract, the authors then demonstrated that the α2, α5 and β4 subunits are necessary for the somatic manifestations of nicotine withdrawal by using the α2, α5 and β4 knockout mice (Jackson, Martin et al. 2008, Salas, Sturm et al. 2009). Interestingly, knockout β2 subunit or blockade of α6 containing nAChRs by the selective antagonist (α-conotoxin H9A) decreased anxiety-related behavior and blocked the withdrawal induced conditional place aversion but the somatic signs of nicotine withdrawal are unaltered (Jackson, Martin et al. 2008).

In agreement with these studies, our lab showed that chronic nicotine treatment upregulated gene expression of β3 and β4 nAChR subunits in somatostatin positive neurons in the IPN, and infusion of the β4 nAChR antagonist SR16584 in the IPN elicited somatic signs of nicotine withdrawal (Zhao-Shea, Liu et al. 2013).

Taken together, these studies indicate that α2, α5 and β4 containing nAChRs in the MHb-IPN pathway contribute to the physical symptoms of nicotine withdrawal whereas α2, β2 and α6 contribute to the affective component of withdrawal (Antolin-Fontes, Ables et al. 2014).

Nicotine intake and aversion

Nicotine intake shows an inverted U-shaped dose effect curve, in which the ascending limb reflects an increase in reinforcing efficacy that is not readily satisfied, whereas the descending limb reflects satiation as well as aversive properties of high doses of nicotine (Morel, Fattore et al. 2014).

It has been shown that the α5* nAChRs play an important role in regulating nicotine intake (Fowler, Lu et al. 2011). In detail, α5 knockout mice self-administer significantly greater quantities of nicotine than their wild-type littermates, and this enhanced intake in the mutant mice was blocked by virus-mediated re-expression of α5 nAChR subunits specifically in the MHb–IPN tract (Fowler, Lu et al. 2011). In addition, they found that the α5 KO mice diminished induction of c-Fos immunoreactivity in IPN in response to nicotine injections, suggesting that IPN neurons were relatively insensitive to nicotine in the mutant

mice (Fowler, Lu et al. 2011). Moreover, lidocaine-induced inactivation of the MHb and IPN or blockade of the NMDA receptor mediated transmission in the MHb-IPN pathway increased nicotine self-administration in rats (Fowler, Lu et al. 2011).

Consistent with these findings, overexpression of β4 nAChR subunits in the MHb–IPN tract reduced consumption of nicotine in mice and enhanced aversion to nicotine during the conditional place aversion procedure (Frahm, Slimak et al. 2011). Moreover, virus-mediated expression of mutant α5 subunit gene (α5 D398N variant, which decreases the function of α5-containing nAChRs), reduced aversion to nicotine and enhanced nicotine intake in the β4 subunit-overexpressing mice (Frahm, Slimak et al. 2011). In addition, several SNPs have been found in the β4 subunit gene, which are related to the cigarette consumption in human (Liang, Salas et al. 2005). When these β4 variants are overexpressed in the mice MHb by virus-mediated gene expression system, the mice showed aversion or preference for nicotine depending on whether the variants increase or decrease nicotine currents (Slimak, Ables et al. 2014).

Taken together, nAChRs in the MHb-IPN tract control the aversion of nicotine. High dose nicotine activates the MHb through α5 and/or β4-containing nAChRs and gives a negative motivational signal in turn blocking the nicotine intake.

I.F. Nicotine, nAChR and anxiety

In both human and animal studies, it has been shown that nicotine has effects on anxiety and depression, but nicotine treatment can be either anxiolytic or anxiogenic depending on the regimen of administration (acute, different chronic regimens, withdrawal), the anxiety model tested (elevated plus maze, social interaction, light-dark box, mirrored chamber), the route of nicotine administration (i.p., s.c., i.v., smoked), the time course of administration as well as the behavioral state of the experimental subjects (relaxed, stressed, in nicotine withdrawal) (Picciotto, Brunzell et al. 2002).

For example, in the social interaction test, acute, systemic nicotine can be either anxiolytic or anxiogenic in rats: low doses (0.01. and 0.1 mg/kg) were anxiolytic and high doses 0.5 and 1.0 mg/kg were anxiogenic (File, Kenny et al. 1998). At low dose, the effect was time dependent: at 5 min low-dose nicotine was anxiogenic, at 30 min it was anxiolytic, and at 60 min it produced a second anxiogenic response (File, Kenny et al. 1998). In contrast, in elevated plus maze test, systemic acute injection of nicotine (0.5 and 1 mg/kg, i.p. or 0.35 mg/kg i.c.) had anxiogenic effects in rats (Ouagazzal, Kenny et al. 1999, Olausson, Akesson et al. 2001). Similarly, nicotine elicits an anxiogenic response 7 min but not 30 min after nicotine i.p. injection with doses of 0.25 and 0.5 mg/kg in mice (O'Neill and Brioni 1994, Zarrindast, Homayoun et al. 2000). Taken together, these studies suggest that low dose (0.01 mg/kg - 0.05 mg/kg) of acute nicotine administration has anxiolytic effect; whereas high dose (0.5 mg/kg) of acute nicotine administration has anxiogenic effect in mice (File, Kenny et al. 1998,

Ouagazzal, Kenny et al. 1999, Zarrindast, Homayoun et al. 2000, Cheeta, Tucci et al. 2001, McGranahan, Patzlaff et al. 2011, Varani, Moutinho et al. 2012).

Interestingly, it has been shown that nicotine can both activate and desensitizes nAChRs at different concentration: at low concentration, nicotine desensitize nAChR (preferentially β2* nAChRs), which makes them unavailable to be further activated by nicotine (Lester and Dani 1995, Fenster, Rains et al. 1997, Pidoplichko, DeBiasi et al. 1997, Mansvelder, Keath et al. 2002, Buccafusco, Shuster et al. 2007). This evidence suggests that desensitizing nAChRs is anxiolytic whereas activating nAChRs is anxiogeneic. Recently, a study by Brunzell lab proved this idea. They showed that low-dose nicotine (0.05 mg/kg) pretreatment blocks high dose nicotine (0.5 mg/kg) induced anxiogenic effect in light–dark box assay and EPM assay, confirming that low dose of nicotine desensitized nAChRs in the brain and prevented them from further activation by high dose of nicotine treatment, in turn blocking its anxiogenic effect (Anderson and Brunzell 2015).

In addition, it also has been shown that selective inhibition of β2* nAChRs by DhβE or low dose of 5I-A85380 (0.001 mg/kg) reduces anxiety in elevated plus maze test and marble burying test (Turner, Castellano et al. 2010, Anderson and Brunzell 2012, Anderson and Brunzell 2015).This evidence suggests that high doses of nicotine may induce anxiogenic effect via high-affinity β2*nAChRs. This idea was proved by Brunzell lab by showing that genetic disruption of β2 nAChR

or pharmacological block of β2 by DHβE blocked anxiogenic-like effects of 0.5 mg/kg nicotine (Anderson and Brunzell 2015).

The studies in the genetically modified mice also showed that nAChRs are involved in anxiety. For α4* nAChRs, knockout mice lacking the α4 subunit and the hypersensitive L9'A α4 mice showed increased anxiety in the elevated plus maze and the mirrored chamber (Ross, Wong et al. 2000, Labarca, Schwarz et al. 2001, Picciotto, Brunzell et al. 2002). For α5* nAChRs, only female α5KO mice, but not the male mice, displayed anxiolytic-like phenotype in the elevated plus maze, not in the open field activity and light-dark box (Gangitano, Salas et al. 2009). For α7* nAChRs, knockout mice lacking the α7 subunit showed lower level of anxiety than wild type mice in the open field test, but not in the light-dark box (Paylor, Nguyen et al. 1998). For β2* nAChRs, knockout mice lacking the β2 subunit did not show difference in the anxiety level compared to wild type mice in the elevated plus maze, light dark exploration test and mirriored chamber test (Picciotto, Zoli et al. 1997).

In conclusion, the large variety of nAChRs expressed in all the brain regions is critical in modulating anxiety, and defining the site specific roles of individual receptor subtypes could be useful in drug development to cure the anxiety disorder.

CHAPTER II

Medial habenula cholinergic neurons are involved in anxiety

Contributions:

Jennifer Ngolab made the virus construct. Liwang Liu did the electrophysiological recordings. All other research was done by me. Dr. Andrew Tapper wrote part of the body of the text, while I made the Figures, Materials and Methods and provided feedback on the other sections.

II.A. Introduction

Up to 40 million patients suffer from anxiety disorders in the United States alone highlighting the need for identification of the underlying neuroanatomical bases and molecular underpinnings of anxiety (Kessler, Chiu et al. 2005).

Multiple brain regions are involved in the anxiety disorders, such as Amygdala, BNST, PFC, hippocampus, etc (Adhikari 2014). Recently, the role of Hb-IPN tract in anxiety has attracted much attention.

The habenula (Hb) is a small, epithalamic structure, which can be divided into medial (MHb) and lateral (LHb) sub-regions (Hikosaka 2010). The Hb projects to its target brain regions through a conspicuous bundle of axons that form the fasciculus retroflexus (fr).

The LHb receives the input mainly from the basal ganglia and send output to the rostromedial tegmental nucleus that is involved in the modulation of dopamine (DA) release from the substantia nigra pars compacta and ventral tegmental area (VTA) (Kaufling, Veinante et al. 2009, Balcita-Pedicino, Omelchenko et al. 2011, Hong, Jhou et al. 2011, Lecca, Melis et al. 2011). Activation of the LHb signals aversion (Hong, Jhou et al. 2011).

On the other hand, the MHb receives the major inputs via a white matter bundle, the stria medullaris (Herkenham and Nauta 1977, Qin and Luo 2009). The triangular septal nucleus (TSN) and septofimbrial nucleus (SFi) release

glutamate and ATP to the MHb (Herkenham and Nauta 1977, Qin and Luo 2009), whereas Nucleus of Diagonal band (NDB) and the medial septum (MS) send GABAergic input to the MHb (Qin and Luo 2009). In addition, MHb also has the highest expression of nicotinic acetylcholine receptors (nAChRs) (Marks, Smith et al. 1998), but where the cholinergic input comes from is still unclear.

The MHb mainly projects to IPN via another white matter bundle, the fasciculus retroflexus. The dorsal MHb innervate the lateral IPN and release Substance P, while the cholinergic neurons in the ventral MHb innervate the ventral IPN (Contestabile, Villani et al. 1987) and release ACh and Glu at different transmission modes (Herkenham and Nauta 1979, Contestabile and Flumerfelt 1981, Ren, Qin et al. 2011). This highly restricted neurotransmitter expression and projection pattern suggest that the subnuclei might have specific functions.

Human imaging studies and the rodent pharmacological studies have shown that MHb is involved in anxiety (Thornton and Bradbury 1989, Morris, Smith et al. 1999, Amat, Sparks et al. 2001, Ullsperger and von Cramon 2003). Interestingly, selective ablation of septal glutamatergic ventral MHb afferents reduces anxiety-like behavior in mice, while selective ablation the bed nucleus of the anterior commissure (BAC) dorsal MHb afferents enhanced fear responses, suggesting a role for the different subregion of MHb in controlling anxiety and fear (Yamaguchi, Danjo et al. 2013). However, how the ventral cholinergic neurons controls anxiety is still unclear.

Optogenetics, which combines genetics and optics, can control the specific neuronal activity (Fenno, Yizhar et al. 2011). Channelrhodopsin (ChR) is a light-activated cation channel which can induce action potentials and “turn the neurons on” when stimulated with blue light (Fenno, Yizhar et al. 2011). In contrast, halorhodopsin (NpHR) is a light-gated chloride pump, which can induce hyperpolarization to turn neurons off when stimulated with yellow light (Fenno, Yizhar et al. 2011). Here, in this chapter, we will use NpHR or ChR2 to silence or activate the cholinergic neurons, respectively, and test the hypothesis that the cholinergic neurons in the MHb control anxiety via the nAChRs.

II.B. Materials and methods

Mice

C57BL/6J and ChAT-Cre mice were used in experiments as indicated. As described above, ChAT-Cre knock-in mice, were purchased from Jackson Laboratories (stock number: 006410) and bred in the UMMS animal facility. For ChAT-Cre mice, genotypes were determined by PCR as previously described (Rossi, Balthasar et al. 2011) and also on Jackson Laboratories website. PCR of mouse tail genomic DNA was performed with three specific primers, WT F (5′-GTT TGC AGA AGC GGT GGG-3′), mutant F (5′-CCT TCT ATC GCC TTC TTG ACG -3′) and Common R (5′-AGA TAG ATA ATG AGA GGC TC -3′). These primers amplify DNA fragments of 272 bp in wild-type (WT) mice, and 350 bp in ChAT-Cre mutant mice. DNA fragments were separated by agarose gel

electrophoresis and visualized with ethidium bromide. Breeding was conducted by mating heterozygous pairs. Mice were group-housed four mice/cage on a 12-h light dark cycle with lights on at 7:00 a.m. and off at 7:00 p.m, and given food and water ad libitum. Male mice were used for all experiments. Mice were at least 8 weeks old at the start of each experiment. Behavioral experiments were performed during the light phase of the light-dark cycle.

Independent groups of animals were used for each behavioral experiment unless otherwise noted. All experiments were conducted in accordance with the guidelines for care and use of laboratory animals provided by the National Research Council, as well as with an approved animal protocol from the Institutional Animal Care and Use Committee of the University of Massachusetts Medical School.

Surgical procedures for virus microinjection

Packaging of AAV-Ef1A-DIO-ChR2-eYFP, AAV-Ef1A-DIO-NpHR-eYFP and AAV-eGFP plasmids into AAV2 viral particles was done by the University of Massachusetts Medical School Viral Vector Core. For viral particle injection, ChAT-Cre mice were anesthetized with a mixture of ketamine (100 mg/kg) and xylazine (10 mg/kg) (VEDCO). The surgical area was shaved and disinfected. Mice were placed in a stereotaxic frame (Stoelting Co.) with mouse adaptor and a small incision was cut in the scalp to expose the skull. Using bregma and lambda as landmarks, the skull was leveled in the coronal and sagittal planes.

The viral particles ($1x10^{12}$ viral particles/µl) were injected into the ChAT-Cre mice MHb according to the coordinates: AP, -1.94, ML, 0.2, DV, -2.25. The viral particles (1.5 µl/side) were injected bilaterally at a flow rate of 0.3 µl/min. The injection needle was kept in place for 5 min post-injection. The incision was sutured and mice were returned to their home cages.

Optic fiber placement and the optic stimulation

Infected ChAT-Cre mice with optic fiber implants were gently connected to a patch cable using a mating sleeve (Doric Lenses). The optic fiber was attached through an FC/patch cable adaptor to a fiber-coupled LED light source. Yellow light pulses (593 nm) or blue light pulse (470 nm) were generated through an LED driver.

To activate the neurons by ChR2, low frequency stimulation (5 Hz trains of blue light pulses 20 s on, 10 s off, 300 mA current) was delivered over the course of 20 min in the marble burying test (MBT) and 5 min in the elevated plus maze (EPM). In the high frequency stimulation, 50 Hz trains of blue light pulses (20 s on, 10 s off, 300 mA current) were delivered over the 10 min of locomotor test.

To silence the neurons by NpHR, constant light (593 nm) stimulation (20 s on, 10 s off) was delivered over the course of 20 min in the marble burying test (MBT) and 5 min in the elevated plus maze (EPM).

After recording, the optic cannula was disconnected from the LED patch cable. Mice were euthanized and the brains were harvested for analysis of virus injections and fiber implantations.

Electrophysiology

For the electrophysiological recording, ChAT-Cre mice were infected with the virus when the mice were 3 weeks old. Four weeks later, brains were quickly removed and placed in oxygenated ice-cold high sucrose artificial cerebrospinal fluid (SACSF) containing kynurenic acid (1 mM, Sigma, St. Louis, MO). SACSF solution contained (in mM): 250 sucrose, 2.5 KCl, 1.2 $NaH_2PO_4•H_2O$, 1.2 $MgCl_2•6H_2O$, 2.4 $CaCl_2•2H_2O$, 26 $NaHCO_3$, 11 D-Glucose. Coronal brain slices containing IPN brain regions (~180 μm) were made using a Leica VT1200 vibratome. Spontaneous EPSCs were obtained in the whole-cell configuration and gap free acquisition mode in Clampex (Axon Instruments). Neurons were held at a resting membrane potential of -70 mV. For optical recordings, eYFP/eGFP-positive neurons were identified under fluorescence microcopy. In the ChR2 expressing neurons, 30 sec trains of blue light were applied to neurons under current clamp. In the NpHR expressing neurons, constant yellow light was applied to neurons under current clamp. All recordings were filtered at 1 kHz using the amplifier's four-pole, low-pass Bessel filter, digitized at 10 kHz with an Axon Digidata 1440A interface and stored on a personal computer. ACSF was

used for bath solution and contained (in mM): 125 NaCl, 2.5 KCl, 1.2 $NaH_2PO_4•H_2O$, 1.2 $MgCl_2•6H_2O$, 2.4 $CaCl_2•2H_2O$, 26 $NaHCO_3$, 11 D-Glucose.

Marble burying test (MBT)

As described in our previous paper (Zhao-Shea, Liu et al. 2013), mice were habituated in the standard mouse cage with ~5 - 6 cm layer of bedding for 2 days (45 min/day) before the test. On the test day, 15 clean 1.5 cm glass marbles were evenly spaced in five rows of three, each 4 cm apart on the thick of bedding. A mouse was placed in its test cage and left for 30 minutes, and the number of marbles buried (to 2/3 their depth) with bedding was counted every 5 min or after 30 min (as noted in the figures), then mice were removed from their test cages.

Elevated plus maze (EPM)

As described in our previous paper (Zhao-Shea, Liu et al. 2013), the experimental apparatus consisted of a central axis and four arms elevated 45 cm above the floor, with each arm positioned at 90° relative to the adjacent arms. One red fluorescent light arranged at 100 cm above the maze was used as the source of illumination. The mice were individually placed in the center of the maze with their heads facing one of the open arms and allowed 5 min of free exploration. The number of entries into the open and closed arms, and the total time spent in the open and closed arms were measured by MED-PC IV software (MED Associates, Inc.). The time spent in open and closed arms was calculated as standard anxiety indices. The total number of arm entries was considered as

an index of locomotor activity. The apparatus was cleaned thoroughly between trials. Trials in which mice froze in the initial arm without moving were not included in the analysis.

Guide cannula placement

As described in our previous paper (Zhao-Shea, Liu et al. 2013), the guide cannulas were surgically implanted at least 3 days prior to the experiment. Mice were anesthetized with a mixture of ketamine (100 mg/kg) and xylazine (10 mg/kg) (VEDCO) and placed on a stereotaxic frame (Stoelting Co.). The surgical area was shaved and disinfected and the skull was exposed. Using bregma and lambda as landmarks, the skull was leveled in the coronal and sagittal planes. A hole was drilled and stainless steel guide cannulas were inserted into the brain and secured to the skull with instant adhesive. The coordinates relative to bregma were: MHb (AP, -1.94, ML, ±0.2, DV, -2.25) or IPN (AP, -3.4, DV, -4.75). The scalp incision was stitched and dental cement was used to stabilize the cannula on the skull. After surgery, the mice were kept on a heating pad to prevent hypothermia. Mice were allowed to recover in individual cages for at least 3 days prior to drug infusion and behavioral testing.

Intra-MHb and intra-IPN infusions

Mice were anesthetized with 2% isoflurane via a nose cone adaptor at a flow rate of 800 ml/L. Once anesthetized, an infusion cannula designed to reach −0.25 mm below the guide cannula was inserted into the guide cannula.

Mecamylamine is a nonselective antagonist of nAChR and we use a relatively low dose according to the literature (Levin, Briggs et al. 1994, Kim and Levin 1996, Wickham, Solecki et al. 2013)

Vehicle (ACSF), mecamylamine (2 µg/µl, 1µl) or AP-5 (1 µg/µl, 1µl) was infused at a rate of 1 µl/min. After infusion, the infusion cannula was left in place for 2 minutes prior to retraction. Mice were placed back into their home cages and the behavior tests were conducted after the mice were totally awake. After completion of behavioral experiments, mice were culled, brains isolated, and cannula placement verified. To verify the guide cannula placement, the brains were cut in 30 µm sections and the location of the guide cannula was determined by neutral red staining using light microscopy. In addition, the injection sites were double verified histologically by microinjection of DiI cell labeling solution (Invitrogen). Only mice with cannulas in the right placement were included in the statistical analysis.

Data analysis

Data were analyzed using One- or Two-way ANOVA followed by Bonferroni post hoc tests or t-tests as indicated. Results were considered significant at $p < 0.05$. All data are expressed as mean ± S.E.M.

II.C. Results

nAChR activity in the MHb but not the IPN regulates anxiety-like behavior in mice

Cholinergic neurons of the MHb robustly express nAChRs (Grady, Moretti et al. 2009). To test the hypothesis that MHb nAChRs regulate anxiety-like behavior we selectively infused saline or the non-specific nAChR antagonist, mecamylamine (2 μg) into the MHb through guide cannulas targeting this brain region in adult C57Bl/6J mice (Fig. II-1). Following infusions, mice were tested in two assays of anxiety-like behavior, the elevated plus maze (EPM) and marble burying test (MBT). After behavioral tests, guide cannula placement and drug infusions were verified as described (See Methods and Fig. II-3). Infusion of mecamylamine into the MHb significantly increased the time spent on the EPM open arms compared to a saline infusion (t_{17}=2.94, $p < 0.01$, Fig. II-1C). Mice receiving mecamylamine infusions did not differ in total open arm entries compared to saline-infused animals, indicating that differences in open arm time did not simply reflect an effect of the drug on general locomotor activity (Fig. II-1E). In the MBT test, infusion of mecamylamine decreased the number of marbles buried compared to a saline infusion (t_{27}=3.74, $p< 0.001$, Fig. II-1G). While blockade of nAChRs at the level of dendrites and soma may directly regulate MHb neuronal excitability, nAChRs are also expressed in presynaptic terminals where they facilitate neurotransmitter release (Grady, Moretti et al. 2009). To test the hypothesis that terminal MHb nAChRs regulate anxiety-like behavior, we also infused mecamylamine (2 μg) and saline in the IPN, the output

region of MHb projections. Infusion of mecamylamine did not significantly affect performance on the EPM or MBT compared to saline IPN infusion (Fig. II-1D, 1F, 1H). Interestingly, cholinergic MHb neurons have recently been found to synthesize and release glutamate into the IPN (Qin and Luo 2009). To test the hypothesis that glutamatergic signaling in the IPN modulates anxiety-like behavior, we infused saline or the NMDA receptor antagonist, AP-5 (1 μg) into the IPN prior to the EPM and MBT assays (Fig. II-2). Mice that received AP-5 IPN infusions in the EPM test spent significantly less time in the open arms compared to mice receiving a saline infusion (t_9=2.46, Fig. II-2A, top), whereas total arm entries did not differ between groups (Fig. II-2A, bottom). Similarly, AP-5-infused animals buried more marbles compared to saline-infused animals in the MBT assay (t_9=3.59, Fig. II-2B). Together, these data indicate that nAChRs in dendrites/soma, but not presynaptic terminals, of MHb neurons inherently modulate anxiety-like behaviors. Furthermore, glutamatergic signaling in the IPN modulates anxiety-like behavior; whereas signaling via IPN nAChRs does not.

Silencing of MHb cholinergic neurons decreases anxiety-like behaviors

To test the hypothesis that MHb cholinergic neurotransmission is involved in anxiety-like behavior, we selectively expressed halorhodopsin in MHb cholinergic neurons to silence neurotransmission in the IPN of mice while measuring anxiety-like behavior by the EPM and MBT. Halorhodopsin (version 3.0) with an eYFP tag (eNpHR-eYFP) was expressed in the MHb of ChAT-Cre mice, in which

Cre is under the control of the ChAT promoter, using AAV2-mediated gene delivery of a plasmid containing eNpHR-eYFP in a double-inverted open reading frame (Fig. II-4A) (Gradinaru, Thompson et al. 2008). Four weeks post-infection, strong eYFP signal was observed in ChAT-expressing neurons and terminals innervating the IPN, indicating proper localization to cholinergic MHb neurons (Fig. II-4B, top). Light stimulation of current-clamped eNpHR-eYFP-positive neurons in MHb slices from eNpHR-eYFP-infected ChAT-Cre mice dramatically silenced action potential firing (Fig. II-4B, bottom). These data confirmed that eNpHR-eYFP was expressed and functional in cholinergic neurons of the MHb.

To test the hypothesis that neurotransmission from cholinergic MHb inputs to the IPN modulated anxiety-like behavior, ChAT-Cre mice were infected with AAV2-eNpHR-eYFP or control virus (AAV2-eGFP) with subsequent implantation of optic cannulas targeting the MHb terminal inputs to the IPN (Fig. II-4C). Light stimulation (593 nm) was applied through the optic fiber cannula for the entirety of the MBT and EPM assays (20 s light on, 10 s light off for 25 min, Fig. II-4D). Mice expressing halorhodopsin and receiving light stimulation spent significantly more time in the open arms of the EPM compared to control mice receiving light stimulation (t_{10} = 2.79, p = 0.019, Fig. II-4E, left). Importantly, total arm entries between groups did not differ, indicating that silencing of MHb cholinergic inputs did not affect locomotor activity (Fig. II-4E, right). In the MBT, at the end of the assay there was a significant decrease in the cumulative number of marbles buried in light-stimulated halorhodopsin-expressing ChAT-Cre mice compared to

light-stimulated control virus-expressing ChAT-Cre mice (Fig. II-4F, inset, t_{17}=3.826, $p < 0.01$).

To test the hypothesis that activation of MHb cholinergic neurons is sufficient to increase the anxiety-like behavior, we selectively expressed channelrhodopsin with an eYFP tag (ChR2-eYFP) in the MHb of ChAT-Cre mice using the same strategy as describe above (Fig. II-5A) (Fenno, Yizhar et al. 2011). Four to six weeks post-infection, significant eYFP signal was observed in MHb ChAT-expressing neurons and terminals innervating the IPN, indicating proper localization to cholinergic neurons (Fig. II-5B, top). Light stimulation of ChR2-eYFP-positive neurons in MHb slices from ChR2-eYFP-infected ChAT-Cre mice elicited robust trains of action potentials (Fig. II-5B, bottom). In contrast, neurons from mice with control virus infection did not respond to light (data not shown). These data confirmed that ChR2-eYFP was expressed and functional within the MHb.

To activate MHb cholinergic neurons in vivo, ChAT-Cre mice were infected with AAV2-ChR2-eYFP or control (AAV2-eGFP) virus and optic cannulas were implanted targeting the IPN in mice 4–6 weeks post-infection (Fig. II-5C). Blue light (via 473 nM LED) was delivered to the IPN in vivo through the optic fiber during the entirety of the MBT and EPM assays (5Hz, 20 s light on, 10 s light off for 25 min) (Fig. II-5D). The time spent in the open arms and the total arm entries of the EPM did not differ between the mice expressing ChR2 receiving light

stimulation and control mice receiving light stimulation (Fig. II-5E). In the MBT, at the end of the assay there was a significant increase in the cumulative number of marbles buried in light-stimulated ChR2-expressing ChAT-Cre mice compared to light-stimulated control virus-expressing ChAT-Cre mice (Fig. II-5F, inset, t_{16}=2.245, $p < 0.05$).

Together, these data indicate that MHb cholinergic neuron inputs to the IPN modulate anxiety-like behavior.

Activation of MHb cholinergic neurons induced hypolocomotion

As the cholinergic neurons in the MHb release Glu with low frequency (10 Hz) stimulation and ACh at high frequency (50 Hz) stimulation (Ren, Qin et al. 2011), here we test the hypothesis that high stimulation-induced ACh release will cause the aversive-like behavior. 4-6 weeks after ChAT-Cre mice were infected with AAV2-ChR2-eYFP or control (AAV2-eGFP) virus, the novel cage locomotor activity was measured for 5 min without the light stimulation, and there was no difference between the groups (Fig. II-6A.B.C). When the blue light was turned on for the next 10 min, the ChR2-expressing mice showed hypolocomotion compared to the control mice (t_{20}=3.974, $p<0.001$, Fig. II-6C), and the hypolocomotion gradually recovered to the same as control mice after the blue light was turned off (Fig. II-6A.B.C). These data indicate that ACh release from the MHb to the IPN induced hypolocomotion.

II.D. Discussion

Previous work indirectly demonstrated a role for the MHb in anxiety regulation, either through lesioning of the habenula itself or through selective ablation of presumed septal glutamatergic inputs into the MHb (Yamaguchi, Danjo et al. 2013). Interestingly, a recent study indicated that cholinergic MHb neurons synthesize and co-release the neurotransmitter glutamate, in addition to ACh (Ren, Qin et al. 2011). Our data indicate that nAChRs expressed at the level of the soma/dendrites of these neurons likely regulate neuronal activity and anxiety, because mecamylamine infusion into the MHb reduced anxiety-like behaviors, whereas blockade of MHb presynaptic nAChRs in the IPN or IPN nAChRs themselves did not affect anxiety-like behavior. In contrast, blockade of NMDA receptors in the IPN decreased anxiety-like behavior. These data indicate that glutamate release, but not ACh release, from dual cholinergic/glutamatergic MHb neurons regulates anxiety-like behavior.

Furthermore, here we showed that MHb cholinergic neurons, which are clustered in the ventral portion of the MHb, regulate anxiety-like behavior directly using optogenetics. Silencing MHb cholinergic neuronal inputs to the IPN reduced anxiety-like behaviors in both the EPM and MBT assays. On the other hand, activating MHb cholinergic neuronal input to the IPN at the low frequency (5 Hz) has a trend to increase anxiety-like behavior in the MBT.

While optogenetics provide an important tool to precisely define the relationship between neuronal activity and behavior in a given circuit, the endogenous

mechanisms that may regulate this activity still need to be studied. In addition, the expression of our control eGFP virus used in this study is not Cre-dependent, therefore, eGFP could express not only in cholinergic neurons but also in other neurons within the targeted region. This nonspecific expression of eGFP could possible influence the results. For future studies, Cre-dependent AAV-EGFP should be used.

In addition, the mice showed hypolocomotion when we activating MHb cholinergic neuronal input to the IPN at the high frequency (50 Hz). These data suggest that the high frequency stimulation induced ACh release from MHb to IPN. As IPN talks to VTA and Substantial Nigra (Lammel, Lim et al. 2014, Zhao-Shea, DeGroot et al. 2015), the release of ACh to IPN might indirectly influence the dopamine release from dopaminergic area into striatum, in turn reducing the locomotion in mice. In addition, we conclude that the low frequency induced glutamate release and high frequency induced ACh release from the MHb to the IPN might mediate different behavior in mice.

Together, our data indicate that MHb cholinergic neuron activity regulates anxiety-like behaviors. In addition, nAChR signaling in MHb cholinergic neurons are involved in the anxiety-like behavior. Thus, nicotinic acetylcholine autoreceptors in MHb cholinergic neurons should be considered molecular targets for novel anxiolytic therapeutics.

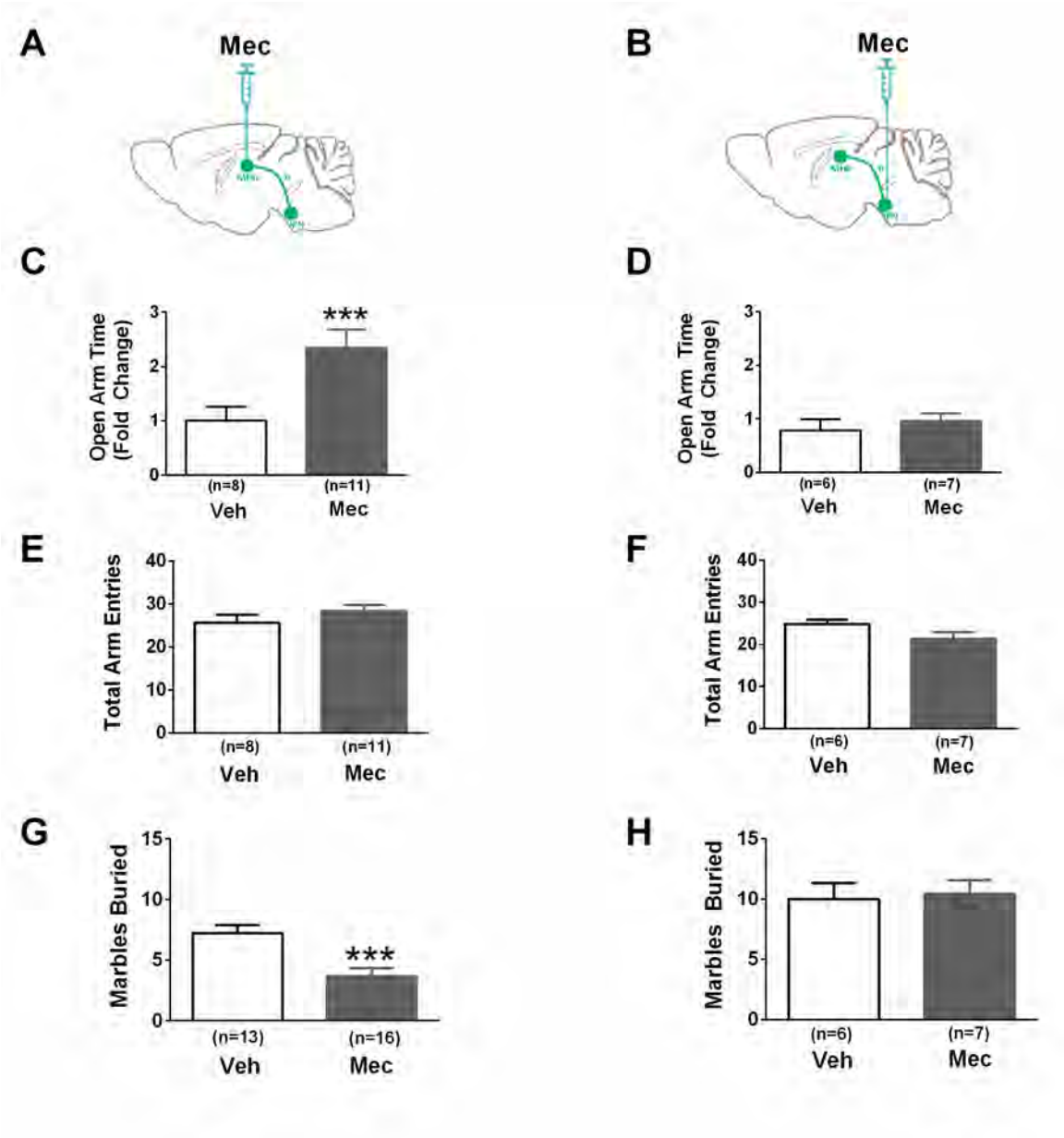

Figure II-1. nAChR activity in the MHb but not the IPN regulates anxiety-like behavior in mice.

Mecamylamine (Mec) or vehicle (Veh) was infused into the MHb (A, C, E, G) or IPN (B, D, F, H) prior to testing in the EPM and MBT assays. Infusion of Mec (2 µg) in the MHb increased time spent in the open arms of the EPM compared to Veh (C), while not affecting total arm entries (E). In the MBT, Mec infusion decreased the number of marbles buried (G). Infusion of Mec into the IPN did not significantly influence time spent in the open arms (D) or total arm entries (F) in the EPM, nor did it affect number of marbles buried in the MBT compared to Veh infusion (H). Data are expressed as average values ± S.E.M. *** $p < 0.001$, Student"s t-test.

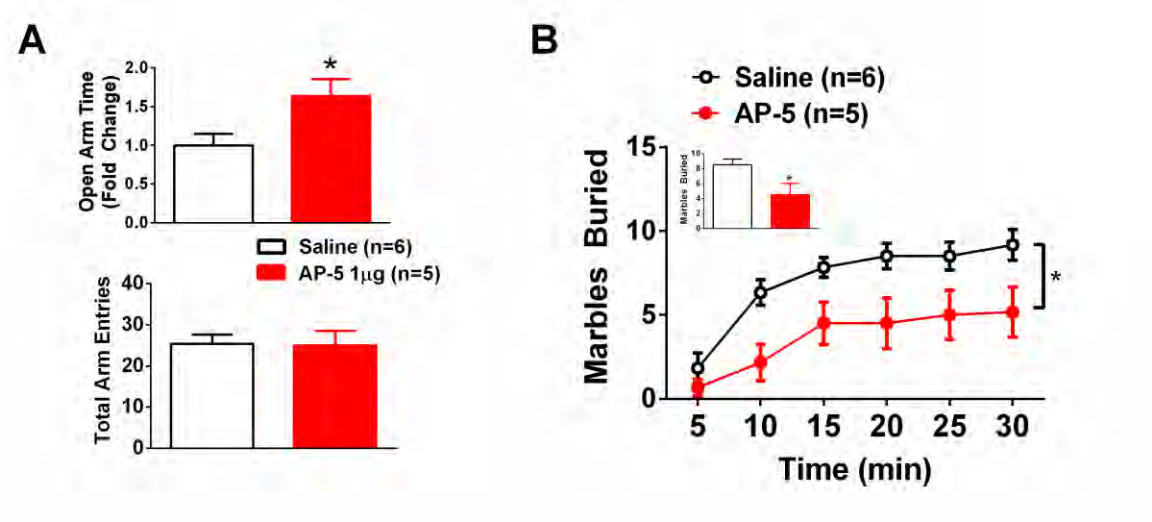

Figure II-2. Blockade of NMDA receptors in the IPN reduces anxiety-like behavior in C57BL/6J mice.

AP-5 (1 μg) or Saline was infused into the IPN prior to testing in the EPM and MBT assays. Infusion of AP-5 in the IPN increased time spent in the open arms of the EPM compared to Saline (A, top) while not affecting total arm entries (A, bottom). In the MBT, AP-5 infusion decreased number of marbles buried at different time points (B) and the end of the assay (B, inset). Data are expressed as average values ± S.E.M. * $p < 0.05$. Student‟s t-test is used to analyze the inset.

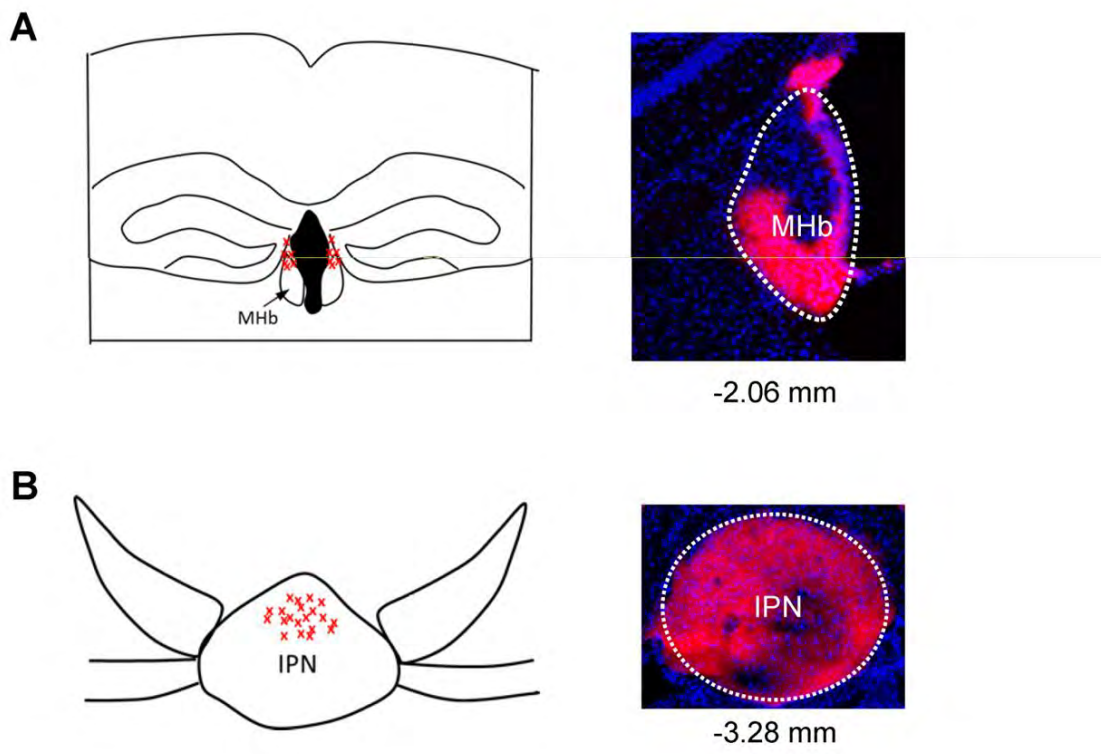

Figure II-3. Verification of cannula placement and drug infusions.

Depiction of a representative coronal section from MHb (A, left) and IPN (B, left). Red "x"s" indicate location of guide cannula tracks as identified by neutral red staining. Note that infusion cannula project 0.25 mm past guide cannulas. A representative image of dye infusion post-behavior experiments for double verification of infusion location is also shown (A, B, right).

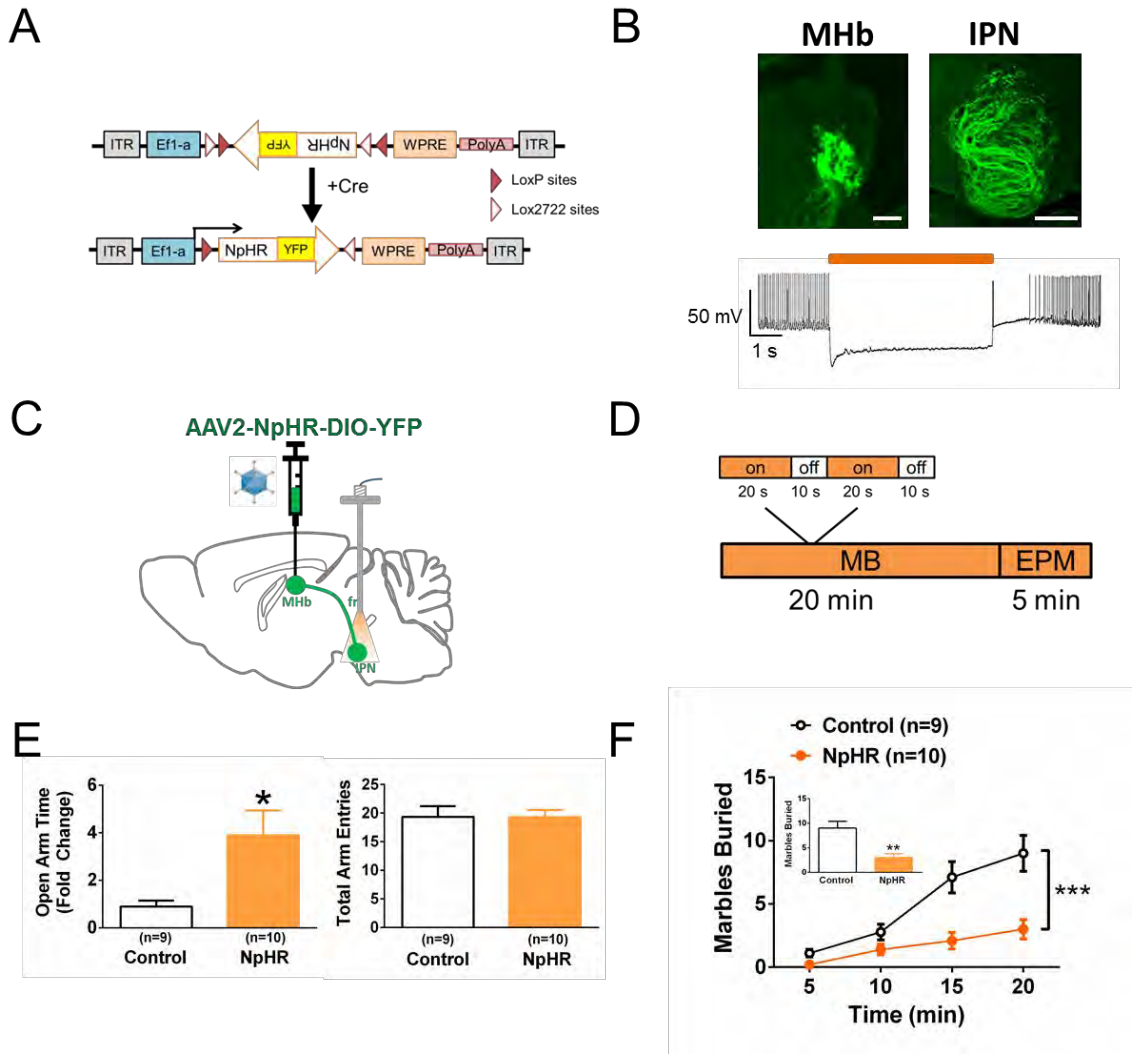

Figure II-4. Silencing of MHb cholinergic neurons decreases anxiety-like behaviors.

A. Schematic diagram of the double-floxed Cre-dependent AAV vector expressing NpHR-YFP cDNA under the control of an Ef-1α promoter. Expression of Cre induces recombination and causes the cDNA insert to flip into the sense orientation.

B. Representative micrographs showing NpHR expression in the MHb and IPN (top). Representative whole-cell current clamp recording from an AAV-NpHR-infected neuron in the MHb exposed to 593 nm yellow light (yellow bar)(bottom).

C and D. Schematic diagram of the experimental strategy and neurotransmission silencing protocol.

E. Average time spent in the open-arm (left), and total-arm entries (right) in the EPM during light stimulation in ChAT-Cre mice infected with control virus or AAV2-NpHR-eYFP. F. The average number of marbles buried in the MBT in control or AAV2-NpHR-eYFP-infected ChAT-Cre mice at baseline prior to light stimulation and during light stimulation is shown. Inset, averaged marbles buried at t=20 min. * $p < 0.05$, **$p < 0.001$, ***$p < 0.001$. Student"s t-test is used to analyze the inset.

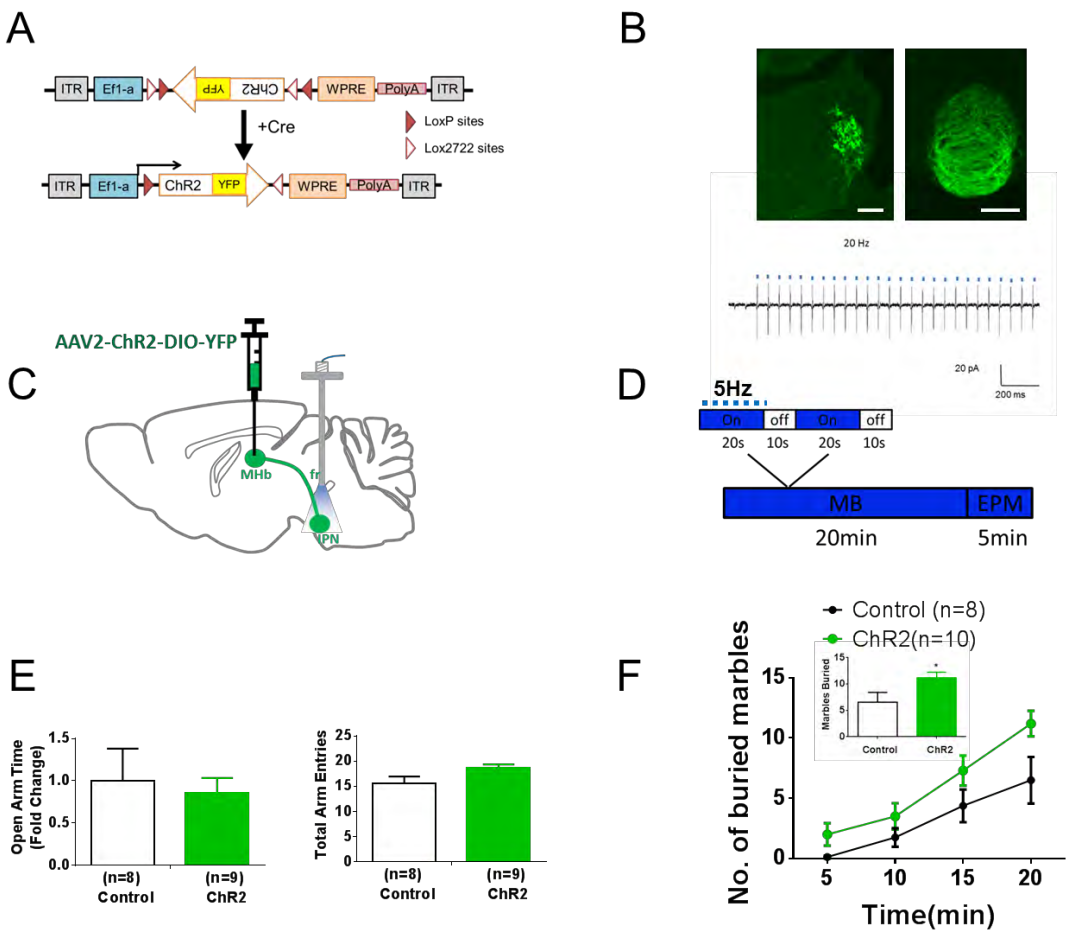

Figure II-5. Activating of MHb cholinergic neurons has tendency to change anxiety-like behaviors.

A. Schematic diagram of the double-floxed Cre-dependent AAV vector expressing ChR2-YFP cDNA under the control of an Ef-1α promoter. Expression of Cre induces recombination and causes the cDNA insert to flip into the sense orientation.

B. Representative micrographs showing ChR2 expression in the MHb and IPN (top). Representative whole-cell current clamp recording from an AAV-ChR2-

infected neuron in the MHb exposed to 473 nm blue light (blue dots, 20 Hz) (bottom).

C and D. Schematic diagram of the experimental strategy and neurotransmission stimulating protocol.

E. Average time spent in the open-arm (left), and total-arm entries (right) in the EPM during light stimulation in ChAT-Cre mice infected with control virus or AAV2-ChR2-eYFP.

F. The average number of marbles buried in the MBT in control or AAV2-ChR2-eYFP-infected ChAT-Cre mice at baseline prior to light stimulation and during light stimulation is shown. Inset, averaged marbles buried at t=20 min. * $p < 0.05$, **$p < 0.001$, ***$p < 0.001$. Student"s t-test is used to analyze the inset.

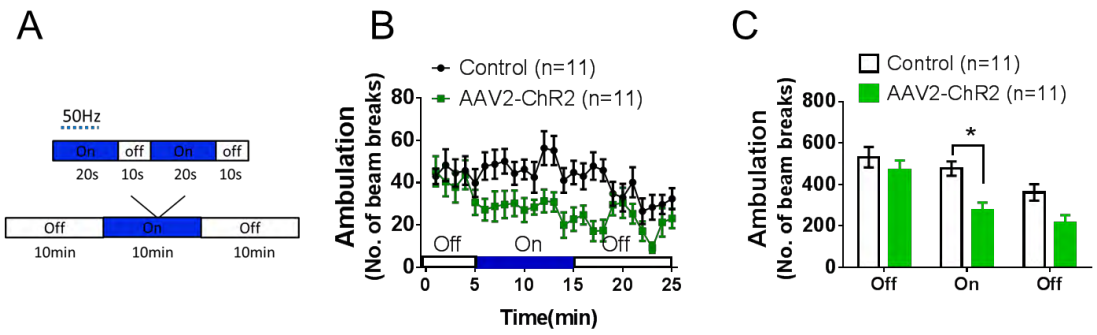

Figure II-6. Activation of MHb cholinergic neurons induced hypolocomotion.

A. Schematic diagram of the experimental stimulating protocol.

B. Average ambulation during light stimulation in ChAT-Cre mice infected with control virus or AAV2-ChR2-eYFP.

C. The average total ambulation in the light-on or light-off period in control or AAV2-ChR2-eYFP-infected ChAT-Cre mice.* $p < 0.05$, **$p < 0.001$, ***$p < 0.001$.

Chapter III

nAChRs in the MHb cholinergic neurons are critical for anxiety

Contributions:

Jennifer Ngolab made the virus construct. Liwang Liu did the electrophysiological recordings. Rubing Zhao-Shea did the qRT-PCR. All other research was done by me. Dr. Andrew Tapper wrote part of the body of the text, while I made the Figures, Materials and Methods and provided feedback on the other sections.

III.A. Introduction

Anxiety disorders are the most common mental illnesses in the United States, affecting 40 million adults in the United States alone, clearly highlighting the need for identification of the underlying neuroanatomical bases and molecular underpinnings of anxiety (Kessler, Chiu et al. 2005). Recently, the habenulo-interpeduncular pathway has been hypothesized to modulate anxiety (Yamaguchi, Danjo et al. 2013). MHb projects to its primary target brain region, IPN, through a conspicuous bundle of axons called the fasciculus retroflexus (fr) , and the IPN in turn projects to the median and dorsal raphe nuclei, as well as other brain regions (Morley 1986). Selective ablation of septal glutamatergic MHb afferents reduces anxiety-like behavior in mice, suggesting a role for the MHb in controlling anxiety (Yamaguchi, Danjo et al. 2013).

nAChRs are ligand-gated ion-channels that are activated by the endogenous neurotransmitter, ACh (Improgo, Scofield et al. 2010). Twelve mammalian genes encoding neuronal nAChR subunits have been identified (α2-α10, β2-β4) and five subunits coassemble to form either homomeric (like α7) or heteromeric (like α4β2) receptors (Dani and Bertrand 2007). Cholinergic signaling through nAChRs has been shown to be involved in anxiety (Picciotto, Brunzell et al. 2002), for instance the mice lacking the α4 subunit showed increased anxiety in the elevated plus-maze assay (Ross, Wong et al. 2000).

It has been shown that nicotinic AChRs are highly expressed in the MHb-IPN tract (Marks, Smith et al. 1998). Cholinergic neurons within the MHb robustly express almost all the nAChR subunits (such as α3, α4, α5, α6, α7, β2, β3 and β4 subunit). Interestingly, cholinergic neurons within the MHb robustly express rare neuronal nAChR subtypes containing the α3 and β4 subunits, as well as the α4 subunit among others (Fonck, Nashmi et al. 2009, Salas, Sturm et al. 2009, Fowler, Lu et al. 2011). However, whether cholinergic signaling via nAChRs specifically in MHb cholinergic neurons modulates anxiety state is unknown. Thus, we focused on testing the hypothesis that activation of MHb cholinergic neurons via nAChR signaling modulates anxiety.

III.B. Materials and methods

Mice

C57BL/6J, α4 L9'A, α4 KO, and ChAT-Cre mice were used in experiments as indicated. ChAT-Cre knock-in mice, were purchased from Jackson Laboratories (stock number: 006410) and bred in the UMMS animal facility. Breeding was conducted by mating heterozygous pairs. For ChAT-Cre mice, genotypes were determined by PCR as previously described (Rossi, Balthasar et al. 2011) and also on Jackson Laboratories website. PCR of mouse tail genomic DNA was performed with three specific primers, WT F (5′-GTT TGC AGA AGC GGT GGG-3′), mutant F (5′-CCT TCT ATC GCC TTC TTG ACG -3′) and Common R (5′-AGA TAG ATA ATG AGA GGC TC -3′). These primers

amplify DNA fragments of 272 bp in wild-type (WT) mice, and 350 bp in ChAT-Cre mutant mice. DNA fragments were separated by agarose gel electrophoresis and visualized with ethidium bromide. L9'A mice and α4 KO mice on a C57BL/6J background have been described previously (Ross, Wong et al. 2000, Tapper, McKinney et al. 2004). Mice were group-housed four mice/cage on a 12-h light-12 h dark lighting cycle with lights on at 7:00 a.m. and off at 7:00 p.m, and given food and water *ad libitum*. Male mice were used for all experiments. Mice were at least 8 weeks old at the start of each experiment. Behavioral experiments were performed during the light phase of the lighting cycle.

Independent groups of animals were used for each behavioral experiment unless otherwise noted. All experiments were conducted in accordance with the guidelines for care and use of laboratory animals provided by the National Research Council, as well as with an approved animal protocol from the Institutional Animal Care and Use Committee of the University of Massachusetts Medical School.

Immunostaining

Mice were injected with saline (i.p.) for three days prior to the start of the experiment to habituate them to handling and to reduce c-Fos activation due to stress. On the experiment day, C57BL/6J, L9'A and α4 KO mice were injected with nicotine (1 mg/kg or 3 mg/kg) or saline (i.p.).

Ninety minutes after the injection, all mice were deeply anesthetized with sodium pentobarbital (200 mg/kg, i.p.) and perfused transcardially with 10 ml of 0.01 M phosphate-buffered saline (PBS) followed by 10 ml of 4 % paraformaldehyde in 0.01 M sodium phosphate buffer (pH 7.4). Brains were removed and post-fixed for 2 h with the same fixative and cryoprotected in sodium phosphate buffer containing 30% sucrose until brains sank. MHB serial coronal sections (20 μm) were cut on a microtome (Leica CM 3050S, Leica Microsystems Inc.) and collected into a 24-well tissue culture plate containing 1 X PBS. After rinsing sections in PBS twice for 5 min, they were treated with 0.4 % Triton X-100 PBS (PBST) twice for 2 min, followed by incubation in 2% BSA/PBS for 30 min. Sections were washed with PBS once and then incubated in a cocktail of primary antibodies for ChAT (Goat, 1:100, Millipore) and c-Fos (rabbit polyclonal, 1:800, Santa Cruz) in 2% BSA/PBS overnight at 4° C. The sections were then washed with PBS three times for 5 min followed by incubation in secondary fluorescent labeled antibodies (donkey anti-rabbit Alexa Fluor® 488 and donkey anti-goat Alexa Fluor® 594, 1:500, Molecular Probes, Inc., Eugene, USA) at room temperature in dark for 30 min. After washing with PBS five times for 5 min/wash, sections were mounted on slides by using VECTASHIELD® Mounting Medium (Vector laboratories, Inc., Burlingame, CA). The number of positive neurons was counted under a fluorescence microscope (Zeiss, Carl Zeiss MicroImaging Inc., NY) at a magnification of 40X. Neurons were counted as signal positive if

intensities were at least two times higher than that of the average value of background (sections staining without primary antibodies).

Engineering of viral plasmids

The yellow fluorescent protein (YFP) -tagged α4 nAChR subunit cDNA construct is commercially available (Addgene plasmid 15245) and has been described previously (Nashmi, Dickinson et al. 2003). Using a Quickchange Site-Directed Mutagenesis Kit (Agilient Technologies), PCR mutagenesis was used to convert the 9' leucine of the M2 pore-forming domain to a serine (changing the codon from CTT to TCT). This mutation has been shown to render nAChRs containing the Leu9'Ser α4 subunit to be hypersensitive to agonists, including ACh (Labarca, Nowak et al. 1995, Labarca, Schwarz et al. 2001). Constructs were verified through sequence analysis (Genewiz). The mutated cDNA inserts were subsequently removed from the pCI-neovector by digestion with EcoRI. pAAV-EF1a-DIO-hChR2(H134R)-EYFP-WPRE-pA was digested using AscI and NheI to excise the hChR2-YFP insert. T4 DNA polymerase (NEB) was used to fill overhangs followed by blunt ligation to subclone the L9'S α4-YFP nAChR subunit cDNA between two pairs of distinct lox sites (loxP and lox2722). Orientation of insert and verification of lox sites was confirmed through sequence analysis.

Surgical procedures for virus microinjection

Packaging of AAV-Ef1A-DIO-L9'S-YFP plasmids into AAV2 viral particles was done by the University of Massachusetts Medical School Viral Vector Core. For

viral particle injection, ChAT-Cre mice were anesthetized with a mixture of ketamine (100 mg/kg) and xylazine (10 mg/kg) (VEDCO). The surgical area was shaved and disinfected. Mice were placed in a stereotaxic frame (Stoelting Co.) with mouse adaptor and a small incision was cut in the scalp to expose the skull. Using bregma and lambda as landmarks, the skull was leveled in the coronal and sagittal planes. The AAV2-Ef1A-DIO-L9'S-YFP viral particles ($1x10^{12}$ viral particles/µl) were injected into the ChAT-Cre mice MHb according to the coordinates: AP, -1.94, ML, 0.2, DV, -2.25. The viral particles (1.5 µl/side) were injected bilaterally at a flow rate of 0.3 µl/min. The injection needle was kept in place for 5 min post-injection. The incision was sutured and mice were returned to their home cages.

Electrophysiology

For the electrophysiological recording in this experiment, ChAT-Cre mice were infected with the virus when the mice were 3 weeks old. Four weeks later, brains were quickly removed and placed in oxygenated ice-cold high sucrose artificial cerebrospinal fluid (SACSF) containing kynurenic acid (1 mM, Sigma, St. Louis, MO). SACSF solution contained (in mM): 250 sucrose, 2.5 KCl, 1.2 $NaH_2PO_4•H_2O$, 1.2 $MgCl_2•6H_2O$, 2.4 $CaCl_2•2H_2O$, 26 $NaHCO_3$, 11 D-Glucose. Coronal brain slices containing lPN (~180 µm) were made using a Leica VT1200 vibratome. Spontaneous EPSCs were obtained in the whole-cell configuration and gapfree acquisition mode in Clampex (Axon Instruments). For whole-cell

responses to ACh, neurons were held at -70 mV and ACh (0.3 mM) was applied via bath perfusion for 10 min. Whole cell responses to ACh were measured in the presence of atropine (1 μM) to block muscarinic receptors, bicuculline (20 μM) to block $GABA_A$ receptors, CNQX (10 μM) to block AMPA receptors, and AP5 (50 μM) to block NMDA receptors. All recordings were filtered at 1 kHz using the amplifier's four-pole, low-pass Bessel filter, digitized at 10 kHz with an Axon Digidata 1440A interface and stored on a personal computer. ACSF was used for bath solution and contained (in mM): 125 NaCl, 2.5 KCl, 1.2 $NaH_2PO_4•H_2O$, 1.2 $MgCl_2•6H_2O$, 2.4 $CaCl_2•2H_2O$, 26 $NaHCO_3$, 11 D-Glucose.

Marble burying test (MBT)

Four weeks after the virus infection, the mice were subjected to the MBT. As described in our previous paper (Zhao-Shea, Liu et al. 2013), mice were habituated in the standard mouse cage with ~5 - 6 cm of bedding for 2 days (45 min/day) before the test. On the test day, 15 clean 1.5 cm glass marbles were evenly spaced in five rows of three, each 4 cm apart on the bedding. A mouse was placed in its test cage and left for 30 minutes, and the number of marbles buried (to 2/3 their depth) with bedding was counted every 5 min or after 30 min (as noted in the figures), then mice were removed from their test cages.

For the mecamylamine injection experiment, mice were injected with mecamylamine (0.3 mg/kg, i.p.). Thirty minutes later, mice were assessed in the MBT.

Elevated plus maze (EPM)

Four weeks after the virus infection, the mice were studied using for the EPM test. As described in our previous paper (Zhao-Shea, Liu et al. 2013), the experimental apparatus consisted of a central axis and four arms elevated 45 cm above the floor, with each arm positioned at 90° relative to the adjacent arms. One red light arranged at 100 cm above the maze was used as the source of illumination. The mice were individually placed in the center of the maze with their heads facing one of the open arms and allowed 5 min of free exploration. The number of entries into the open and closed arms, and the total time spent in the open and closed arms were measured by MED-PC IV software (MED Associates, Inc.). The time spent in open and closed arms was calculated as standard anxiety indices. The total number of arm entries was considered as an index of locomotor activity. The apparatus was cleaned thoroughly between trials. Mice that froze in the initial placed arm without moving were not included in the analysis.

For the mecamylamine injection experiment, mice were injected with mecamylamine (0.3 mg/kg, i.p.). Thirty minutes later, mice were subjected to the EPM.

Guide cannula placement

As described in our previous paper (Zhao-Shea, Liu et al. 2013), the guide cannulas were surgically implanted at least 3 days prior to the experiment. Mice

were anesthetized with a mixture of ketamine (100 mg/kg) and xylazine (10 mg/kg) (VEDCO) and placed in a stereotaxic frame (Stoelting Co.). The surgical area was shaved and disinfected and the skull bone was exposed. Using bregma and lambda as landmarks, the skull was leveled in the coronal and sagittal planes. A hole was drilled and stainless steel guide cannulas were inserted into the brain and secured to the skull with instant adhesive. The coordinates relative to the bregma were: MHb (AP, -1.94, ML, 0.2, DV, -2.25). The scalp incision was stitched and dental cement was used to stabilize the cannula on the skull. After surgery, the mice were kept on a heating pad to prevent hypothermia. Mice were allowed to recover in individual cages for at least 3 days prior to drug infusion and behavioral testing.

Intra-MHb infusions

Mice were anesthetized with 2% isoflurane via a nose cone adaptor at a flow rate of 800 ml/L. Once anesthetized, an infusion cannula designed to reach −0.25 mm below the guide cannula was inserted into the guide cannula. Vehicle or mecamylamine (0.5 or 2 μg/μl, 1μl) was infused at a rate of 1 μl/min. After infusion, the infusion cannula was left in place for 2 minutes prior to retraction. Mice were placed back into their home cages and the behavior tests were conducted 30 min after the drug infusion. After completion of behavioral experiments, mice were culled, brains isolated, and cannula placement verified. To verify the guide cannula placement, the brains were cut in 30 μm sections and

the location of the guide cannula was determined by neutral red staining using light microscopy. In addition, the injection sites were double verified histologically by microinjection of DiI cell labeling solution (Invitrogen). Only mice with cannulas in the right placement were included in the statistical analysis.

Locomotor activity

Locomotor activity was recorded using an automated system (San Diego Instruments, La Jolla, CA, USA) with photobeams, which recorded ambulation (consecutive beam breaks). A translucent cage was placed between photobeams. Individual mice were moved from their home cage to this cage, and ambulatory activity was defined as the successive interruption of two of the four beams crossing the cage. All data were presented as total ambulations.

For the baseline locomotor activity experiment, four weeks after the virus infection, mice were placed individually in a novel cage and recorded for 60 min for their baseline locomotor activity.

For the locomotor activity after the nicotine injection, an independent group of mice were recorded for the locomotor activity in a novel cage right after nicotine i.p. injection (1.5 mg/kg) for 90 min.

Data analysis

Data were analyzed using One- or Two-way ANOVA followed by Bonferroni post hoc tests or t-tests as indicated. Results were considered significant at $p < 0.05$. All data are expressed as means ± SEM.

III.C. Results

nAChRs are highly expressed in MHb cholinergic neurons

Cholinergic neurons of the MHb exhibit strong expression of genes encoding distinct nAChR subunits (Sheffield, Quick et al. 2000, Grady, Moretti et al. 2009) suggesting that they could serve as a point of regulation for anxiety-like behavior.

To determine the precise repertoire of nAChR subunits specifically expressed in MHb cholinergic neurons, cholinergic neurons were laser-microdissected and neuronal nAChR subunit gene expression (α2-α7 and β2-β4 nAChR subunit genes) was measured using quantitative RT-PCR (Table III-1). All nAChR subunit genes except α2 were detected in cholinergic MHb neurons. Expression of the nAChR α3 and α4 subunit genes was relatively strong compared to the house-keeping gene GAPDH; whereas, expression of the α5, α6, and α7 genes was less robust. In addition, expression of the nAChR β2 β3 and β4 subunit genes was high relative to GAPDH.

α4* nAChRs are necessary and sufficient for nicotine activation of MHb cholinergic neurons

As α4 nAChR subunit gene expression was highly expressed in the MHb, we verified α4 subunit functional expression by measuring nicotine activation of MHb cholinergic neurons in two complementary mouse lines using the immediate early gene c-Fos as a molecular marker of neuronal activation (Cole, Saffen et al. 1989). For this analysis we used the α4 knockout (α4 KO) mouse line which does not express chrna4 and the L9'A mouse line, a knock-in mouse line that expresses a single point mutation in chrna4 that renders nAChRs hypersensitive to agonist (Ross, Wong et al. 2000, Tapper, McKinney et al. 2004). When challenged with 1 mg/kg nicotine, one-way ANOVA indicated a significant main effect of genotype on the number of c-Fos immunopositive MHb neurons ($F_{4, 10}$ = 73.6, $p < 0.001$). Post-hoc analysis indicated L9'A animals exhibited prominent c-Fos expression in MHb (Fig.III-1 A, B) compared to WT or α4 KO mice after 1 mg/kg nicotine challenge. Conversely, when challenged with 3 mg/kg nicotine, WT mice exhibited significant c-Fos expression in MHb; whereas c-Fos expression was dramatically reduced in MHb of α4 KO mice.

Together, these data indicate that functional nAChRs containing the α4 subunit are critical for nicotine activation of MHb cholinergic neurons.

“AChR detectors” are functionally expressed in MHb cholinergic neurons

To test the hypothesis that activation of nAChRs specifically in MHb cholinergic neurons inherently regulates anxiety-like behavior, we selectively expressed novel mutant α4 nAChR subunits that render nAChRs hypersensitive to ACh

("Ach detectors") in MHb cholinergic neurons of adult mice. This was done by engineering a viral plasmid for expression of mutated α4 nAChR subunits selectively in Cre-expressing neuronal populations. This plasmid includes the α4 nAChR subunit cDNA containing an agonist-hypersensitive L9'S mutation in the M2 transmembrane sequence in addition to a yellow fluorescent protein (YFP) tag, engineered in the M3-M4 intracellular loop, where it does not interfere with expression or function of nAChRs (Labarca, Nowak et al. 1995, Labarca, Schwarz et al. 2001, Nashmi, Dickinson et al. 2003). Specifically, the L9'S-YFP cDNA was sub-cloned into the double-inverted open (DIO) reading frame of the pAAV-EF1a-DIO viral plasmid in the antisense orientation (i.e., the same expression plasmid used for the halorhodopsin experiments described in Chapter II). Thus, the cDNA insert is flanked by two pairs of distinct Lox sites that regulate L9'S-YFP α4 subunit cDNA expression by rearranging the cDNA into the sense orientation wherever Cre recombinase is expressed (Fig. III-2A) (Tsai, Zhang et al. 2009). To selectively infect cholinergic MHb neurons, L9'S-YFP AAV2 viral particles were intracranially injected into the MHb of ChAT-Cre mice. As a control, AAV2-eGFP particles (not Cre dependent) were similarly injected into the MHb of ChAT-Cre mice. Mice were allowed to recover 4-6 weeks post-infection to maximize plasmid expression. To verify expression, brains from infected animals were sliced and immunolabeled for ChAT and YFP (Fig. III-2B). YFP-expression was primarily restricted to the ventral MHb (i.e., where cholinergic neurons are clustered) and in ChAT-immunopositive neurons from L9'S-YFP-infected animals.

To confirm functional expression, acute coronal sections containing the MHb were isolated and whole-cell currents in response to ACh were measured from YFP- or GFP (control)-positive neurons using patch-clamp electrophysiology. Bath application of 300 μM ACh elicited inward currents in both control and L9'S-YFP-infected neurons (Fig. III-2C). However, currents in L9'S-YFP-infected neurons were significantly larger compared to controls, indicating increased functional expression of nAChRs in these animals (Fig. III-2C, $p < 0.01$, Mann-Whitney test). Together, these data indicate that L9'S nAChR subunits were properly expressed in MHb cholinergic neurons and formed "gain-of-function" nAChR ACh detectors to boost nAChR signaling in MHb cholinergic neurons.

"ACh detector" expressing mice showed increased anxiety-like behavior

To test the hypothesis that increased nAChR signaling in MHb cholinergic neurons modulates anxiety, we evaluated anxiety-like behavior in the EPM and MBT assays. In the EPM, mice infected with the L9'S-YFP virus spent significantly less time in the open arms compared to control-infected mice ($t_{19.4} = 2.24$, $p < 0.05$, Fig. III-2E, left). Total arm entries between groups did not differ (Fig. III-2E, right). In the MBT, L9'S-YFP-infected animals buried significantly more marbles at each time point in the assay, but most importantly, there was an overall increase in the number of marbles buried at the end of the assay (Fig. III-2F, inset, T-Test, $p< 0.001$). To determine if increased burying in L9'S-expressing mice compared to control mice was a non-specific phenotype elicited by

increased locomotor activity, we measured ambulation during one hour in both groups (Fig. III-2D). Two-way ANOVA indicated that locomotor activity did not significantly differ between groups.

To test the hypothesis that increased anxiety-like behavior in L9'S-infected mice was due to ACh-mediated activation of the agonist-hypersensitive nAChRs in cholinergic MHb neurons, control and L9'S-infected mice were challenged with either saline or a low dose of the nAChR antagonist mecamylamine (0.3 mg/kg, i.p.) prior to testing in the EPM and MBT assays (Fig. III-3). In the EPM, two-way ANOVA indicated an overall main effect of virus ($F_{1, 33}$ =9.64, $p < 0.01$) and drug injection ($F_{1, 33}$ = 7.83, $p < 0.01$) and significant virus × drug interaction ($F_{1,33}$ = 5.41, $p<0.05$). Post-hoc analysis revealed that mice expressing L9'S nAChRs in MHb cholinergic neurons spent significantly less time in the open arms of the EPM after saline treatment compared to control mice receiving saline (Fig. III-3A, $p<0.01$). Mecamylamine injection to L9'S expressing animals significantly increased time spent in the open arm compared to a saline injection (Fig. III-3A, $p<0.01$); whereas the low dose of antagonist did not significantly alter time spent in the open arms in control mice. Two-way ANOVA indicated that neither virus infection nor drug injection significantly altered total arm entries in the EPM (Fig. III-3B). In the MBT assay, mecamylamine did not significantly alter the number of marbles buried in control animals compared to a saline injection (Fig. III-3C). Mecamylamine significantly reduced the number of marbles buried in mice expressing L9'S nAChRs in MHb cholinergic neurons compared to a saline

injection at each time point and such that, at the end of the assay, the cumulative number of marbles buried was significantly reduced ($p < 0.001$, Fig. III-3D, inset). To verify that systemic antagonist injections were actually acting at mutant nAChRs in the MHb, we implanted cannulas targeting the MHb and infused vehicle or mecamylamine (0.5 μg, Fig. III-4) in the MHb of L9'S-expressing and control ChAT-Cre mice prior to testing in the EPM and MBT assays. In the EPM, two-way ANOVA indicated a significant effect of virus ($F_{1, 28} = 8.74$, $p < 0.01$) and drug infusion ($F_{1, 28} = 4.52$, $p < 0.05$), and a virus × infusion interaction ($F_{1, 28} = 6.23$, $p < 0.05$). Post-hoc analysis revealed that in control-virus expressing mice, 0.5 μg mecamylamine had little effect compared to vehicle infusion; whereas the antagonist significantly increased time spent in the open arms compared to a vehicle infusion in L9'S-expressing ChAT-Cre mice (Fig. III-4A). Infusion of mecamylamine did not alter total arm entries (Fig. III-4B). Similarly, infusion of 0.5 μg mecamylamine did not alter marble burying in control mice compared to vehicle infusion (Fig. III-4C) but significantly reduced the number of marbles buried in the MBT of L9'S-expressing ChAT-Cre mice compared to vehicle ($p < 0.0001$, Fig. III-4C). Proper placement of cannulas and drug infusions were verified after behavioral experiments as described in Methods (Fig. III-5). Together, these data indicate that L9'S expression in MHb cholinergic neurons increased anxiety-like behavior through increased endogenous activation of L9'S α4* nAChRs.

“ACh detector” expressing mice showed prolonged hypolocomotion by high dose of nicotine

In addition, we also tested the reaction of L9'S-expressing ChAT-Cre mice to high dose nicotine. When challenged with a high dose of nicotine (1.5 mg/kg), control virus expressing mice showed hypolocomotion for 30 min, and gradually recovered to the baseline at 60 min (Fig. III-6A). In contrast, the L9'S-expressing ChAT-Cre mice showed a prolonged hypolocomotion for 60min, but after the recovery, the peak of the locomotor activity is lower than the control mice (Fig. III-6A). The quantification of the total ambulation over the first 90 min showed that there is a significant difference between the two groups (Fig. III-6B).

IV.D. Discussion

Cholinergic signaling through nAChRs has been implicated in a variety of physiological and pathophysiological processes including attention, striatal dopamine release, and nicotine dependence (Guillem, Bloem et al. 2011, Threlfell, Lalic et al. 2012, Picciotto and Kenny 2013). However, behavioral responses mediated by cholinergic signaling have been difficult to properly assess likely due to a predominant neuromodulatory role of ACh.

Here we first test the necessity and sufficiency of the α4 subunit for the MHb cholinergic neuron activation. We showed that the α4 KO mice lacked c-Fos expression when challenged with high dose of nicotine, while L9'A mice showed significantly more c-Fos expression compared to the wild type mice when

challenged with low dose of nicotine (1 mg/kg). These results suggest that α4 nAChRs are necessary and sufficient for nicotine induced neuronal activation in the MHb cholinergic neurons, which is consistent with a previous study (Fonck, Nashmi et al. 2009).

In addition, it has been shown that systemic (i.p.) nicotine (0.5 mg/kg) has anxiogenic effect in mice mainly via β2* nAChRs in the brain (Zarrindast, Homayoun et al. 2000, Anderson and Brunzell 2015), but we did not find c-fos expression in MHb after 1 mg/kg nicotine injection. It has been shown that GABA receptors are highly expressed in MHb, suggesting that there is a strong inhibitory projection to MHb. In addition, the diversity of distinct nAChR subtypes found in MHb is huge compared to other brain areas, since most nAChR subunits are expressed in MHb (Dineley-Miller and Patrick, 1992; Marks et al., 1992). It is possible that the activation of MHb neurons by nicotine is more difficult compared to other brain regions, due to the strong GABA inhibition and the high expression of the relatively low affinity nAChR subtypes.

On the other hand, c-fos, has been extensively used as a marker for the neuronal activation since 1987 (Hunt, Pini et al. 1987), but it does not necessarily mean there is no neuronal activation without c-fos expression. Therefore, it is also possible that 1 mg/kg nicotine injection activated the MHb neurons but it is not enough to induce the c-Fos expression.

Then, to test the behavioral function of endogenous role of nAChRs in the MHb-IPN circuitry, we have designed a system to express Leu9′Ser α4 nAChR subunits that render nAChRs hypersensitive to ACh in discreet neuron population using viral mediated gene delivery combined with the Cre-Lox system. These ACh detectors should facilitate identification of the behavioral role of ACh through nAChR signaling in individual circuits. For the current work, we focused on the MHb-IPN axis which robustly expresses a wide variety of nAChR subtypes (Grady, Moretti et al. 2009). Our data indicate that expression of α4 nAChR subunit ACh detectors selectively in MHb cholinergic neurons increased anxiety-like behavior. Anxiety was alleviated by blocking the hypersensitive nAChRs with a low dose of antagonist or locally within the MHb, indicating that heightened anxiety was mediated through activation of ACh detector nAChRs and not due to additional factors such as nAChR desensitization or excitotoxicity. Thus, our data directly implicate nAChRs on cholinergic MHb neurons specifically in regulating anxiety. Our data also suggest that cholinergic signaling via nAChRs expressed in MHb cholinergic neurons is an endogenous mechanism governing the regulation of anxiety-like behaviors.

In addition, we also found that the expression of α4 nAChR subunit ACh detectors selectively in MHb cholinergic neurons caused prolonged hypolocomotion in the mice. In Chapter II, we have shown that high frequency stimulation of MHb cholinergic neurons - presumably induced ACh release in the IPN - induced hypolocomotion. These two lines of evidence together suggest that

the high dose of nicotine may induce ACh release in the IPN, and the hypersensitive L9'S ACh detector is more sensitive to high dose of nicotine, thus the mice showed prolonged hypolocomotion. Previous studies have shown that the α3 and β4 nAChRs are necessary for nicotine-induced hypolocomotion using the α3KO mice and β4KO mice (Salas, Cook et al. 2004). As α3 and β4 are highly expressed in the MHb-IPN tract, together with our data, it suggests that the nAChRs in the MHb-IPN tract are critical for nicotine induce hypolocomotion.

Table III-1. Relative Gene Expression of nAChR subunit genes in MHb cholinergic neurons.

α2	α3	α4	α5	α6	α7	β2	β3	β4
N.D.	-2.41 ±0.36	-5.04 ±0.42	-9.72 ±0.57	-11.59 ±0.51	-9.63 ±0.55	-5.11 ±0.20	-4.99 ±0.53	-4.30 ±0.31

Values represent the change in the threshold cycle ($^{-\Delta Ct}$) compared with GAPDH. n = 4. N.D., Not detected.

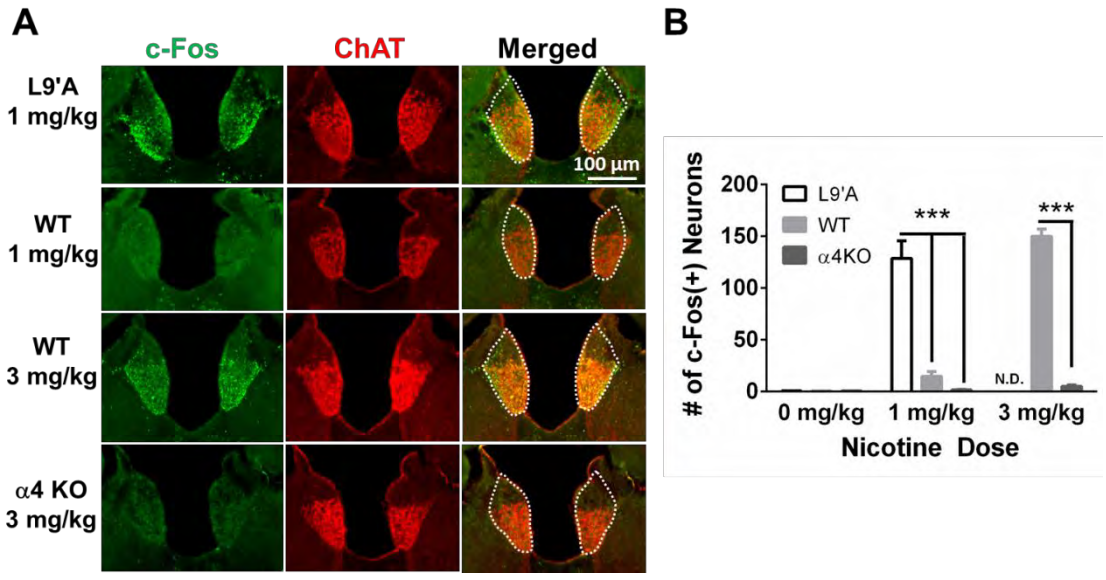

Figure III-1. α4* nAChRs are necessary and sufficient for nicotine activation of MHb cholinergic neurons.

A. Representative images of coronal sections from the MHb of C57BL/6J wild type mice, α4 knockout mice or Leu9'Ala mutant mice injected with saline or nicotine. Immunolabeling was performed to detect c-Fos expression (green, left columns) and ChAT expression (red, middle columns). Merged images are represented in the right column. The MHb is highlighted by the white-dotted line.

B. Quantification of the number of c-Fos immunopositive neurons within the MHb after each drug treatment (10–15 slices analyzed per mouse, n = 3 mice/treatment). *** p <0.001. One-way ANOVA with Tukey Post-hoc analysis.

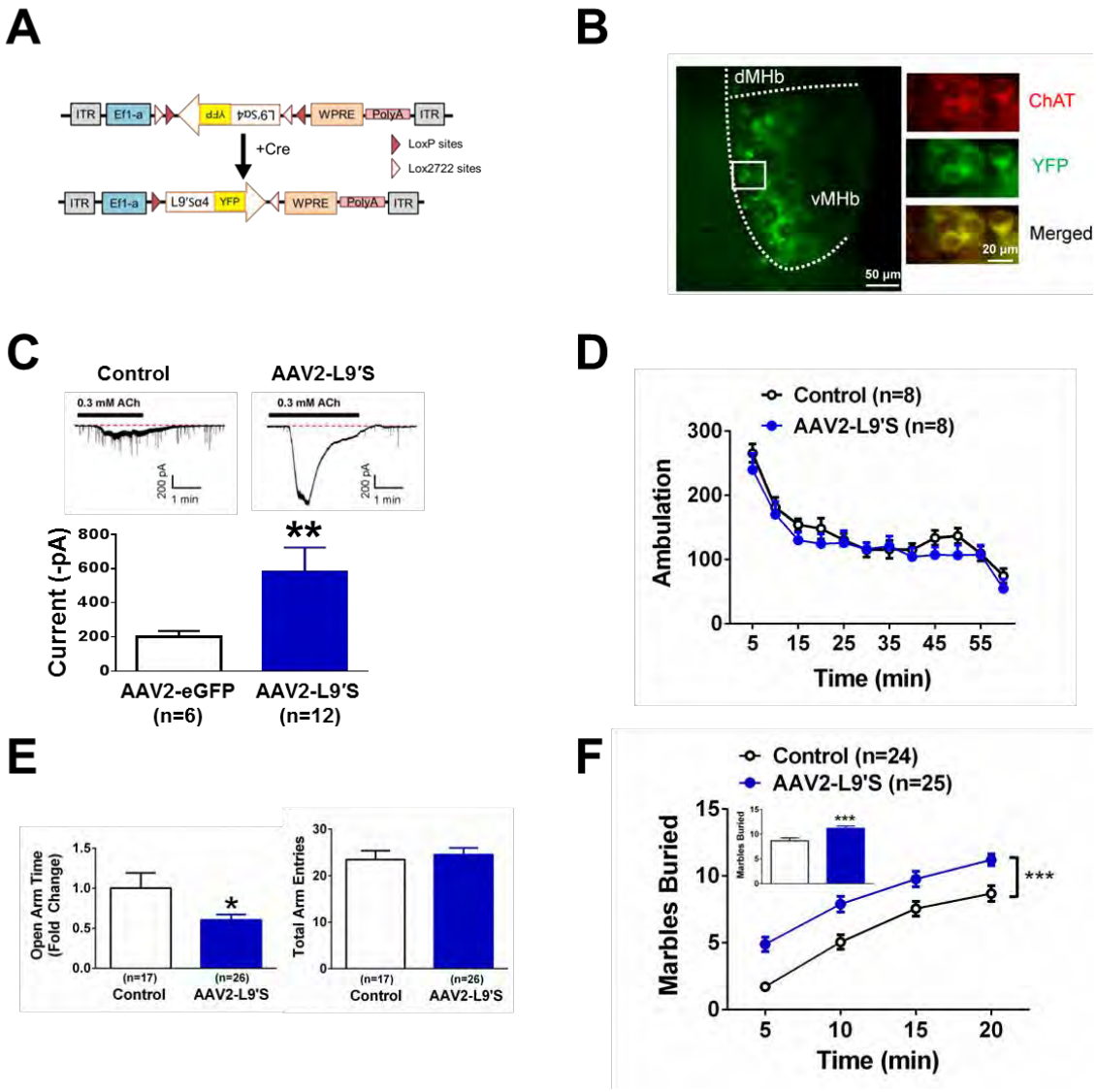

Figure III-2. Selective expression of agonist-hypersensitive α4* nAChRs in MHb cholinergic neurons.

A. Schematic diagram of the double-floxed Cre-dependent AAV vector expressing L9„S α4-YFP nAChR subunit cDNA under the control of the Ef-1α promoter.

B. Left, Representative images of coronal sections illustrating the expression of L9„S-YFP (green signal) in the MHb (20x). Right, 60x photomicrograph from the section indicated in the square outline of the 20x image. Cholinergic signal (red, top panel), YFP signal (green, middle panel) and merged signals (yellow, bottom panel) are shown.

C. Representative whole-cell voltage-clamp recording from eGFP-positive (left, control) or L9'S-YFP-positive neurons (right) in response to 0.3 mM ACh in acute MHb slices from ChAT-Cre mice. Average currents recorded from eGFP- and L9'S-YFP-positive neurons are shown below. ** $p < 0.01$, Student"s t-test.

D. Locomotor activity (ambulation) did not differ between Control-infected and AAV2 L9'S-infected ChAT-Cre mice. Each data point represents summed 5 min total ambulation.

E. Time spent in the open arms of the EPM in Control- and AAV2 L9'S-infected ChAT-Cre mice (left). Total EPM arm entries of each group (right). *$p < 0.05$, Student"s t-test.

F. Cumulative number of buried marbles at different time points in the MBT from Control-infected and AAV2 L9'S-infected ChAT-Cre mice. Inset, averaged marbles buried at t=20 min. Data are expressed as average values ± S.E.M. *$p < 0.05$, ** $p < 0.01$, *** $p < 0.001$. Student"s t-test is used to analyze the inset.

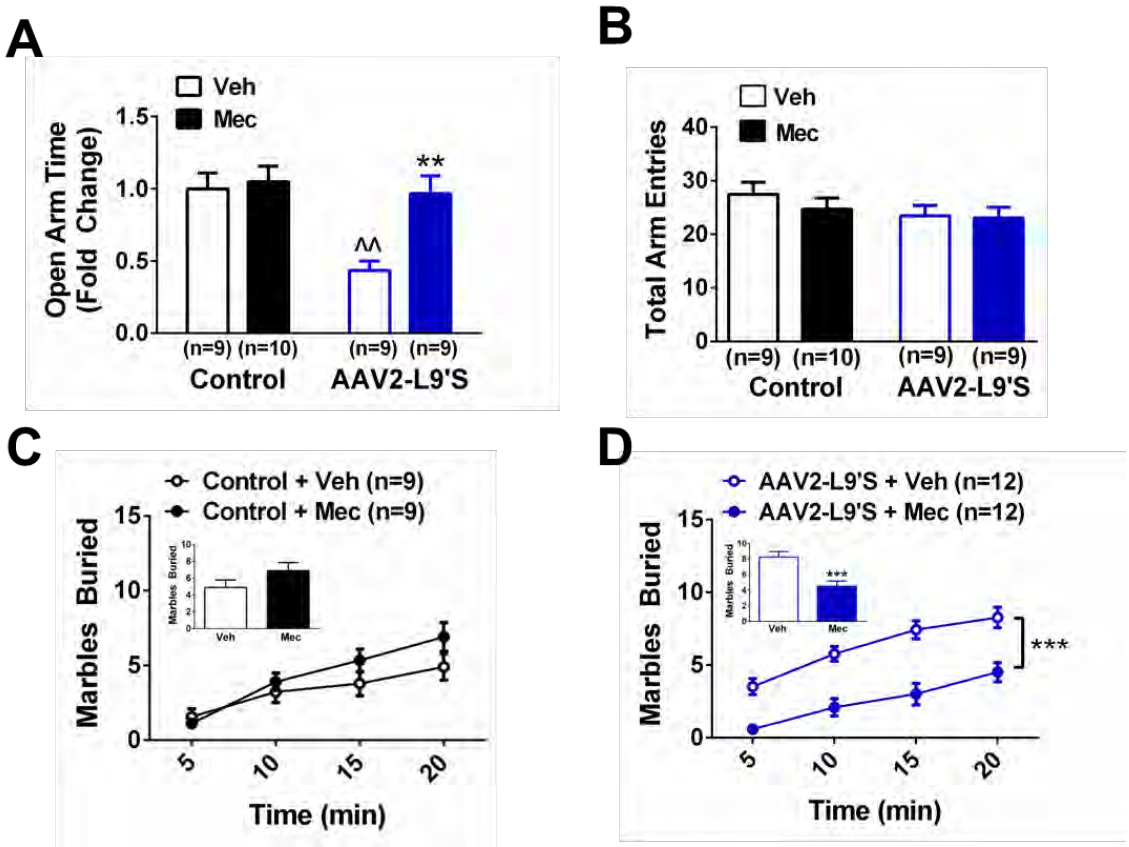

Figure III-3. Increased anxiety-like behavior is mediated by increased nAChR activity in mice expressing Leu9'Ser α4-YFP nAChRs in MHb cholinergic neurons.

A. Time spent in the open arms of the EPM in Control- and AAV2 L9'S-infected ChAT-Cre mice after challenge with Vehicle (Veh) or low dose mecamylamine (Mec, 0.3 mg/kg, i.p.).

B. Total EPM arm entries of each group from panel A.

C. Cumulative number of buried marbles at different time points in the MBT from control-infected ChAT-Cre mice challenged with Veh or Mec. Inset, averaged marbles buried at t=20 min.

D. Cumulative number of buried marbles at different time points in the MBT from AAV2-L9'S-infected ChAT-Cre mice challenged with Veh or Mec. Inset, averaged marbles buried at t=20 min. Data are expressed as average values ± S.E.M. ^^p<0.01 compared to control group with Veh. ** p < 0.01, *** p < 0.001 compared to within group vehicle.

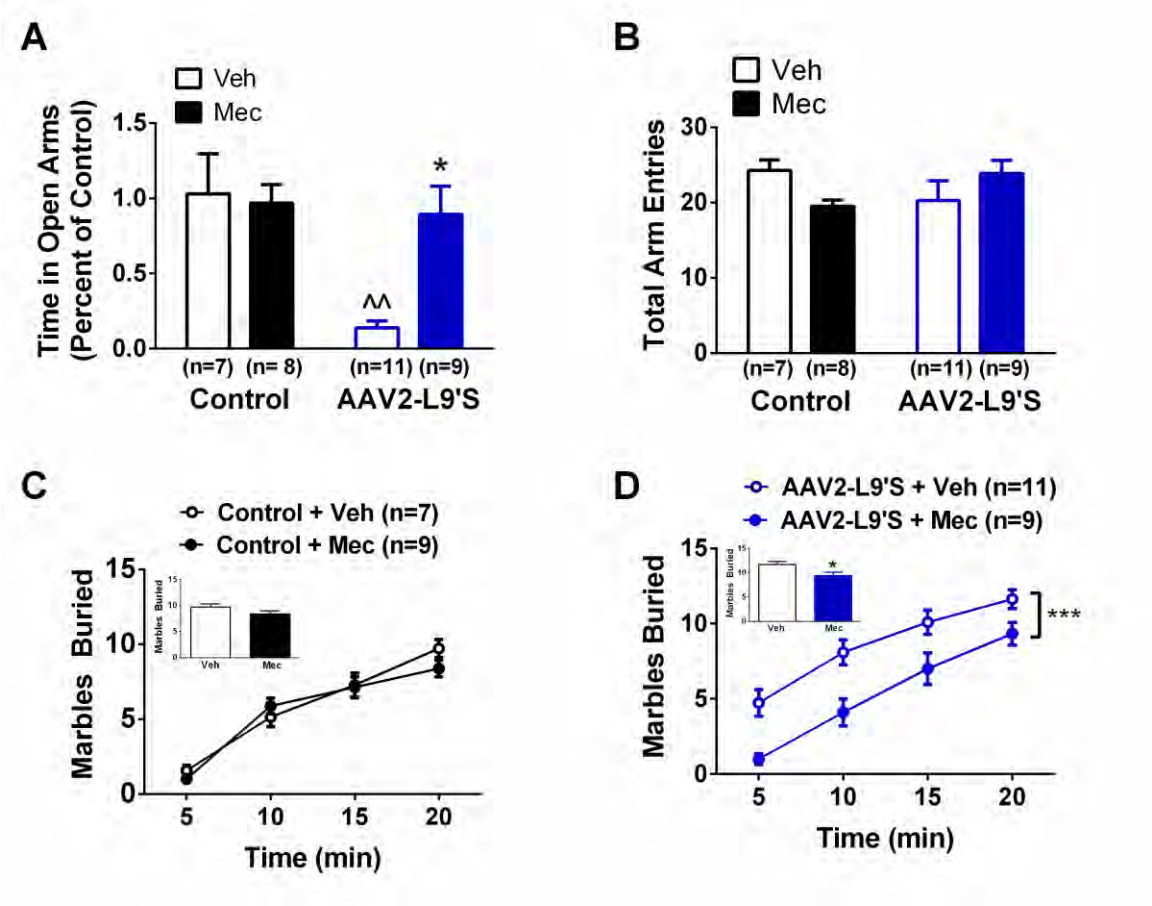

Figure III-4. Infusion of mecamylamine in the MHb of L9'S α4-YFP nAChR-expressing ChAT-Cre mice alleviates increased anxiety-like behavior.

A. Time spent in the open arms of the EPM in Control- and AAV2 L9'S-infected ChAT-Cre mice after infusion of vehicle (Veh) or low dose mecamylamine (Mec, 0.5 μg).

B. Total EPM arm entries of each group from panel A.

C. Cumulative number of buried marbles at different time points in the MBT from control-infected ChAT-Cre mice infused with Veh or Mec.

D. Cumulative number of buried marbles at different time points in the MBT from AAV2-L9'S-infected ChAT-Cre mice infused with Veh or Mec. Data are expressed as average values ± S.E.M. ^^p<0.01 compared to between group control. * p < 0.05, *** p < 0.001 compared to within group vehicle.

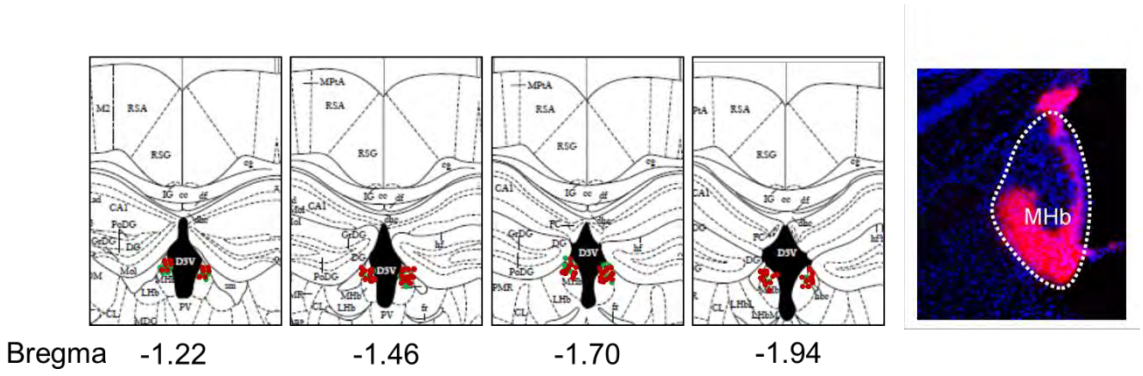

Figure III-5. Verification of cannula placement and drug infusions.

Depiction of representative coronal sections from MHb at coordinates relative to bregma in mm as indicated. Green circles indicate guide cannula placements from L9„S mice infused with mecamylamine in Chapter III. Red circles indicate cannula placements from control- or nicotine-treated mice infused with different nAChR antagonists in Chapter IV. Note that infusion cannulas project 0.25 mm past guide cannulas. Right image shows representative dye infusions post-behavior experiments to double verify infusion location.

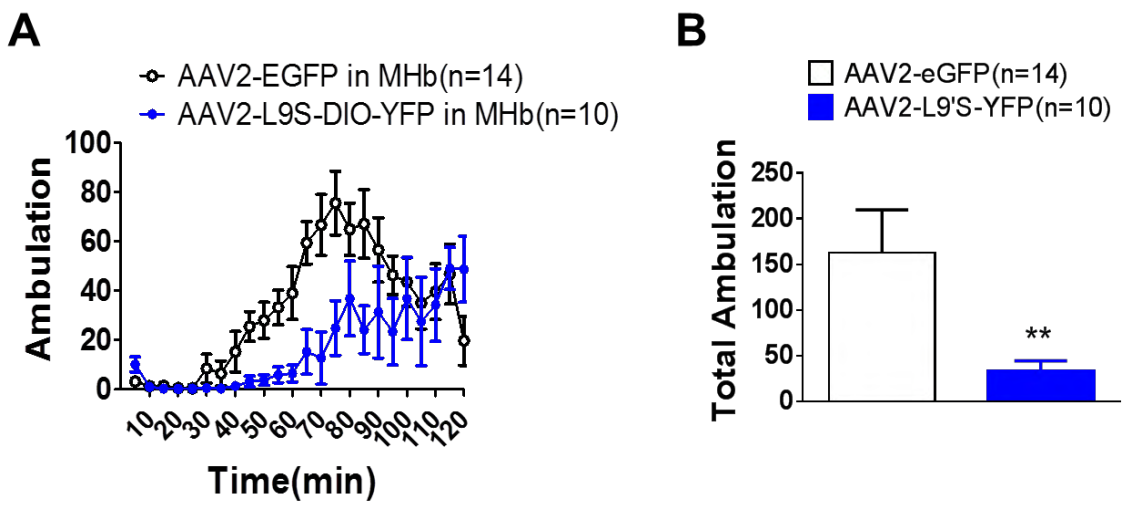

Figure III-6. Activation of MHb cholinergic neurons by nicotine modulates hypolocomotion

A. Average number of ambulation in the novel cage locomotion test following the nicotine (1.5 mg/kg, i. p.) injection in the mice with AAV2-eGFP or AAV2-L9'S infection.

B. Average total number of ambulation of first 90 min in the mice treated as A. t-test was used for statistics. * $p < 0.05$, ** $p < 0.01$, *** $p < 0.001$

CHAPTER IV

nAChRs upregulation on MHb cholinergic neurons are critical for nicotine withdrawal symptoms

Contributions:

Jennifer Ngolab made the virus construct. Liwang Liu did the electrophysiological recordings. Rubing Zhao-Shea did the qRT-PCR. All other research was done by me. Dr. Andrew Tapper wrote part of the body of the text, while I made the Figures, Materials and Methods and provided feedback on the other sections.

IV.A. Introduction

Despite considerable educational and legislative efforts, tobacco use kills approximately 6 million people annually, which makes nicotine addiction the primary cause of preventable mortality in the world (Picciotto and Kenny 2013). Smokers attempting to quit oftentimes relapse, because during the tobacco cessation, the dependent individuals will show the unpleasant withdrawal symptoms (Benowitz 2008), which include somatic (physical), and affective withdrawal symptoms (Kenny and Markou 2001). Rodent somatic symptoms include increased scratching, head nods and body shakes (Damaj, Kao et al. 2003, Grabus, Martin et al. 2005); whereas affective symptoms include anxiety and aversion (Jackson, Martin et al. 2008).

Nicotine, the addictive component of tobacco smoke, mediates its pharmacological effect by binding to, activating, and/or desensitizing neuronal nicotinic acetylcholine receptors (nAChRs) (Improgo, Scofield et al. 2010). The nAChRs are cation selective ligand-gated ion-channels that can be activated by the endogenous neurotransmitter, acetylcholine (ACh) (Improgo, Schlichting et al. 2010). Twelve mammalian genes encoding nAChR subunits have been identified (α2-α10, β2-β4) and five subunits coassemble to form a functional receptor (Dani and Bertrand 2007). Because multiple distinct alpha subunits can combine with multiple distinct beta subunits, the potential number of nAChR subtypes is vast and is usually brain region-specific (Millar and Gotti 2009).

One of the most robust nAChR-expressing circuits in the central nervous system is the medial habenulo-interpeduncular pathway(Leslie, Mojica et al. 2013). Interestingly, cholinergic neurons within the MHb robustly express rare neuronal nAChR subtypes containing the α3 and β4 subunits, as well as the α4 subunit among others (See Page 85, Table III-1) (Fonck, Nashmi et al. 2009, Salas, Sturm et al. 2009, Fowler, Lu et al. 2011).

While the neurocircuitry underlying withdrawal remains to be completely elucidated, the habenular-interpeduncular axis has recently been implicated in nicotine intake and aversion (Fowler, Lu et al. 2011, Frahm, Slimak et al. 2011). It has been shown that direct infusion of the non-specific nAChR antagonist, mecamylamine, into the interpeduncular nucleus (IPN) can precipitate somatic withdrawal in nicotine-dependent mice, suggesting that the habenulor-interpeduncular axis may be important for the expression of somatic signs of nicotine withdrawal (Zhao-Shea, Liu et al. 2013). In addition, knock-out mice that do not express nAChR α2, α5, or β4 subunits, which are particularly abundant in the MHb-IPN tract, exhibit fewer withdrawal symptoms during nicotine withdrawal (Salas, Sturm et al. 2009). However, how nAChRs on the MHb cholinergic neurons modulates nicotine withdrawal is still unknown. Thus, in this chapter, we focused on testing the hypothesis that nAChRs on MHb cholinergic neurons are involved in affective nicotine withdrawal symptoms.

IV.B. Materials and methods

Animals

C57BL/6J mice, α4 knock-out (α4KO) mice and their wild type (WT) littermates were used for the experiments in this chapter. The genetic engineering of the α4KO mouse line has been described previously (Ross, Wong et al. 2000). The α4KO mouse line has been back-crossed to a C57BL/6J background for at least nine generations. All the mice used in the experiments were bred in our animal facilities. The mice were group housed four mice/cage on a 12-h light, 12-h dark lighting cycle with lights on at 7:00 a.m. and off at 7:00 p.m, and given food and water ad libitum. Mice were at least 8 weeks old at the beginning of each experiment. Behavioral experiments were performed during the light cycle. Independent groups of animals were used for each behavioral experiment unless otherwise noted.

All experiments were conducted in accordance with the guidelines for care and use of laboratory animals provided by the National Research Council (National Research Council Institute for Laboratory Animal 1996), as well as with an approved animal protocol from the Institutional Animal Care and Use Committee of the University of Massachusetts Medical School.

Drugs and drinking solutions

Nicotine and control drinking solutions were prepared from nicotine hydrogen tartrate or L-tartaric acid (Sigma-Aldrich), which were dissolved in tap water with concentrations of 200 μg/ml (nicotine base) and 300 μg/ml, respectively. Saccharin Sodium (Fisher Scientific) was added to each solution to sweeten the taste with a concentration of 3 mg/ml. For brain infusions, mecamylamine (2 μg, 1 μl), Dihydro-β-erythroidine hydrobromide (DHβE) (3 μg, 1 μl), SR16584 (2 μg, 1 μl) and α-conotoxin MII [E11A] (5 μM, 1 μl) were dissolved in artificial cerebrospinal fluid (ACSF) prior to delivery. Mecamylamine is a nonselective antagonist of nAChR and we use a relatively low dose according to the literature (Levin, Briggs et al. 1994, Kim and Levin 1996, Wickham, Solecki et al. 2013). DHβE is a competitive nAChR antagonist, selective for the α4* nAChRs (IC_{50} values are 0.19 and 0.37 μM for α4β4 and α4β2 receptors respectively) (Harvey, Maddox et al. 1996) and we use a relatively low dose according to the literature (Raybuck and Gould 2010, Wickham, Solecki et al. 2013). SR 16584 is a selective antagonist of the α3β4 nAChR subtype (IC_{50} = 10.2 μM), and we chose the dose base on the previous literature (Zaveri, Jiang et al. 2010, Zhao-Shea, Liu et al. 2013). α-conotoxin MII [E11A] is an antagonist selectively for α6* nAChRs (IC_{50} = 0.15 nM). At higher dose, α-conotoxin MII [E11A] can also block α3β2 nAChR (IC_{50} = 8.72 nM) (McIntosh, Azam et al. 2004, Wickham, Solecki et al. 2013). Here we use a dose that is relatively low (8.8ng/side) according to the literature and it supposed to selectively antagonize the α6* nAChRs (Wickham, Solecki et al. 2013).

Laser Capture micro-dissection.

Six weeks after nicotine or control solution exposure, mice were decapitated and the brains were removed, snap-frozen in dry ice-cooled 2-methylbutane (−60 °C) and stored at −80 °C. Coronal serial sections (10 μm) of medial habenula were cut using a cryostat (Leica Microsystems Inc.) and mounted on pre-cleaned glass slides (Fisher Scientific). The sections were immediately placed in a slide box on dry ice until completion of sectioning, followed by storage at −80 °C. A quick immunofluorescence staining protocol was used to identify cholinergic neurons. First, frozen sections were allowed to thaw for 30 s. Slides were immediately fixed in ice-cold acetone for 4 min and then washed in PBS, incubated with mouse anti-ChAT primary antibody (Millipore, 1: 50 dilution for 10 min), washed in PBS once, followed by incubation in secondary fluorescently-labeled antibodies (Molecular Probes; donkey anti-goat Alex Fluor 594, 1: 100) for 10 min. The slides were washed in PBS once, and then subsequently dehydrated in graded ethanol solution (30 s each in 70% ethanol, 95% ethanol, 100% ethanol, and once for 5 min in xylene). Slides were allowed to dry for 5 min. All antibodies were diluted in PBS, including 2% BSA and 0.2% Triton X-100. PBS and dH_2O were treated with diethylpyrocarbonate (DEPC) for RNA preservation. All ethanol solutions and xylene were prepared fresh to preserve RNA integrity. A Veritas Microdissection System Model 704 (Arcturus Bioscience) was used for laser capture microdissection (LCM). ChAT immunopositive neurons were captured on CapSure Macro LCM caps (Arcturus Bioscience) for total RNA isolation.

Real-time PCR

Total RNA was extracted from individual samples using a Micro Scale RNA Isolation Kit (Ambion). RNA samples extracted from cholinergic neurons of chronic nicotine or control MHb were reverse-transcribed into cDNA using a TaqMan Reverse Transcription Kit (Applied Biosystems). Quantitative reverse transcription-PCR (qRT-PCR) was performed using an Applied Biosystems 7500 Real-Time System and TaqMan assays (Applied Biosystems). Samples containing no reverse transcriptase were used as negative controls. Relative gene expression differences between control-treated mice and chronic nicotine-treated mice were calculated using the $2^{-\Delta\Delta Ct}$ method. Expression values are relative to glyceraldehyde-3-phosphate dehydrogenase (GAPDH). Samples were analyzed in triplicate. Student"s t-test was used for statistical analysis.

Western blot

For antibody test, α4, α6, β3, β4 knockout mice and their wild type litter mates were used (these mice brains are gifts from Picciotto lab and verified the genotype by PCR as described previously by them) (Picciotto, Zoli et al. 1995, Orr-Urtreger, Goldner et al. 1997, Xu, Gelber et al. 1999, Ross, Wong et al. 2000, Champtiaux and Changeux 2002). For the chronic nicotine treatment experiment, C57BL/6 mice were treated with nicotine-containing water for 6 weeks (described above) and the brains were removed for western blot. MHb was punched out and

three of them from the same treatment group were pooled together as one sample to get enough protein.

The tissue was lysed in RIPA buffer (Radioimmunoprecipitation assay buffer) containing protease inhibitors and protein concentrations were determined using the Bradford protein assay (Pierce). After boiling, approximately 30 µg of each sample was loaded in each well and separated by 10% SDS–polyacrylamide gel electrophoresis (SDS-PAGE) and transferred to nitrocellulose membranes. Blots were blocked with 5% milk in phosphate-buffered saline with 0.05% (v/v) Tween-20 (PBST) for 60 min at room temperature, washed three times in PBST for 5 min, and then incubated at 4 degrees overnight in primary antibody diluted in PBST [α4 nAChR (rabbit, 1:500), β3 nAChR (rabbit, 1:500), or β4 nAChR (rabbit, 1:500), from Alomone Labs]. Blots were washed three times in PBST and incubated in secondary antibody for 60 min at room temperature (HRP-Goat anti-rabbit IgG, 1:2000, from Santa Cruz). Blots were washed three times in PBST, and then immunoreactive bands were detected with Super Signal West Dura (Pierce). The images were captured using a Versa Doc Imaging station (Biorad). Nonsaturating bands were quantified using Quantity One software (Biorad).

Electrophysiological recording

Mice were treated with chronic nicotine water or control solution for 3 weeks starting from 3 weeks old. Brains were quickly removed and placed in oxygenated ice-cold high sucrose artificial cerebrospinal fluid (SACSF)

containing kynurenic acid (1 mM, Sigma, St. Louis, MO). SACSF solution contained (in mM): 250 sucrose, 2.5 KCl, 1.2 $NaH_2PO_4•H_2O$, 1.2 $MgCl_2•6H_2O$, 2.4 $CaCl_2•2H_2O$, 26 $NaHCO_3$, 11 D-Glucose. Coronal brain slices (~180 μm) containing MHb brain regions were made using a Leica VT1200 vibratome. Current responses to ACh or nicotine were obtained in the whole-cell configuration and gap-free acquisition mode in Clampex (Axon Instruments). Neurons were held at a resting membrane potential of -70 mV. For whole-cell responses to nicotine and ACh, neurons were held at -70 mV and nicotine (10 μM) or ACh (300 μM) was applied via bath perfusion for 10 min. Whole-cell responses to agonists were measured in the presence of atropine (1 μM) to block muscarinic receptors, bicuculline (20 μM) to block $GABA_A$ receptors, CNQX (10 μM) to block AMPA receptors, and AP5 (50 μM) to block NMDA receptors. All recordings were filtered at 1 kHz using the amplifier's four-pole, low-pass Bessel filter, digitized at 10 kHz with an Axon Digidata 1440A interface and stored on a personal computer. ACSF was used for bath solution and contained (in mM): 125 NaCl, 2.5 KCl, 1.2 $NaH_2PO_4•H_2O$, 1.2 $MgCl_2•6H_2O$, 2.4 $CaCl_2•2H_2O$, 26 $NaHCO_3$, 11 D-Glucose.

Marble burying test (MBT)

As described in our previous paper (Zhao-Shea, Liu et al. 2013), mice were habituated in the standard mouse cage with ~5 - 6 cm layer of bedding for 2 days (45 min/day) before the test. On the test day, 15 clean 1.5 cm glass marbles

were evenly spaced in five rows of three, each 4 cm apart on the bedding. A mouse was placed in its test cage and left for 30 minutes, and the number of marbles buried (to 2/3 their depth) with bedding was counted every 5 min or after 30 min (as noted in the figures), then mice were removed from their test cages.

Elevated plus maze (EPM)

As described in our previous paper (Zhao-Shea, Liu et al. 2013), the experimental apparatus consisted of a central axis and four arms elevated 45 cm above the floor, with each arm positioned at 90° relative to the adjacent arms. One red light arranged at 100 cm above the maze was used as the source of illumination. The mice were individually placed in the center of the maze with their heads facing one of the open arms and allowed 5 min of free exploration. The number of entries into the open and closed arms, and the total time spent in the open and closed arms were measured by MED-PC IV software (MED Associates, Inc.) The time spent in open and closed arms was calculated as an index of anxiety. The total number of arm entries was considered as an index of locomotor activity. The apparatus was cleaned thoroughly between trials. Mice that froze in the initial arm without moving were not included in the analysis.

Guide cannula placement

As described in our previous paper (Zhao-Shea, Liu et al. 2013), the guide cannulas were surgically implanted at least 3 days prior to the experiment. Mice were anesthetized with a mixture of ketamine (100 mg/kg) and xylazine (10

mg/kg) (VEDCO) and placed on a stereotaxic frame (Stoelting Co.). The surgical area was shaved and disinfected and the skull bone was exposed. Using bregma and lambda as landmarks, the skull was leveled in the coronal and sagittal planes. A hole was drilled and stainless steel guide cannulas were inserted into the brain and secured to the skull with instant adhesive. The coordinates relative to the bregma were: MHb (AP, -1.94, ML, 0.2, DV, -2.25). The scalp incision was stitched and dental cement was used to stabilize the cannula on the skull. After surgery, the mice were kept on a heating pad to prevent hypothermia. Mice were allowed to recover in individual cages for at least 3 days prior to drug infusion and behavioral testing.

Intra-MHb infusions

Mice were anesthetized with 2% isoflurane via a nose cone adaptor at a flow rate of 800 ml/L. Once anesthetized, an infusion cannula designed to reach −0.25 mm below the guide cannula was inserted into the guide cannula. Vehicle or drug was infused at a rate of 1 µl/min. After infusion, the infusion cannula was left in place for 2 min prior to retraction. Mice were placed back into their home cages and the behavior tests were conducted after the mice were awake. After completion of behavioral experiments, mice were culled, brains isolated, and cannula placement verified. To verify the guild cannula placement, the brains were cut in 30 µm sections and the location of the guide cannula was determined by neutral red staining using light microscopy. In addition, the injection sites were

double verified histologically by microinjection of DiI cell labeling solution (Invitrogen). Only mice with cannulas in the right placement were included in the statistical analysis.

Data analysis

Data were analyzed using One- or Two-way ANOVA followed by Bonferroni post hoc tests or t-tests as indicated. Results were considered significant at $p < 0.05$. All data are expressed as means ± SEM.

IV.C. Results

α4* nAChRs are critical for the increased anxiety during nicotine withdrawal

Withdrawal from drugs of abuse, including nicotine, is a stressor and anxiogenic (Tsai, Zhang et al. 2009). To test the hypothesis that nAChRs containing the α4 subunit are critical for the increased anxiety during nicotine withdrawal, we measured anxiety-like behaviors during nicotine withdrawal in nicotine-dependent WT and α4 KO mice. Nicotine dependence was induced via 4-6 weeks of nicotine-laced drinking water as reported previously (Zhao-Shea, Liu et al. 2013). Nicotine-naïve mice received either nicotine solution or control solution. Withdrawal was induced by replacing the nicotine solution with water and behaviors were measured 24 hours post nicotine cessation. Interestingly, while nicotine-dependent WT mice undergoing withdrawal displayed decreased time-

spent in the open arms of the EPM and increased marble burying, withdrawn nicotine-dependent α4 KO mice did not differ in anxiety-like behaviors compared to nicotine naïve α4 KO mice, indicating that α4* nAChRs are necessary for increased anxiety during nicotine withdrawal (Fig. IV-1 A-C).

nAChRs in the MHb cholinergic neurons are critical for the increased anxiety during nicotine withdrawal

To test the hypothesis that the anxiogenic effects of nicotine withdrawal are mediated, in part, through increased MHb α4* nAChR signaling, we measured anxiety in the EPM and MBT assay during spontaneous withdrawal from nicotine or control solution in C57Bl/6J mice. Mice were implanted with cannulas targeting the MHb and infused with vehicle or subtype selective nAChR antagonists including the α6* nAChR-selective antagonist α-conotoxin MII [E11A], the α4β2* nAChR-selective antagonist DHβE, and the α3β4 nAChR selective antagonist SR16584 prior to testing (McIntosh, Azam et al. 2004). In the EPM, two-way ANOVA revealed a significant main effect of drug infusion ($F_{3,72}$ = 9.68, $p < 0.0001$) and significant drug infusion × chronic treatment interaction ($F_{3,72}$ = 7.01, $p < 0.001$). Posthoc analysis indicated that infusion of the antagonists into the MHb did not significantly modulate time spent in the open arms of the EPM in nicotine-naïve mice compared to vehicle infusion (Fig. IV-2A). However, mice undergoing nicotine withdrawal and infused with vehicle spent less time in the open arms compared to nicotine-naïve animals ($p < 0.05$) and time spent in the

open arms was significantly increased by infusion of α-conotoxin MII [E11A] ($p < 0.001$) and DHβE ($p < 0.01$), but not SR16584. Total arm entries in the EPM did not significantly differ between nicotine-naïve and –dependent mice regardless of antagonist infusion into the MHb. In the MBT, marble burying was not significantly affected by antagonist infusion in nicotine-naïve mice; whereas mice undergoing nicotine withdrawal had significantly increased marble burying compared to control mice ($p < 0.001$). This increase was significantly decreased by MHb infusion of the antagonist α-conotoxin MII [E11A] ($p < 0.01$) and DHβE ($p < 0.05$), but not SR16584. Proper placement of cannulas and drug infusions were verified after behavioral experiments by the neutral red staining and dye infusion (Fig. III-5).

These data suggest that anxiety induced by the stress of nicotine withdrawal is mediated by increased signaling through α6* and α4β2* nAChRs in the MHb.

Chronic nicotine treatment upregulates α6 nAChRs in MHb neurons

Both in humans and in rodents, long-term exposure to nicotine will cause the upregulation of nAChRs in the brain (Nashmi, Xiao et al. 2007, Govind, Vezina et al. 2009). To test the hypothesis that chronic nicotine treatment upregulates the nAChRs in the MHb, we measured the expression level of nAChRs in the MHb cholinergic neurons by qRT-PCR and western blot.

Mice were treated with nicotine water or control solution for 4-6 weeks, as described above. The cholinergic neurons in the MHb were dissected by the

laser capture micro dissection and the nAChR subunit (α2-α7 and β2-β4 nAChR subunit) gene expression was detected by qRT-PCR. In both control mice and nicotine treated mice, all nAChR subunit genes except α2 were detected in cholinergic MHb neurons. As we showed in Chapter II, expression of the nAChR α3 and α4 subunit genes was relatively strong compared to the house-keeping gene GAPDH; whereas, expression of the α5, α6, and α7 genes was less robust. In addition, expression of the nAChR β3 and β4 subunit genes was high relative to GAPDH (Table IV-1). These results are consistent with a previous report (Sheffield, Quick et al. 2000). Interestingly, the paired t-test showed that significantly higher level of expression of the α6 subunit gene in the chronic nicotine treated mice compared to the control mice (Table IV-1), which indicated α6 gene was upregulated by chronic nicotine treatment.

To check whether the nAChR subunits were also upregulated in the protein level, we performed western blot assays.

First, we tested the nAChR subunit antibody specificity by comparing the immunoreactive bands in the specific nAChR subunit knockout mice and their corresponding wild type litter mates. The western blot results showed that the bands in the α4, α6 or β3 knockout mice are equivalent to their corresponding wild type litter mate, but the band in the β4 knockout mice showed a robust decrease compare to its wildtype litter mate (Fig. IV-3A). These results suggest that the β4 subunit antibody is specific, but unfortunately the antibodies for α4 α6

or β3 are not specific under the conditions used. However, when using Bradford assay to quantify protein concentration, SDS in RIPA buffer might cause high backgrounds. Therefore, the protein we loaded might not be accurate, contributing to an inaccurate outcome.

Second, we use the specific β4 subunit antibody to test whether the β4 protein level was upregulated after chronic nicotine treatment. As the bands shown in Fig. IV-3B (left), the β4 subunit immunoactive bands are similar between the nicotine naïve group and chronic nicotine treated group. The quantification of the bands showed that there is no significant difference between the two groups (Fig IV-3B, right) under the conditions used, which is consistent with the qRT-PCR results.

α6/α4β2* nAChRs in MHb neurons were functionally upregulated in chronic nicotine-exposed mice

To test the hypothesis that α6/α4β2* nAChRs in MHb neurons were functionally upregulated in chronic nicotine-exposed mice, we measured whole-cell responses to nicotine in MHb neurons from nicotine-naïve and nicotine-dependent animals and tested current sensitivity to α-conotoxin MII [E11A], DHβE, and SR16584. As a recent study indicated that α6* nAChRs are predominantly located in the medial ventral portion of the MHb, we focused our recordings on this sub-region (Shih, Engle et al. 2014). In control mice, 10 μM nicotine elicited robust whole-cell currents. One-way ANOVA revealed a significant main effect of antagonist on current amplitude (Kruskal-Wallis test, $p <$

0.001). Dunn‟s post-hoc test indicated that currents were relatively insensitive to 100 nM α-conotoxin MII [E11A], but were significantly blocked by DHβE and SR16584 (Fig IV-2D, left). In MHb neurons from chronic nicotine-treated mice, whole-cell responses were significantly larger compared to control neurons (Mann-Whitney test, $p < 0.05$) (Fig IV-2D, right). In addition, one-way ANOVA indicated a significant main effect of antagonist on nicotine response ($F_{3, 60} = 34.17$, $p < 0.0001$) (Fig IV-2E). Unlike nicotine-naïve mice, post-hoc analysis revealed that whole-cell responses from nicotine-treated mice were significantly reduced in the presence of α-conotoxin MII [E11A], as well as DHβE and SR16584 (Fig IV-2E). Together, these data indicate an increase in functional α6* nAChRs in the MHb after chronic nicotine treatment.

Recently, we identified a novel nAChR subtype containing both α4 and α6 subunits within the VTA that is sensitive to α6* nAChR antagonists as well as DHβE (Zhao-Shea, Liu et al. 2011, Liu, Zhao-Shea et al. 2012). To test if α4* nAChRs are expressed within the medial ventral sub-region of the MHb, we measured whole-cell responses to ACh in WT and α4 KO mice. Peak ACh induced current amplitudes were significantly reduced in α4 KO mice compared to WT (Fig. IV-1D), which suggest that α4 and α6 subunit may co-assemble with each other in the medial ventral sub-region of the MHb.

IV.D. Discussion

Previous studies have implicated the MHb in physical nicotine withdrawal behaviors (Antolin-Fontes, Ables et al. 2014). In this study, we found that chronic nicotine increased gene expression of CHRNA6, the gene encoding the α6 nAChR subunit. In addition, nAChRs containing the α6 subunit were functionally upregulated in the MHb, as upregulated currents were more sensitive to a selective α6* nAChR antagonist compared to currents from nicotine-naïve animals. These data are consistent with a recent study showing that mice harboring α6 subunits with an eGFP tag exhibited an increase in fluorescent signal in MHb after chronic nicotine treatment compared to control mice, suggesting α6 subunit upregulation after nicotine exposure (Henderson, Srinivasan et al. 2014).

Importantly, we previously identified a novel nAChR containing both α4 and α6 subunits in DAergic neurons of the VTA (Zhao-Shea, Liu et al. 2011, Liu, Zhao-Shea et al. 2012). Here, we showed that nicotinic currents in the MHb subregion that predominantly express the α6 subunit also contain the α4 subunit. These data suggest that α4α6* nAChRs are upregulated by chronic nicotine exposure and contribute to increased anxiety-like behavior during nicotine withdrawal (Zhao-Shea, Liu et al. 2011, Liu, Zhao-Shea et al. 2012, Shih, Engle et al. 2014).

Interestingly, while the α3β4 nAChR-selective antagonist SR16584 significantly blocked nicotine-induced whole cell currents in the medial ventral portion of the MHb, it did not affect anxiety during nicotine withdrawal. While α6* and α4*

nAChRs have unique expression patterns in discrete sub-nuclei of the MHb, α3β4* nAChR are expressed throughout. Thus, nAChR signaling in MHb sub-nuclei may have opposing roles in modulating affective behaviors such that blockade of α3β4* nAChRs throughout the MHb ultimately may have little effect in modulating behavior output compared to α6/α4* nAChR antagonists which would be expected to block signaling in distinct MHb subregions. Alternatively, the concentration of SR16584 used for our analysis may have blocked non-α3β4* nAChRs. Regardless, these data indicate that heightened anxiety during nicotine withdrawal is mediated by increased nAChR signaling in the MHb, especially the α4α6* nAChRs. Thus, nAChRs expressed in MHb cholinergic neurons should be considered molecular targets for smoking cessation therapeutics.

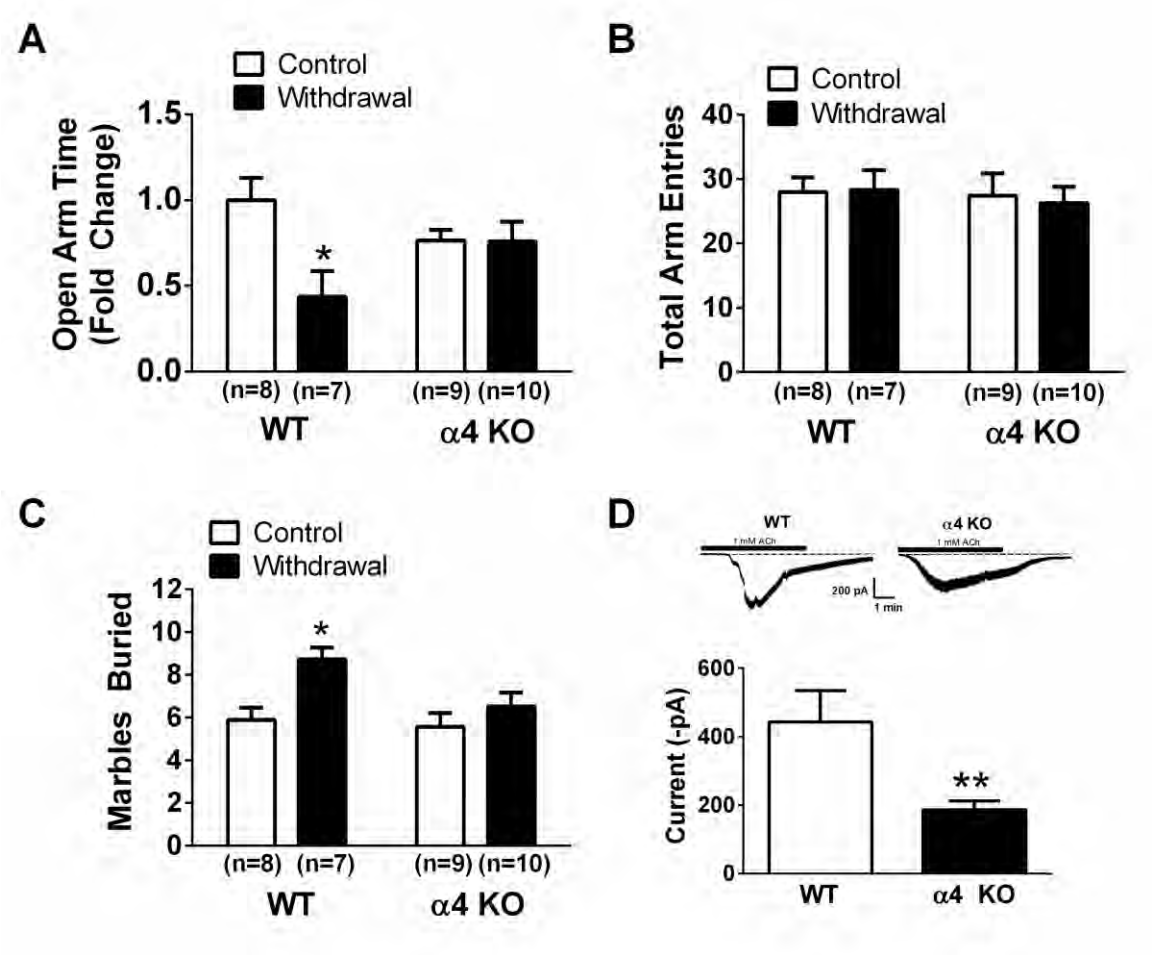

Figure IV-1. Expression of α4* nAChRs is necessary for affective nicotine withdrawal symptoms.

A. Time spent in the open arms of the EPM in control and nicotine withdrawn WT and α4 KO mice.

B. Total arm entries in the EPM from the groups in panel A.

C. Total number of marbles buried in the MBT in control and nicotine withdrawn WT and α4 KO mice. For A-C, * $p < 0.05$, ** $p < 0.01$, Two-way ANOVA, Bonferroni post-hoc.

D. Representative whole-cell traces from the medial ventral portion of the MHb in WT and α4 KO mice (top). Averaged peak current in response to 10 mM nicotine in WT and α4 KO mice (bottom). * $p < 0.05$, ** $p < 0.01$, unpaired t-test.

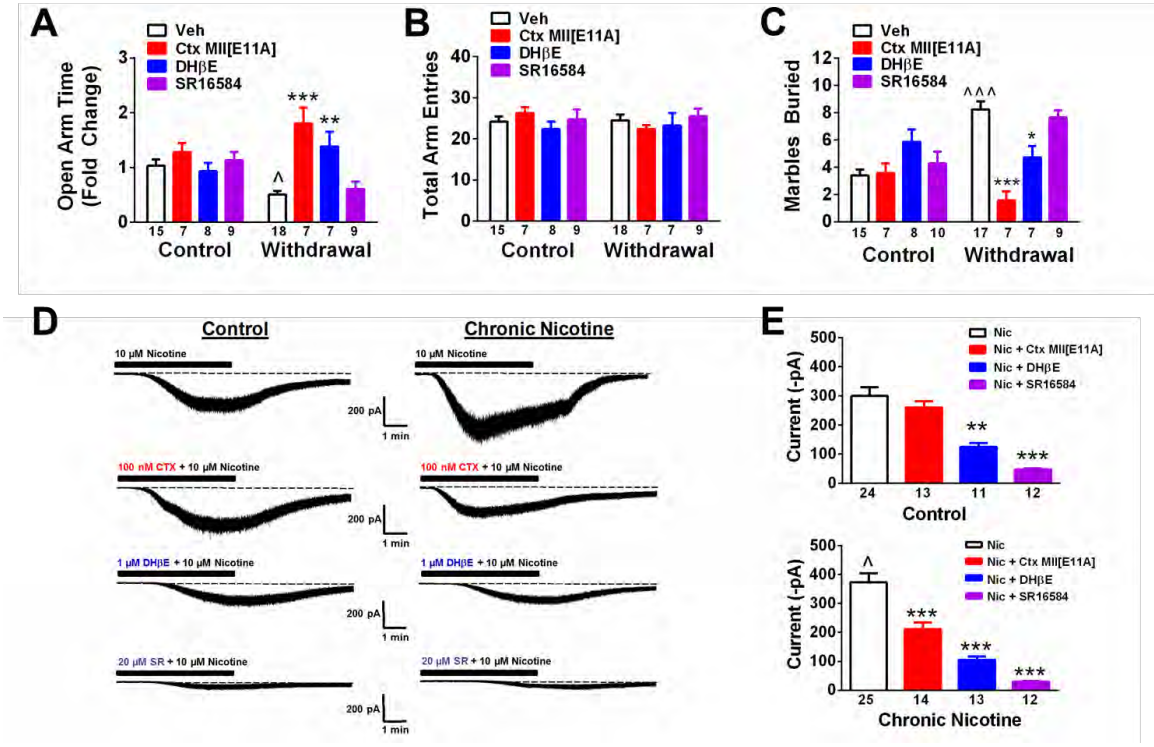

Figure IV-2. Nicotine regulation of MHb α4/α6β2* nAChRs mediates increased anxiety during nicotine withdrawal.

A. Time spent in the open arms of the EPM in control and nicotine withdrawn mice after vehicle (Veh), α-conotoxin MII[E11A] (α-Ctx[E11A]), DHβE, or SR16584 infusion into the MHb.

B. Total arm entries in the EPM from the groups in panel A.

C. Total number of marbles buried in the MBT (t = 20 min) in control and nicotine withdrawn mice after Veh, α-Ctx [E11A], DHβE, or SR16584 infusion into the MHb. For A-C, data are expressed as average values ± S.E.M. ^p<0.05, ^^p<0.01 compared to control group with Veh infusion. ***p < 0.01, ***p < 0.001 compared to Veh within groups. Two-way ANOVA, Bonferroni post-hoc.

D. Representative whole-cell response to 10 μM nicotine under control conditions and in the presence of 100 nM α-Ctx[E11A], 1 μM DHβE, or 20 μM SR16584 in MHb slices from control-treated mice (left recordings) and chronic nicotine-treated mice (right recordings).

E. Averaged peak whole-cell current responses to 10 μM nicotine from the indicated groups as recorded in panel D from control mice (top) or chronic nicotine-treated mice (bottom). Data are expressed as average values ± S.E.M. ^p<0.05, ^^p<0.01 compared to control group with Nic only. ***p < 0.01, ***p < 0.001 compared to Nic only within groups.

Table IV-1. Relative gene expression of nAChR subunit genes in MHb cholinergic neurons in control and nicotine treated mice.

	α2	α3	α4	α5	α6	α7	β2	β3	β4
Control	N.D.	-2.41 ±0.36	-5.04 ±0.42	-9.72 ±0.57	-11.59 ±0.51	-9.63 ±0.55	-5.11 ±0.20	-4.99 ±0.53	-4.30 ±0.31
Nicotine	N.D.	-1.97 ±0.68	-4.80 ±0.17	-10.04 ±0.25	-10.47 ±0.28	-9.65 ±0.20	-5.16 ±0.33	-4.63 ±0.49	-4.15 ±0.53
Fold-Change[#]	N.D.	1.76 ±0.57	1.21 ±0.16	0.85 ±0.16	2.34 ±0.39*	1.03 ±0.13	1.04 ±0.20	1.49 ±0.39	1.35 ±0.43

Values represent the change in the threshold cycle ($^{-\Delta\Delta Ct}$) compared with GAPDH. * $p < 0.05$. [#] Nicotine compared to control calculated as $2^{-\Delta\Delta Ct}$, * $p < 0.05$, n = 4/treatment. N.D., Not detected.

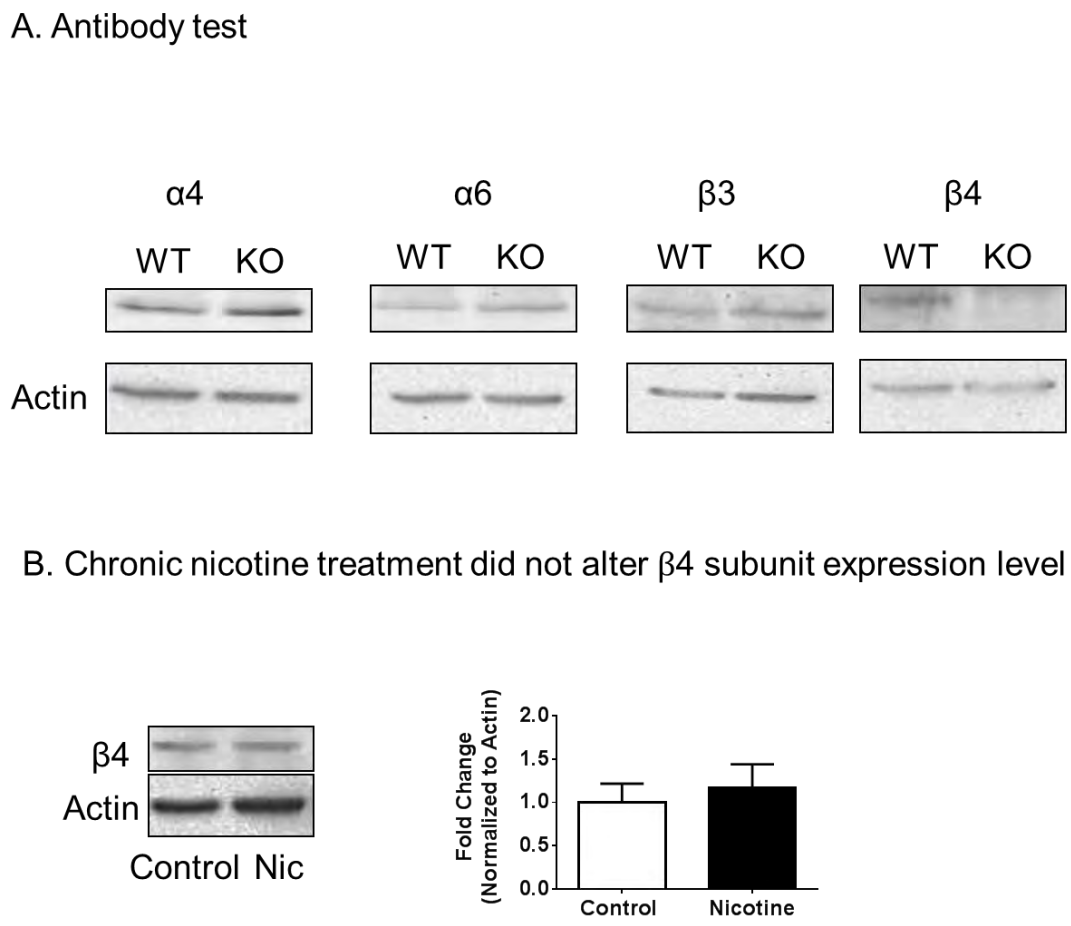

Figure IV-3 Chronic nicotine treatment did not upregulate β4 subunit expression level.

A. Antibody specificity tests were done for the α4, α6, β3, β4 subunits in the knockout mice and corresponding wild type littermate by western blot analysis. Actin is used for endogenous control.

B. Chronic nicotine treatment did not upregulate the β4 expression level.

Left, representative western blot of β4 subunit in nicotine treated or control treated mice; Right, quantitated results of western blots (n=3). Data are

expressed as average values ± S.E.M. Statistical analysis was performed by student-t test ($p>0.05$).

CHAPTER V

Cholinergic input to the medial habenula

is not from the septal-diagonal band area

Contributions:

Jennifer Ngolab made the virus construct. All other research was done by me. I wrote the body of the text and made the Figures.

V.A. Introduction

The medial habenula is a key connection between the limbic forebrain and midbrain. The medial habenula receives major inputs via a white matter bundle called stria medullaris (sm) (Herkenham and Nauta 1977, Qin and Luo 2009). The most prominent input is from the two nuclei in the posterior septum: the triangular septal nucleus (TSN) and septofimbrial nucleus (SFi), which release glutamate and ATP to the MHb (Herkenham and Nauta 1977, Qin and Luo 2009). It also has been shown that the GABAergic inputs to the MHb are from the Nucleus of Diagonal band (DB) and the medial septum (MS) (Qin and Luo 2009). In addition, physiological and neurochemical studied have shown that the MHb also has the highest expression of nicotinic acetylcholine receptors (nAChRs) (Sheffield, Quick et al. 2000). Evidence from the lesion studies indirectly showed that the NDB or posterior septum might send the cholinergic input to the MHb, but more precise research still needs to be done (Contestabile and Fonnum 1983).

As mentioned in Chapter II, AAV2-ChR2-YFP were designed to express only in the Cre-positive neurons, and its expression is robust, therefore AAV2-ChR2-YFP can be used as a tracer to study the precise projection of certain neuron population from a specific brain area. Here, we tested whether cholinergic input arises from DB, MS, TSN or SFi using AAV2-ChR2 as a tracer.

V.B. Materials and methods

Mice

ChAT-Cre knock-in mice were purchased from Jackson Laboratories (stock number: 006410) and bred in the UMMS animal facility. Breeding was conducted by mating heterozygous pairs. For ChAT-Cre mice, genotypes were determined by PCR as previously described (Rossi, Balthasar et al. 2011) and also on Jackson Laboratories website. PCR of mouse tail genomic DNA was performed with three specific primers, WT F (5′ -GTT TGC AGA AGC GGT GGG-3′), mutant F (5′ -CCT TCT ATC GCC TTC TTG ACG -3′) and Common R (5′ -AGA TAG ATA ATG AGA GGC TC -3′). These primers amplify DNA fragments of 272 bp in wild-type (WT) mice, and 350 bp in ChAT-Cre mutant mice. DNA fragments were separated by agarose gel electrophoresis and visualized with ethidium bromide. Mice were group-housed four mice/cage on a light dark cycle with lights on at 7:00 a.m. and off at 7:00 p.m, and given food and water *ad libitum*. Male mice were used for all experiments. Mice were at least 8 weeks old at the start of each experiment. Behavioral experiments were performed during the light phase.

All experiments were conducted in accordance with the guidelines for care and use of laboratory animals provided by the National Research Council, as well as with an approved animal protocol from the Institutional Animal Care and Use Committee of the University of Massachusetts Medical School.

Surgical procedures for virus microinjection

Packaging of AAV-Ef1A-DIO-ChR2-eYFP plasmids into AAV2 viral particles was done by the University of Massachusetts Medical School Viral Vector Core. For viral particle injection, ChAT-Cre mice were anesthetized with a mixture of ketamine (100 mg/kg) and xylazine (10 mg/kg) (VEDCO). The surgical area was shaved and disinfected. Mice were placed in a stereotaxic frame (Stoelting Co.) with mouse adaptor and a small incision was cut in the scalp to expose the skull. Using bregma and lambda as landmarks, the skull was leveled in the coronal and sagittal planes. The viral particles ($1x10^{12}$ viral particles/µl) were injected into the ChAT-Cre mice DB/MS or SFi/TS according to the coordinates: DB: AP, -0.8, ML, ±0.2, DV, 5.0; MS: AP, -0.8, ML, 0, DV, 4.0; SFi: AP, -0.1, ML, 0, DV, 2.75; TS: AP, -0.46, ML, 0, DV, 2.5. The viral particles (1.5 µl/side) were injected bilaterally to DB or unilaterally TS, SFi, MS, at a flow rate of 0.3 µl/min. The injection needle was kept in place for 5 min post-injection. The incision was sutured and mice were returned to their home cages.

Immunostaining

Four weeks after the virus infection, mice were deeply anesthetized with sodium pentobarbital (200 mg/kg, i.p.) and perfused transcardially with 10 ml of 0.01 M phosphate-buffered saline (PBS) followed by 10 ml of 4 % paraformaldehyde in 0.01 M sodium phosphate buffer (pH=7.4). Brains were removed and post-fixed for 2 h with the same fixative and cryoprotected in sodium phosphate buffer containing 30% sucrose until brains sank. MHb serial coronal sections (20 µm) were cut on a microtome (Leica CM 3050S, Leica Microsystems Inc.) and

collected into a 24-well tissue culture plate containing 1 X PBS. After rinsing sections in PBS twice for 5 min, they were treated with 0.4 % Triton X-100 PBS (PBST) twice for 2 min, followed by incubation in 2% BSA/PBS for 30 min. Sections were washed with PBS once and then incubated with primary antibodies for ChAT (Goat, 1:100, AB144P, Millipore) in 2% BSA/PBS overnight at 4° C. The sections were then washed with PBS three times for 5 min followed by incubation in secondary fluorescent labeled antibodies (donkey anti-goat Alexa Fluor® 594, 1:500, Molecular Probes, Inc., Eugene, USA) at room temperature in dark for 30 min. After washing with PBS five times for 5 min/wash, sections were mounted on slides by using VECTASHIELD® Mounting Medium (Vector laboratories, Inc., Burlingame, CA). The YFP signal was detected and picture was taken under the zeiss fluorescence microscope through the YFP fluorescence filter (Zeiss, Carl Zeiss MicroImaging Inc., NY).

V.C. Results

The MS/DB is cholinergic while SFi/TS are not cholinergic

To test whether the main MHb input are cholinergic, we first performed the ChAT staining in mouse brain, which is a marker of cholinergic neurons. Within the MS and DB, we observed densely distributed ChAT-positive neurons (Figure V-1A), however, within the TS/SFi, there are no ChAT-positive neurons (Figure V-1B), suggesting that the TS/SFi is not the source of cholinergic input to the MHb.

MS/DB cholinergic neurons project to the hippocampus not the MHb

To test whether DB cholinergic neurons project to the MHb, we selectively expressed ChR2 in the cholinergic neurons of DB/MS/SFi/TS by injecting AAV2-ChR2-YFP into the ChAT-Cre mice. As expected, ChR2-YFP was not expressed in the SFi/TS, as there were no cholinergic neurons in these brain regions (see above). In contrast, as shown in Figure V-2A, the ChR2-YFP was expressed in the DB/MS cholinergic neurons. Then, we examined the distribution patterns of YFP labeled terminals. There are many YFP-positive terminals observed bilaterally in the hippocampus, but not in the MHb (Figure V-2B), suggesting that DB/MS cholinergic neurons project to the hippocampus but not the MHb.

V.D. Discussion

The MHb has been shown to be involved in several important behaviors. Interestingly, nAChRs are highly expressed in the MHb but where the cholinergic input originates is unclear. Previous lesion studies have shown that DB or the posterior septum might provide the cholinergic input to the MHb, but there is no direct evidence to support that.

It has been shown that ChR2-YFP can be used as an anterograde tracer to study the neural circuitry (Hira, Ohkubo et al. 2013, Saito, Tsujino et al. 2013, Shimano, Fyk-Kolodziej et al. 2013). In this study, using ChR2-YFP as a tracer, we showed that cholinergic neurons that originate from MS/DB project to the hippocampus. No projections from MS/DB to MHb were detected in any of the tracing examination. However, there are no cholinergic neurons in SFi/TS, suggesting that SFi/TS are not the cholinergic input to the MHb, either.

All tracers have their limitations. For ChR2, it has been shown that ChR2 trafficks to the membrane well when expressed at low levels but forms intracellular aggregates at high levels (Lin, Lin et al. 2009, Lin 2011). In our study, we found that ChR2 in MS/DB neurons project to the hippocampus, but not to MHb. Therefore, it is unlikely that ChR2 was not efficiently trafficked to the membrane. In the future study, we could try to use other tracers, including pseudorabies virus, or cholera toxin B subunit, to check the projections from MS/DB to MHb.

It is interesting that the main MHb afferents (MS/DB/SFi/TS) do not send the cholinergic projection to the MHb. MHb is one of the brain regions that have the highest nAChRs expression level, suggesting that there must be strong ACh release to it. Thus, there are two possibilities: 1) Some other unclear brain region sends the cholinergic input to the MHb; or 2) the cholinergic neurons in the MHb release the ACh to themselves to feed forward the neuronal circuit. More studies need to be done to test the possibilities.

In conclusion, MS, DB, SFi, TS do not provide the cholinergic input to the MHb, and the cholinergic input to the MHb still needs to be identified.

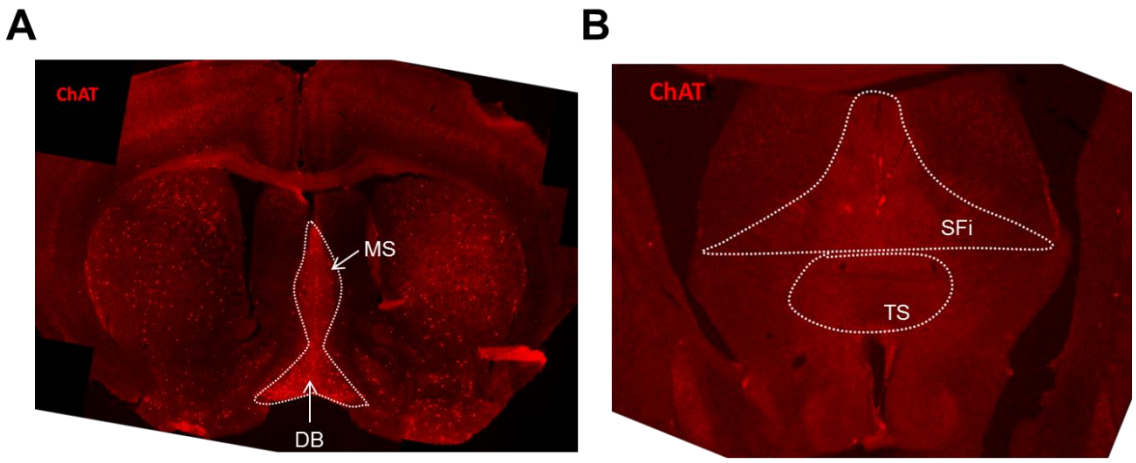

Figure V-1. ChAT expression pattern in the MS, DB, SFi and TS

A is showing that ChAT-positive neurons are clustered in the MS and DB (as shown in dashed line).

B is showing that there are no ChAT-positive neurons in the SFi and TS (as shown in dashed line).

Six mice were injected with virus and 20-25 slices were collected from each mouse. Representative slides were showing here.

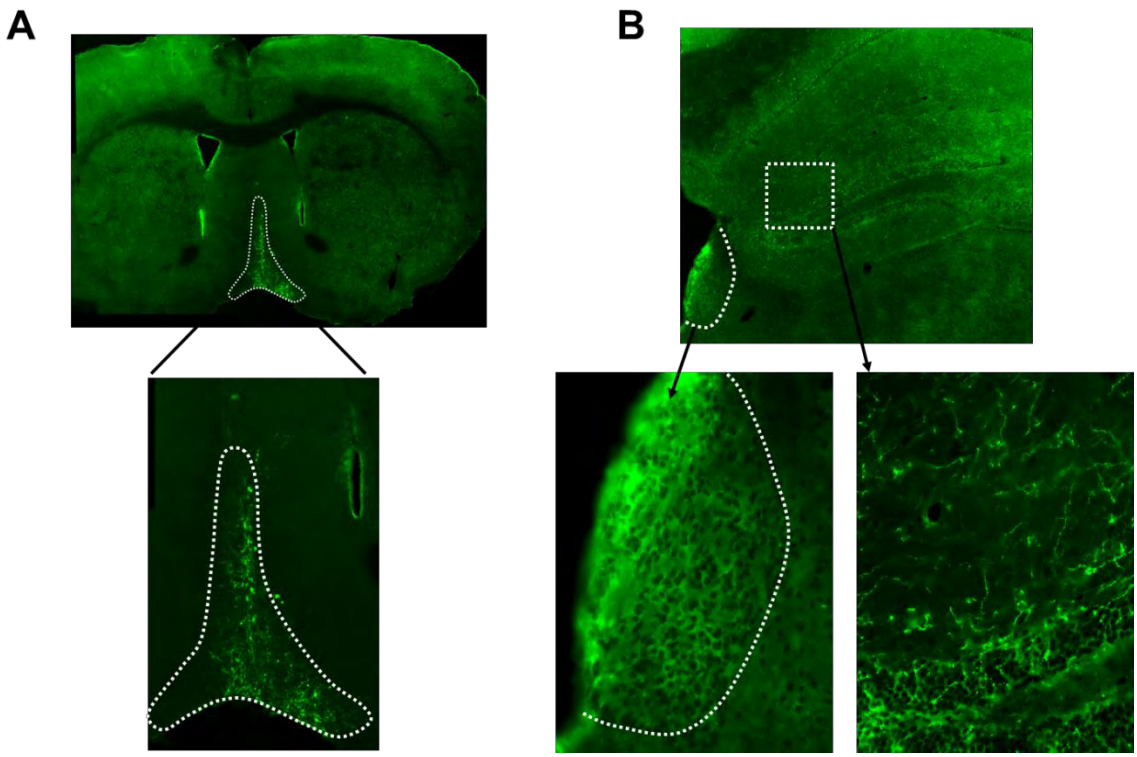

Figure V-2. DB cholinergic neurons project to the hippocampus not the MHb

A.The AAV2-ChR2 was injected into the MS and DB of ChAT-Cre mice. The picture is showing the expression of ChR2-YFP in the MS and DB (dashed line, above 10x, below 20x).

B.The fluorescent images showing the distribution of ChR2-YFP labeled terminals of DB cholinergic neurons. The terminals are mainly located in the hippocampus, not in the MHb (dashed line is MHb, above 10x, below 20x).

Six mice were injected with virus and 20-25 slices were collected from each mouse. Representative slides were showing here.

Chapter VI:

Conclusion, Discussion and Future direction

Conclusion and discussion:

Anxiety disorders are the most common of emotional disorders and the cost is a big burden for society, highlighting the need for identification of the underlying neuroanatomical bases and molecular underpinnings of anxiety (Kessler, Chiu et al. 2005). In the past few decades, research on anxiety disorder has focused on neurochemistry and genetics, and there is also growing interest in identifying the underlying brain circuits. Early on, chemical lesion studies combined with pharmacological studies provide a wealth of information about anxiety brain circuits. Recently, as new techniques emerged and developed, such as high resolution brain image and optogenetics, studies have revealed a major breakthrough and provided more detailed, precise information about the brain circuitry involved in anxiety disorders.

Human and animal studies have shown the neurocircuitry of anxiety, including the amygdala, nucleus accumbens, BNST and hippocampus (Adhikari 2014). Recently the role of the MHb-IPN tract in anxiety and fear has attracted much attention. Previous work indirectly demonstrated a role for the MHb in anxiety regulation, either through lesioning of the habenula itself or through selective ablation of presumed septal glutamatergic inputs into the MHb (Yamaguchi, Danjo et al. 2013). However, whether MHb is directly involved in anxiety and the mechanism by which the MHb-IPN tract regulates anxiety are still unclear.

In Chapter II, by using optogenetics, we showed that MHb cholinergic neurons, which are clustered in the ventral portion of the MHb, regulate anxiety-like behavior directly. Silencing MHb cholinergic neuronal inputs to the IPN by NpHR reduced anxiety-like behaviors in both the EPM and MBT assays. As MHb cholinergic neurons release glutamate at 10 Hz stimulation or ACh at 50 Hz stimulation (Ren, Qin et al. 2011), we also tested whether glutamate and ACh mediate different behaviors in the mice. When the MHb cholinergic neurons were activated by low frequency of stimulation (5 Hz), the mice tend to increase the anxiety. It has been demonstrate that MHb cholinergic neurons display spontaneous tonic firing of 2-10 Hz (Gorlich, Antolin-Fontes et al. 2013). Therefore, the stimulation paradigm in this experiment could be influenced by the pacemaking activity of the neurons themselves. In the future experiments, we could try some different stimulation paradigms (different stimulation frequency, duration, intensity, etc.) and test whether low frequency stimulation-induced glutamate release will increase anxiety. Interestingly, when the MHb cholinergic neurons were activated by high frequency of stimulation (50 Hz), the mice showed hypolocomotion compare to the control group. These results together suggest that the MHb cholinergic neurons modulate anxiety, and the two different neurotransmitters might be involved in different behaviors in mice.

While optogenetics provide an important tool to precisely define the relationship between neuronal activity and behavior in a given circuit, it provides little information regarding the endogenous mechanisms that may regulate this activity.

Previous studied have shown that nAChRs are highly expressed in the MHb-IPN circuit and the diversity of nAChR subtype is vast here. In addition, the nAChRs in the MHb-IPN pathway have been linked to acute nicotine intake and aversion. However, an endogenous role of nAChRs in the MHb-IPN circuitry has not been described.

In chapter II, to test whether MHb nAChRs regulate anxiety-like behavior, we directly infused the non-selective nAChR antagonist, mecamylamine, into the MHb or IPN. Our data showed that only the mecamylamine infused into the MHb, but not the IPN, alleviated the anxiety-like behavior in mice, indicating that nAChRs in dendrites/soma, but not presynaptic terminals, of MHb neurons inherently modulate anxiety-like behaviors. These results also suggest that nAChRs on the presynaptic terminals might be involved in anxiety.

We also infused the NMDA receptor antagonist, AP-5, into the IPN, which resulted in the anxiolytic effect in mice, suggesting that glutamatergic signaling in the IPN modulates anxiety-like behavior, which is consistent with the optogenetics study in Chapter II.

It has been shown that several nAChR subunit genes are expressed in the MHb, but why the diversity of nACh subtype is huge here is unclear. In Chapter III, we checked the precise repertoire of nAChR subunits specifically expressed in MHb cholinergic neurons by laser-microdissected and qRT-PCR. We found that α3, α4,

β2, β3, β4 subunit genes was relatively strong compared to the house-keeping gene GAPDH.

As the α4 subunit is highly expressed in the MHb, in Chapter III, we test the sufficiency and necessity of α4 subunit in the activation of MHb cholinergic neurons in two complementary mouse lines: α4 KO mouse line (a mouse line which does not express chrna4) and L9'A mouse line (a mouse line that expresses a single point mutation in chrna4 that renders nAChRs hypersensitive to agonist). When challenged with low dose of nicotine, only the L9'A mouse, but not wild type mice or α4 KO mice, exhibit increased c-fos (neuronal activation marker) expression in the MHb. In contrast, when challenged with high dose of nicotine, the wild type mice exhibited significant c-Fos expression in MHb cholinergic neurons, while c-Fos expression was dramatically lower in cholinergic MHb neurons of α4 KO mice. Together, these data indicate that functional nAChRs containing the α4 subunit are necessary and sufficient for nicotine activation of MHb cholinergic neurons, which is consistent with a previous study (Fonck, Nashmi et al. 2009). In addition, it has been shown that systemic (i.p.) nicotine (0.5 mg/kg) has anxiogenic effect in mice (Zarrindast, Homayoun et al. 2000), but we did not found c-fos expression in MHb after 1 mg/kg nicotine injection. C-fos, has been extensively used as a marker for the neuronal activation since 1987 (Hunt, Pini et al. 1987), but it does not necessarily mean there is no neuronal activation without c-fos expression. Therefore, it is possible

that 1 mg/kg nicotine injection activated the MHb neurons but it is not enough to induce the c-fos expression.

In order to probe the behavioral consequences of α4* receptors in MHb cholinergic neurons, we designed a system to express “gain-of-function” L9'S α4 nAChR subunits in discrete neuron populations using viral-mediated gene delivery combined with the Cre-Lox system. These novel ACh detectors will facilitate identification of the behavioral role of ACh through nAChR signaling in individual circuits. In Chapter III, our data indicate that cholinergic signaling through nicotinic autoreceptors in MHb cholinergic neurons regulates anxiety-like behavior in mice. In detail, expression of α4 nAChR subunit ACh detectors selectively in MHb cholinergic neurons increased anxiety-like behavior. Anxiety was alleviated by blocking the hypersensitive nAChRs with a low dose of antagonist either systemically or locally within the MHb, indicating that heightened anxiety was mediated through activation of ACh detector nAChRs and not due to additional factors such as nAChR desensitization or excitotoxicity. Together, these data indicate that α4* nAChRs in the MHb cholinergic neuron are critical for the anxiety-like behavior in mice. Alternatively, the expression of hypersensitive α4* nAChRs in the MHb cholinergic neuron could increase the overall sensitivity of the nAChRs, increase the activity of cholinergic neurons, and in turn increase anxiety in mice.

In addition, in Chapter III, we also found that the ACh detector expressing mice showed prolonged hypolocomotion when challenged with high dose nicotine. Interestingly, in Chapter II, we showed that high frequency stimulation of MHb cholinergic neurons, which caused ACh release in the IPN, induced hypolocomotion. These two evidences together suggest that the high dose of nicotine or high frequency of stimulation may induce ACh release in the IPN, and the hypersensitive L9'S ACh detector expressing mice are more sensitive to high dose of nicotine, thus showed prolonged hypolocomotion. Previous studies have shown that the α3 and β4 nAChRs are necessary for nicotine-induced hypolocomotion using the α3KO mice and β4KO mice (Salas, Cook et al. 2004). As α3 and β4 are highly expressed in the MHb-IPN tract, together with our data, it suggests that the nAChRs in the MHb-IPN tract are critical for nicotine induce hypolocomotion.

Previous studies implicated the MHb in physical nicotine withdrawal behaviors as well as acute nicotine intake and aversion. Expression of L9'S α4* nAChRs in MHb cholinergic neurons increased anxiety-like behavior, a predominant affective withdrawal symptom, essentially mimicking what may happen if one or more nAChR subtype was functionally upregulated after chronic nicotine exposure. Confirming this idea, we found that after chronic nicotine treatment, the α6* nAChRs are functionally upregulated (by the qRT-PCR and electrophysiological recording), and the anxiety during nicotine withdrawal was

alleviated by infusion of the α4β2* and the α6* nAChR-selective antagonist into the MHb.

It has been shown that intravenous nicotine self-administration (approximately 1.5 mg free base/kg/day) increased α6* nAChRs expression in VTA/SN and nucleus accumbens (Parker, Fu et al. 2004). In contrast, chronic nicotine treatment by minipump (3–6 mg/kg/day administrated for 14 days) or by drinking water (50–300 μg/ml for up to 6 weeks) decreases the number of α6* receptors in midbrain dopaminergic neurons (Mugnaini, Tessari et al. 2002, Lai, Parameswaran et al. 2005, Perry, Mao et al. 2007, Gotti, Guiducci et al. 2010). It is interesting that the regulation of nAChRs by long-term nicotine treatment in rodents may strongly depend on the dosage of nicotine, the method of nicotine delivery and the brain regions checked.

A recent study showed that mice harboring α6 subunits with an eGFP tag exhibited an increase in fluorescent signal in the MHb after chronic nicotine treatment compared to control mice. In consistence with our data, we both showed that there is a upregulation of α6 subunit in the MHb after nicotine exposure and this upregulation of α6 subunit is critical for anxiety during nicotine withdrawal (Henderson, Srinivasan et al. 2014).

Importantly, we previously identified a novel nAChR containing both α4 and α6 subunits in DAergic neurons of the VTA and show here that nicotinic currents in the MHb subregion that predominantly expresses the α6 subunit also contains

the α4 subunit, suggesting that α4α6* nAChRs are upregulated by chronic nicotine exposure and contribute to increased anxiety-like behavior during nicotine withdrawal (Liu, Zhao-Shea et al. 2012, Liu, Hendrickson et al. 2013, Shih, Engle et al. 2014).

In conclusion, here is our model of MHb cholinergic neuron nAChRs in regulating anxiety-like behaviors:

A) Cholinergic/glutamatergic MHb neurons project to the IPN and these neurons synthesize and co-release the neurotransmitter glutamate, in addition to ACh (Ren, Qin et al. 2011) (Fig VI-1A).

B) In chapter II, we showed that silencing the MHb cholinergic neurons activity reduced anxiety (Fig VI-1B), whereas activating MHb cholinergic neurons with high frequency induced hypolocomotion (Fig VI-1C).

C) In chapter III, our data indicate that nAChRs expressed at the level of the soma/dendrites of these neurons likely regulate neuronal activity and anxiety, because mecamylamine infusion into the MHb reduced anxiety-like behaviors; whereas blockade of MHb presynaptic nAChRs in the IPN or IPN nAChRs themselves did not affect anxiety-like behavior (Fig. VI-1D).

D) In Chapter III, our data suggest that expression of nAChRs that are hypersensitive to agonist specifically in cholinergic/glutamatergic MHb neurons increases anxiety-like behavior presumably through increasing glutamate release into the IPN (Fig. VI-1E).

E) In Chapter IV, during nicotine withdrawal, nAChRs are functionally upregulated, increasing activation of MHb neurons and glutamate release in the IPN leading to increased anxiety-like behavior (Fig. VI-1F).

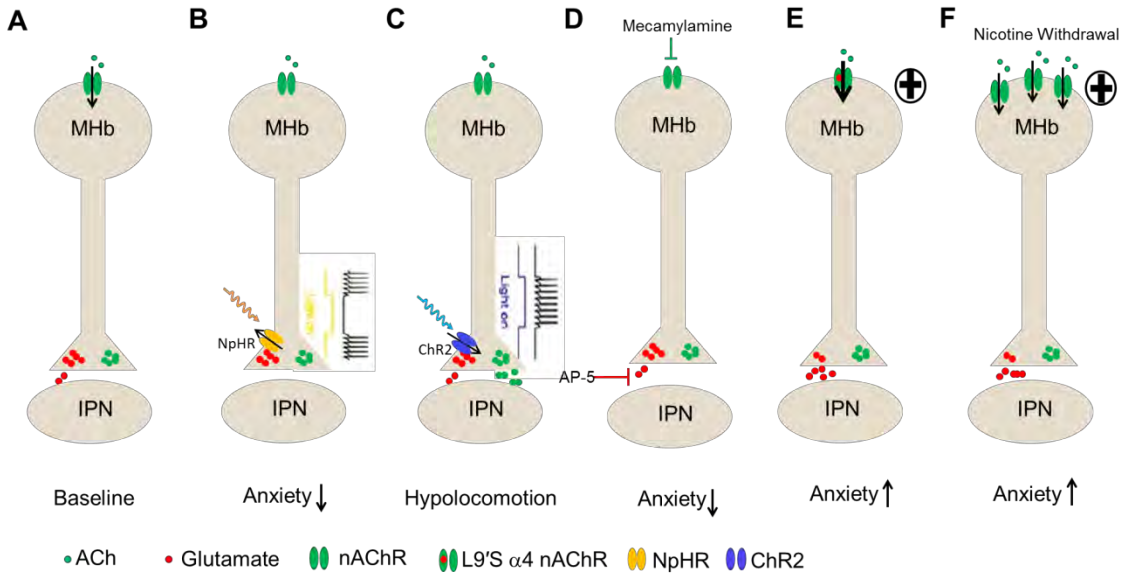

Figure VI-1. Model of MHb cholinergic neuron nAChRs in regulating anxiety-like behaviors.

A. Cholinergic/glutamatergic MHb neurons project to the IPN (baseline).

B. Silencing MHb cholinergic neurons reduced anxiety-like behaviors.

C. Activating MHb cholinergic neurons with high frequency induced hypolocomotion.

D. Blockade of nAChRs in MHb or blockade of NMDA receptors in the IPN reduce anxiety-like behavior.

E. Expression of nAChRs that are hypersensitive to agonist specifically in cholinergic/glutamatergic MHb neurons increases anxiety-like behavior presumably through increasing glutamate release into the IPN.

F. Chronic nicotine treatment upregulate the nAChRs in the MHb. During nicotine withdrawal, upregulated nAChRs increased activation of MHb neurons and glutamate release in the IPN leading to increased anxiety-like behavior.

Future directions

A. Where is the MHb cholinergic input from?

The medial habenula is a key connection between the limbic forebrain and midbrain. Physiological and neurochemical studied have shown that the MHb has the highest expression of nicotinic acetylcholine receptors (nAChRs) (Sheffield, Quick et al. 2000). Evidence from the lesion studies indirectly showed that the NDB or posterior septum might send the cholinergic input to the MHb (Contestabile and Fonnum 1983). However, in Chapter IV, using AAV2-ChR2 as a tracer, we showed that cholinergic neurons that originate from MS/DB project to the hippocampus but not MHb.

MHb is one of the brain regions that have the highest nAChRs expression level, suggesting that there must be strong ACh release to it. Thus, there are two possibilities: 1) Some other unknown brain region sends the cholinergic input to the MHb; or 2) the cholinergic neurons in the MHb release the ACh to themselves to feed forward the neuronal circuit. More studies need to be done to test the possibilities.

To test the first possibility, one can infuse small volume anterograde tracer into MHb and map all the neuronal population that project to it. To screen the candidate cholinergic input to MHb, the anterograde tracer labeled neuronal populations can also be double labeled immunohistochemically with cholinergic neuronal markers, like ChAT. The anterograde tracer and ChAT double positive neuronal population will be the cholinergic input to MHb. On the other hand, one

can also use AAV2-ChR2 as a tracer as I did in this thesis and double confirm this candidate brain region send the cholinergic input to MHb.

To test the second possibility, one can test whether strong stimulation (electrically or optically by ChR2) on MHb will induce ACh release (by microdialysis or electrophysiology) in the MHb cholinergic neurons in the presence of presynaptic ACh release inhibitor. It will be interesting if the cholinergic neurons feed forward themselves, and the behavior output of it will be worth to study.

B. Are MHb cholinergic neurons involved in general anxiety?

Human and animal studies have shown the neurocircuitry of anxiety, including the amygdala, nucleus accumbens, BNST and hippocampus (Adhikari 2014). Recently the role of the MHb-IPN tract in anxiety and fear has attracted much attention. Previous work indirectly demonstrated a role for the MHb in anxiety regulation, either through lesioning of the habenula itself or through selective ablation of presumed septal glutamatergic inputs into the MHb (Yamaguchi, Danjo et al. 2013). Here in my study, we showed that MHb is directly involved in anxiety during nicotine withdrawal. In addition, expression of nAChRs that are hypersensitive to agonist specifically in cholinergic/glutamatergic MHb neurons increases anxiety-like behavior. However, whether the cholinergic neurons in the MHb are involved in general anxiety is still unclear.

To answer this question, one can test whether blocking nAChRs in the MHb will alleviate anxiety in other anxiety or stress animal models (repeated social defeat

model, forced swimming, tail suspension test). On the other hand, one can also test the expression of hypersensitive in MHb cholinergic neurons increases anxiety/stress-like behavior in these animal models.

C. Is MHb-IPN circuit also involved in other drugs of abuse?

Some evidence showed that MHb may contribute to the development of morphine tolerance and withdrawal. For instance, chronic morphine administration (20, 40, 60, 80, 100, and 100 mg/kg three times per day) results in a reduction in acetylcholinesterase (AChE) activity in the MHb, but not IPN (Neugebauer, Einstein et al. 2013). In addition, morphine dependent mice showed increased nicotinic acetylcholine receptor (nAChR) levels in MHb (Neugebauer, Einstein et al. 2013). For cocaine abuse, a study by Maroteaux and Mameli (2012) showed the synaptic plasticity of LHb neurons, but not MHb neurons in mice after exposure to cocaine. Therefore, it is worth studying whether and how the MHb- IPN circuit is involved in regulating response to other drugs of abuse, like morphine and cocaine. If they do, whether all drug abuse share the same mechanism in MHb-IPN circuit to signal anxiety during withdrawal is still questionable.

D. Are other neurotransmitter signalings other than nAChR involved in anxiety?

It has been shown that different subregions of the medial habenula (MHb) use different combinations of neurotransmitter systems (Aizawa, Kobayashi et al. 2012). It could be categorized as exclusively glutamatergic (sMHb), both

substance P-ergic and glutamatergic (dMHb), or both cholinergic and glutamatergic (vMHb) (Aizawa, Kobayashi et al. 2012). How these different neurotransmitter systems involved in different behaviors are still unclear. The cellular mechanism of these neurotransmitter involved in anxiety also need to be studied. One can use the immunostaining, western blot, in combination with pharmacological treatment and behavior test to study the role of different neurotransmitter system of MHb in anxiety.

E. How MHb subregions talk to IPN subregions and control different behavior? The medial habenula sends major inputs to the interpeduncular nucleus (IPN) via fasciculus retroflexus (fr) (Herkenham and Nauta 1977, Carlson, Noguchi et al. 2001). MHb projects to distinct subnuclei of the IPN, and releases three distinct neurotransmitters: ACh, Glu, and SP (Ren, Qin et al. 2011, Aizawa, Kobayashi et al. 2012). The dorsal MHb innervate the lateral IPN (IPL and IPR, described below) in a cluster pattern and release the SP; the ChAT positive neurons in the ventral MHb innervate the ventral IPN (Contestabile, Villani et al. 1987) and the MHbVl part only innervates the dorsal IPN (IPR, described below) (Shih, Engle et al. 2014), and they release ACh and Glu at different transmission modes (Herkenham and Nauta 1979, Contestabile and Flumerfelt 1981, Ren, Qin et al. 2011). This highly restricted neurotransmitter expression and projection pattern suggest that the subnuclei might have specific functions in the brain. To test this idea, one can use subregion specific promoter to drive the expression of ChR/

NpHR or other gain of function/loss of function tools, and test the acitivity change in the cell level and behavior level.

In conclusion, MHb is a key connection between the limbic forebrain and midbrain. It might be involved in several important behaviors, like aversion and anxiety. But the mechanisms underlie that are still largely unknown and need to be further studied.

Appendix 1.

Light illumination is a critical determinant of the behavior of mice in the elevated plus maze

Contributions:

I did all the experiments, wrote all the text, and made all the figures.

A1.A. Introduction

A variety of animal models of anxiety has been developed to screen effects of drugs and to study the psychological and neurochemical basis of anxiety disorders, such as elevated plus maze test (EPM), social interaction test, fear-potentiated startle test, light-dark exploration and mirrored chamber. The elevated plus test is one of the most commonly used animal models. Usually, mice show exploratory behavior on the EPM apparatus and tend to stay in the closed arms of the maze. When the mice were forced onto the open arm, the plasma corticosterone concentrations increased, which is indicative of increased anxiety (File, Zangrossi et al. 1994, Rodgers, Haller et al. 1999). Administration of anxiolytic compound increase the time spent in the open arm and the number of entries to the open arms (Dawson and Tricklebank 1995). The locomotor activity also can be assessed by monitoring the total arm entries to both the closed and open arms in the EPM.

However, when using this assay, researchers often get contradictory results from the same pharmacological experiments. In addition to the sensitivity of the different stains and the dose of drug used in the experiment, the inter–laboratory variability in implementation of the EPM may also be a key factor that causes contradictory results. But, only few studies provide clear information on the detailed experimental design for EPM, such as level of illumination, strain, traits,

habituation and handling the mice. Therefore, the aim of the present study is to test several methodological factors (illumination level, mice strain, food baits, and habituation) that may contribute to the variability in mice behavior in the elevated plus maze.

A1.B. Materials and methods

Animals

C57BL/6J mice and ChAT-Cre mice were used for the experiments in this chapter. All the mice used in the experiments were bred in our animal facilities. For ChAT-Cre mice, genotypes were determined by PCR as previously described (Rossi, Balthasar et al. 2011) and also on Jackson Laboratories website. PCR of mouse tail genomic DNA was performed with three specific primers, WT F (5′-GTT TGC AGA AGC GGT GGG-3′), mutant F (5′-CCT TCT ATC GCC TTC TTG ACG -3′) and Common R (5′-AGA TAG ATA ATG AGA GGC TC -3′). These primers amplify DNA fragments of 272 bp in wild-type (WT) mice, and 350 bp in ChAT-Cre mutant mice. DNA fragments were separated by agarose gel electrophoresis and visualized with ethidium bromide. The mice were group housed four mice/cage on a light-dark cycle with lights on at 7:00 a.m. and off at 7:00 p.m, and given food and water ad libitum. Mice were between 8-10 weeks old for all experiments. Behavioral experiments were performed during the light cycle. Independent groups of animals were used for each behavioral experiment.

All experiments were conducted in accordance with the guidelines for care and use of laboratory animals provided by the National Research Council (National Research Council Institute for Laboratory Animal 1996), as well as with an approved animal protocol from the Institutional Animal Care and Use Committee of the University of Massachusetts Medical School.

Apparatus

The experimental apparatus consisted of a central axis and four arms elevated 45 cm above the floor, with each arm positioned at 90° relative to the adjacent arms. One red light arranged at 100 cm above the maze was used as the source of illumination. The mice were individually placed in the center of the maze with their heads facing one of the open arms and allowed 5 min of free exploration. The number of entries into the open and closed arms, and the total time spent in the open and closed arms were measured by MED-PC IV software (MED Associates, Inc.) The time spent in open and closed arms was calculated as standard anxiety indices. The total number of arm entries was considered as an index of locomotor activity. The apparatus was cleaned thoroughly between trials. Mice that froze in the initial arm without moving were not included in the analysis.

Procedures

Experiment 1: Effect of level of illumination

Experiments were carried out at two different light intensities: low intensity or high intensity. For the low intensity, the level of the illumination on the central platform in the center and both the open arms was 40 lux, whereas for the high intensity, the level of the illumination on the central platform in the center and both the open arms was 400 lux.

Experiment 2: Effect of different stains

C57BL/6J mice and ChAT-Cre mice were used for the experiments.

Experiment 3: Effect of habituation

Mice were divided into two groups: with habituation or no habituation. For the no habituation group, mice were directly taken from the colony room to the behavior room, and put on the EPM apparatus. For the habituation group, mice were put into the behavior room for 30 min, and then put on the EPM apparatus.

Experiment 4: Effect of bait

Mice were divided into two groups: with baits or no baits. For the baits group, standard mouse chow was taken from their home cage and put onto the open arms of the apparatus 1/3 away from the distal end of the open arm. For the no baits group, no food was put onto the apparatus.

Statistics

Data were analyzed using Student"s t-test. Results were considered significant at $p < 0.05$. All data are expressed as means ± SEM.

A1.C. Results

Light intensity

Analysis with the Student t-test shows that in the ChAT-Cre mice line, mice with high intensity condition significantly reduced the time spent in open arms compared to the mice with low intensity condition, from 72.59 ± 7.74s to 18.12 ± 8.70s in the no food group, and from 159.74 ± 31.07s to 42.89 ± 4.04s in the food baits group (Figure A1-1, Figure A1-2A).

Habituation

In the C57BL/6J line, mice with habituation tend to spend less time in the open arm compared to the no habituation group (Figure A1-1, Figure A1-2B), but these differences were not significant.

Strain

Analysis with the student t-test shows that there is no significantly difference between C57BL/6J mice line and ChAT-Cre mice line when they have no habituation (Figure A1-1, Figure A1-2C).

Bait

In all the groups, mice with food baits tended to increase the time spend in the open arm compare to the no food baits groups. Only for the ChAT-Cre mice with low intensity illumination, there is significant difference between the mice with food baits and those without food baits (Student"s t-test, * $p<0.05$). In this condition, time spent in the open arm increase from 72.59 ± 7.74s (no food baits) to 159.74 ± 31.07s (with food baits) (Figure A1-1, Figure A1-2D).

Lomomoter activity

Overall, for the locomotor acitivity, there were no significant differences among all the groups (Figure A1-2).

A1.D. Discussion

In the elevated plus maze test, rodents are placed in the intersection of the four arms of the elevated plus maze and their behavior is typically recorded for 5 min (Montgomery 1955), the behavioral results showed that the mice prefer the closed arms to the open arms. However, when use these animal model, researchers often get contradictory results from the same pharmacological experiments, as the EPM conditions used in different labs might be distinct.

Here we tested several determinants that might influence the behavior of mice in the elevated plus-maze. Our results showed that the level of illumination of the experimental area is a critical determinant of the time spent in the open arm of the mice in EPM. In a highly illuminated room, mice showed a greater avoidance

of the open arms than in a less intensely illuminated one. These results are consistent with previous studies that brightly lit test areas are aversive to many strains of rats and mice (Crawley and Goodwin, 1980; File, 1980; Crawley, 1985; Morato and Castrechini, 1989; Benjamin et al., 1990).

The second factor evaluated here is the baits such as food from the mice home cage which has the familiar smell. The food baits also played an important role in the performance of mice in the EPM. Animals tested with the food baits showed increased time spent in open arms than those without food baits. Especially for the ChAT-Cre line, food baits group significantly spend more time in the open arms. These data suggest that the familiar smell from the food bait and the food itself might have anxiolytic effect on mice, thus mice spend more time in the open arm. In addition, our lab has found that in the ChAT-Cre line, the ChAT expression level is lower than that in the C57BL/6J mice. Together with our data in this study, cholinergic system in the brain might be involved in the feeding behavior and anxiety.

The third factor evaluated here is habituation to the EPM room. Previously, it has been shown that rats did not habituate with repeated test trials. Instead, they appeared to become more anxious as open-arm avoidance increased on the repeated trials (Treit, Menard et al. 1993). Here we showed that habituation to the room also affected level of performance in mice. Mice with habituation spent around 20% less time compare to the mice without habituation. Together with

previous study, we conclude that habituation to either the apparatus or the behavior room has the anxiogenic effect.

We also test the difference between the C57black6 mice line and ChAT-Cre mice line at 40 Lux in absence of habituation, but no significant difference were found.

In summary, when using the elevated plus-maze, the light intensity, habituation and food baits are critical determinants, which should be taken into account by each laboratory when attempting to identify the optimal conditions for their investigation.

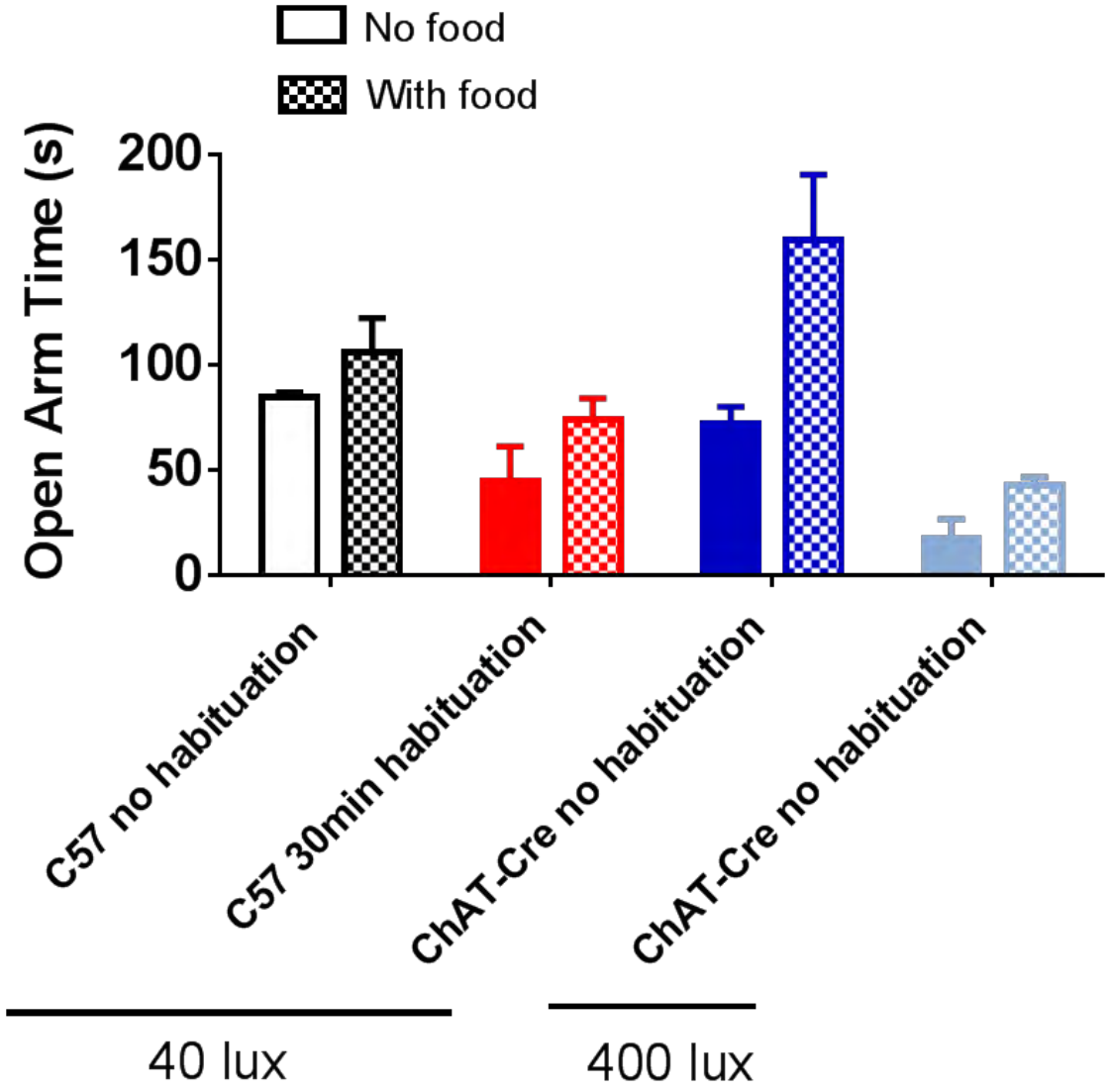

Figure A1-1. Effects of illumination, mice strain, baits, and habituation on the time spent in the open arms of mice in the elevated plus-maze. C57 mice and ChAT-Cre mice line were used at two illumination conditions (40 lux or 400 lux), with or without food baits, with or without habituation. Results are expressed as time spent (seconds) in the open arms (mean ± SEM).

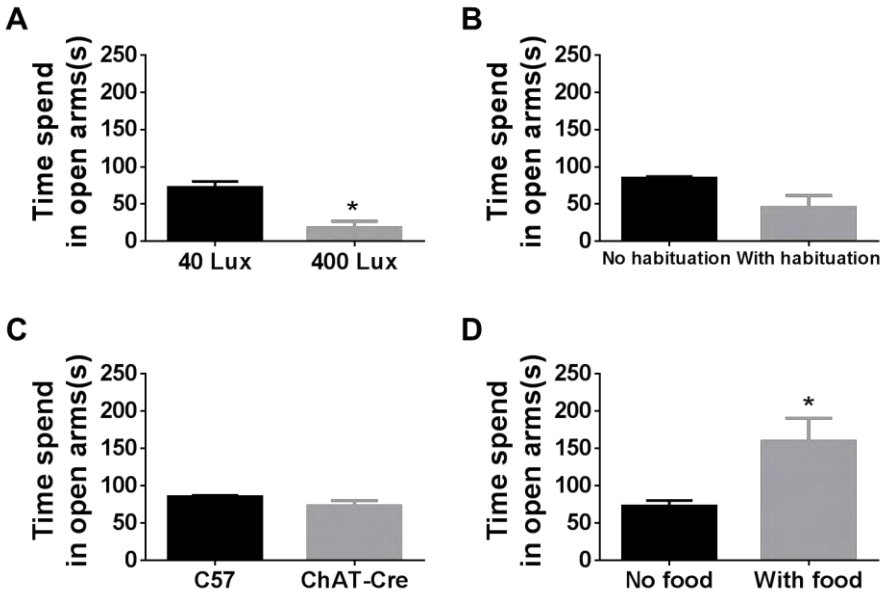

Figure A1-2. Effects of illumination, mice strain, baits, and habituation on the time spent in the open arms of mice in the elevated plus-maze (Data are replotted from Fig. A1-1).

A. ChAT-Cre mice were tested at two illumination conditions (40 lux or 400 lux). Mice with 400 lux intensity spend significantly less time compare to the mice with 40 Lux.

B. In the C57BL/6J line, mice with habituation tend to spend less time in the open arm compared to the no habituation group under 40 lux light intensity.

C. C57BL/6J mice and ChAT-Cre mice spent similar time in the open arm under 40 lux light intensity.

D. ChAT-Cre mice with food baits increase the time spent in the open arm compare to the no food baits groups.

Results are expressed as time spent (seconds) in the open arms (mean ± SEM). For A-D, * $p < 0.05$, Student‟s t-test.

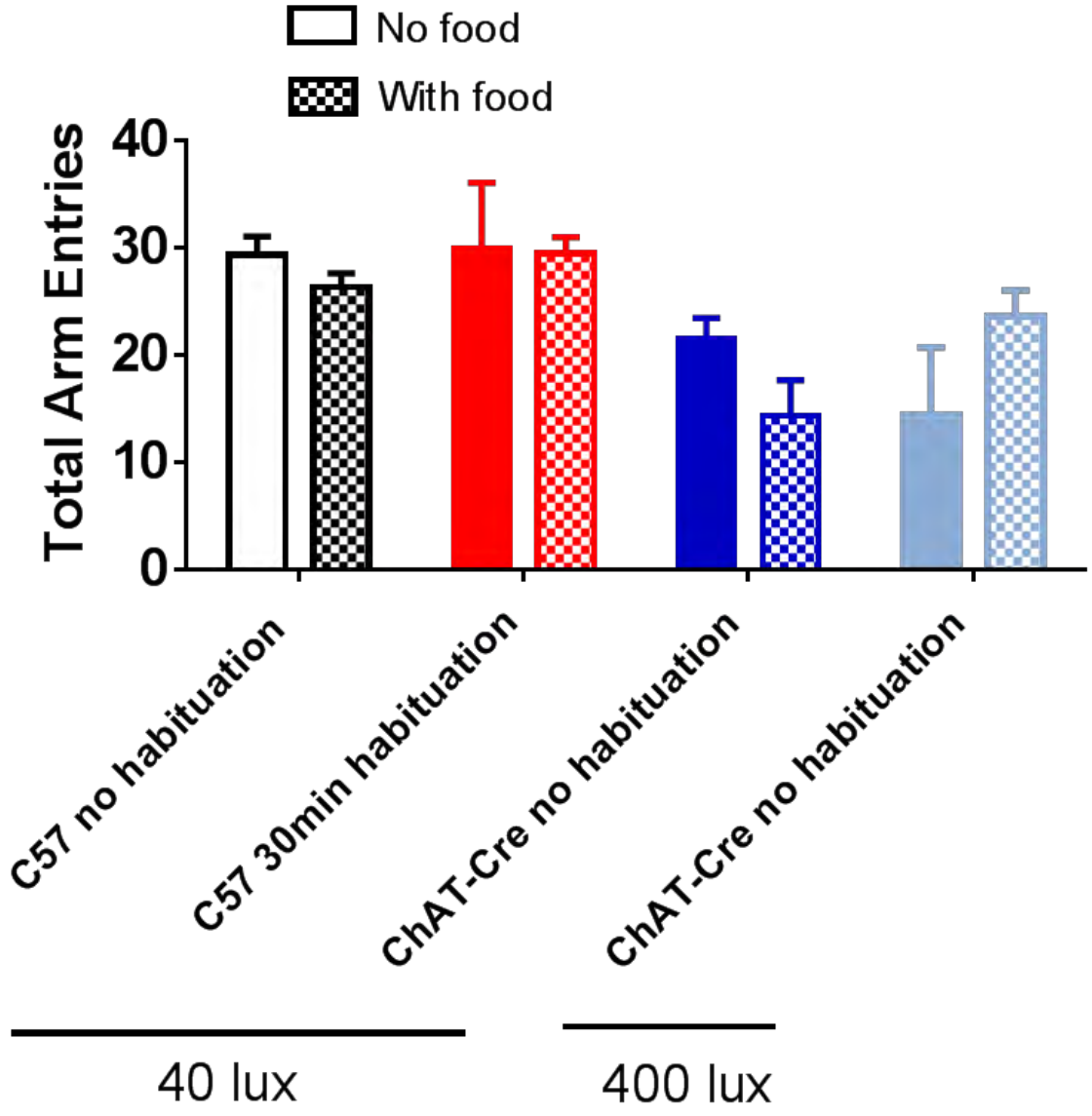

Figure A1-3. Effects of illumination, mice strain, baits, and habituation on the total arm entries of mice in the elevated plus-maze. C57 mice and ChAT-Cre mice were used at two illumination conditions (40 lux or 400 lux), with or without food baits, with or without habituation. Results are expressed as total entries in all the arms (mean ± SEM).

APPENDIX 2.

Dicer expression is essential for adult midbrain dopaminergic neuron maintenance and survival

This chapter has been published separately in:

Pang, X., E. M. Hogan, A. Casserly, G. Gao, P. D. Gardner and A. R. Tapper (2014). Dicer expression is essential for adult midbrain dopaminergic neuron maintenance and survival. Mol Cell Neurosci 58: 22-28.

Contributions:

Eric Hogan and Alison Casserly did the qRT-PCR, Guangping Gao made the virus, I did all the other experiments and made all the figures. Dr. Andrew Tapper and Paul Gardner wrote most of the text.

A2.A. Introduction

MicroRNAs (miRNAs) are small, non-coding RNAs that modulate mRNA expression (Cao, Yeo et al. 2006, Bicker and Schratt 2008, Fiore, Siegel et al. 2008, Pietrzykowski, Friesen et al. 2008, Huang and Li 2009, Karr, Vagin et al. 2009). miRNAs bind to miRNA-recognition elements (MRE), specific sequences usually located in target mRNA 3′-untranslated regions (UTRs) resulting in either mRNA cleavage (Bartel 2004, Huppi, Martin et al. 2005, Martin and Caplen 2006) or inhibition of translation (Ambros 2004, Bartel 2004, Zamore and Haley 2005). In some cases, miRNAs have been shown to increase expression of their target genes (Vasudevan, Tong et al. 2007). miRNAs are derived from long primary transcripts that are sequentially processed by the ribonuclease, Drosha, and the type III RNAse, Dicer. While it is clear that miRNA expression and function is critical during CNS development (Davis, Cuellar et al. 2008, De Pietri Tonelli, Pulvers et al. 2008, Li, Bian et al. 2011, McLoughlin, Fineberg et al. 2012) and neuronal maintenance and survival in some brain regions during post-natal periods (Schaefer, O'Carroll et al. 2007), the role of miRNAs in the adult CNS is still largely unknown.

In the dopaminergic (DAergic) neuron-rich midbrain, a structure critical for voluntary locomotor processing and motivation (Salamone and Correa 2012, Sulzer and Surmeier 2013), miRNA expression is essential for midbrain formation during development and DAergic neuron differentiation. Wnt1-Cre-

mediated conditional loss of Dicer in mice results in embryos with smaller midbrains compared to control embryos (Huang, Liu et al. 2010). In addition, Wnt1-Cre Dicer knock-out (KO) mice express DAergic precursor neurons that do not properly differentiate into DAergic neurons at E12.5. In cell culture, Dicer deletion in DAergic neurons derived from embryonic stem cells, triggers apoptosis and neuronal-like cell death (Kim, Inoue et al. 2007). Finally, conditional knock-out of Dicer in dopamine transporter (DAT)-expressing neurons results in significant death of midbrain DAergic neurons in mice by three weeks of age. However, whether expression of Dicer dependent miRNAs is critical for maintenance and survival of adult midbrain DAergic neuron areas is unknown. We sought to test the hypothesis that Dicer expression, and by extension miRNAs, are critical for DAergic neuron maintenance and survival even in adult animals. To do this, we knocked-out Dicer expression in mice homozygous for a floxed Dicer allele ($Dicer^{flox/flox}$) allowing for conditional knock-out of Dicer in neuronal populations that express Cre (Harfe, McManus et al. 2005). However, to induce Dicer deletion in discreet midbrain areas during adulthood, we delivered Cre into the VTA and SNpc using adeno-associated virus (AAV)-mediated gene delivery.

A2.B. Materials and methods

Animals

Dicer$^{flox/flox}$ mice, which contain loxP sites on either side of exon 23 of the Dicer1 (Dicer1, Dcr-1 homolog (Drosophila)) gene, were purchased from Jackson Laboratories and bred in our animal facilities. Breeding was conducted by mating heterozygous pairs. The mice were group housed four mice/cage on a 12-h light-dark cycle and given food and water ad libitum. Male mice were used for all experiments. Mice were at least 8 weeks old at the beginning of each experiment. All experiments were conducted in accordance with the guidelines for care and use of laboratory animals provided by the National Research Council (National Research Council Institute for Laboratory Animal 1996), as well as with an approved animal protocol from the Institutional Animal Care and Use Committee of the University of Massachusetts Medical School.

Virus microinjection

AAV2-CMV-PI-Cre-ZsGreen and AAV2-eGFP virus particles were provided by the viral vector core facility of the University of Massachusetts Medical School. Dicer$^{flox/flox}$ mice were anesthetized with a mixture of ketamine (100 mg/kg) and xylazine (10 mg/kg) (VEDCO). The surgical area was shaved and disinfected. Mice were placed in a stereotaxic frame (Stoelting Co.) with mouse adaptor and a small incision was cut in the scalp to expose the skull. Using bregma and lambda as landmarks, the skull was leveled in the coronal and sagittal planes. AAV2-Cre-ZsGreen or AAV2-eGFP was injected into either VTA or SNpc. For the VTA, the coordinates were: anterior-posterior (AP), −3.3 mm from bregma;

medial-lateral (ML), ±0.5 mm from midline; dorsal-ventral (DV), −4.0 mm from brain surface. For the SNpc, the coordinates were: AP, −3.0 mm from bregma; ML, ±1.5 mm from midline; DV, −4.0 mm from brain surface. The virus (1×10^{12} viral particles/ml, 0.5 µl/side) was injected at a flow rate of 0.1 µl/min. The injection needle remained in place for 5 min post-injection before slowly being withdrawn.

Genotyping

As described previously (Harfe, McManus et al. 2005), two sets of primers were used to verify the insertion of the loxP site and the deletion of the Dicer gene. The conditional floxed allele was genotyped using primers DicerF1 (5′-CCTGACAGTGACGGTCCAAAG-3′) and DicerR1 (5′-CATGACTCTTCAACTCAAACT-3′), which amplify a DNA fragment that is 351 bp in wild-type (WT) mice, and 420 bp in $Dicer^{flox/flox}$ (Figure A1-1). Four weeks after the AAV2-Cre-ZsGreen virus infection, brain tissue was laser captured (described below). Total DNA was extracted with a tissue DNA extraction kit (DNeasy Blood & Tissue Kit, Qiagen). The deletion allele was genotyped using primers DicerF1 and DicerDel (5′-CCTGAGCAAGGCAAGTCATTC-3′). The band for the deleted allele is 471 bp whereas the band for a WT allele is 1,300 bp (Figure A1-1).

Laser capture microdissection

Eight weeks after virus infection, mice were sacrificed and the brains were removed, snap-frozen in dry ice-cooled 2-methylbutane (−60°C) and stored at −80°C. Coronal serial sections (10 μm) were cut using a cryostat (Leica Microsystems Inc.) and mounted on pre-cleaned glass slides (Fisher Scientific). The sections were immediately placed in a slide box on dry ice until completion of sectioning followed by storage at −80°C. Frozen sections were allowed to thaw for 30 s and then immediately fixed in cold acetone for 4 min. The slides were washed twice in PBS (prepared in DEPC water) and subsequently dehydrated in a graded ethanol series (for 30 s each in 70% ethanol, 95% ethanol, 100% ethanol, and once for 5 min in xylene). Slides were allowed to dry for 5 min. All ethanol solutions and xylene were prepared fresh to preserve RNA integrity. The Veritas Microdissection System Model 704 (Arcturus Bioscience) was used for laser capture microdissection (LCM). ZsGreen- or EGFP-positive neurons were captured on CapSure Macro LCM caps (Arcturus Bioscience) for total RNA isolation.

Real-time PCR

Total RNA was extracted from individual replicate samples using a Micro Scale RNA Isolation Kit (Ambion). miRNAs were amplified from laser-captured material except for miR-133b which was amplified from tissue punches of infected areas due to low yield. RNA samples extracted from ZsGreen- or eGFP-positive neurons were reverse-transcribed into cDNA using a miRNA TaqMan Reverse

Transcription Kit (Applied Biosystems). Quantitative reverse transcription-PCR (qRT-PCR) was performed using an Applied Biosystems 7500 Real-Time System and miRNA TaqMan assays (Applied Biosystems). Samples containing no reverse transcriptase were used as negative controls. Relative gene expression differences between eGFP-positive neurons and ZsGreen-positive neurons were calculated using the $2^{-\Delta\Delta Ct}$ method. Expression values were normalized to expression of sno202, a small nucleolar RNA not produced by Dicer (Politz, Hogan et al. 2009, Brattelid, Aarnes et al. 2011). Samples were analyzed in triplicate. Student's t-test was used for statistical analysis.

Immunohistochemistry

Eight weeks after virus infection, mice were sacrificed and the brains removed to make coronal serial sections (10 μm) and mounted onto pre-cleaned glass slides. Immunolabeling was done as previously described (Zhao-Shea, Liu et al. 2011). Briefly, the sections were immediately placed in a slide box on dry ice until completion of sectioning followed by storage at −80°C. The frozen sections were thawed for 30 s and fixed in 4 % paraformaldehyde in 0.01 M sodium phosphate buffer (pH 7.4). The slides were rinsed in PBS twice for 5 min, and treated with 0.2 % Trition X-100 PBS (PBST) for 5 min followed by incubation in 2 % BSA/PBS for 30 min. Sections were washed with PBS once and then incubated in primary antibodies directed to tyrosine hydroxylase (TH, monoclonal, 1:250 dilution, Santa Cruz Biotechnology) in 2 % BSA/PBS overnight at 4°C. The

sections were washed with PBS three times for 5 min followed by incubation in secondary fluorescent labeled (goat anti-mouse Alexa Fluor 594, 1:300 dilutions, Invitrogen) at room temperature in the dark for 30 min. For NeuN and TH double labeling, the sections were washed with PBS and incubated with primary antibodies NeuN (monolclonal, 1:100 dilution, Millipore) and TH (polyclonal, 1:1000 dilution, Santa Cruz Biotechnology) overnight at 4°C. After PBS washing, the secondary antibodies (goat anti-mouse Alexa Fluor 594 and goat anti-rabbit Alexa Fluor 488, 1:300 dilutions, Invitrogen) were incubated at room temperature in the dark for 30 min. After washing with PBS 5 times for 5 min/wash, sections were covered with cover slides using VECTASHIELD® Mounting Medium (Vector laboratories, Inc.). Neurons were counted as signal-positive if intensities were at least 2 times higher than that of the average value of background (sections stained without primary antibodies).

TUNEL staining

Frozen sections were made as described above at different time points (2 weeks, 4 weeks, 6 weeks and 8 weeks) after virus infection. The TUNEL assay (Roche Diagnostics, Mannheim, Germany) was performed according to the manufacturer's instructions.

Locomotor activity

Locomotor activity was recorded using an automated system (San Diego Instruments, La Jolla, CA, USA) with photobeams, which recorded ambulation

(consecutive beam breaks). Before virus microinjection, mice were placed individually in a novel cage and recorded for 90 min for their baseline locomotor activity. At different time points after the virus infection (4 weeks, 6 weeks, and 8 weeks), locomotor activity was recorded in a novel cage. For amphetamine treatment, mice were placed in a novel cage and activity was recorded for 20 min, followed by an i.p. injection of amphetamine (0.5 mg/kg) or saline. Activity post-injection was recorded for 3 h.

Rotarod test

A rotarod apparatus (San Diego Instruments, San Diego, CA) was used to evaluate motor coordination and balance. Mice were placed on an accelerating rod (4 to 40 rpm) over a period of 300 s. Any mice remaining on the apparatus after 300 s were removed and the rotor rod time scored as 300. The length of time that the mouse remained on the rod (latency to fall) was recorded. Each mouse underwent seven consecutive trials with 10 min intervals between trials.

At the end of each behavioral experiment, brains of mice were isolated, sliced, and stained to verify infection site and loss of DAergic neurons as described above. Mice that were mis-injected were subsequently removed from behavioral analysis.

Data analysis

Data were analyzed using 1- or 2-way ANOVAs as indicated followed by Bonferroni post-hoc tests. Data were analyzed using GraphPad software. Student's t tests were used to analyze fold expression of qRT-PCR data and immunohistochemistry data. Results were considered significant at $p < 0.05$. All data are expressed as the mean ± SEM.

A2.C. Results

To test the hypothesis that Dicer expression is critical for maintenance and survival of DAergic neurons in adult midbrain areas, we selectively expressed Cre recombinase in either the VTA or SNpc of adult (>8 week old) $Dicer^{flox/flox}$ mice. To do this, recombinant adeno-associated virus serotype 2 (AAV2) co-expressing Cre under the control of the CMV promotor and the green fluorescent marker, ZsGreen under the control of the β-actin promotor, were injected into VTA or SNpc. Control mice received AAV2 encoding enhanced green fluorescent protein (eGFP) alone. To verify loss of Dicer expression, 4-6 weeks post AAV2 injection, midbrain areas expressing Cre, identified by expression of ZsGreen under fluorescence microscopy, were isolated and genotyped. Deletion of the floxed NEO-cassette was verified by PCR using primers spanning the floxed region (Fig. A2-1A). To verify loss of miRNA expression, infected areas were laser dissected followed by isolation of small RNAs and quantitation using qRT-PCR. Expression of Cre in midbrain of $Dicer^{flox/flox}$ mice resulted in statistically

significant reduction of common neuronal miRNAs including miR-124a, -328, -9, and -133b (Fig. A2-1B).

To determine the effect of Dicer deletion in the VTA on behavior, Dicer$^{flox/flox}$ mice were infected with AAV2-eGFP (control) or AAV2-Cre-ZsGreen in the VTA, bilaterally. Locomotor activity was monitored weekly 4-8 weeks post infection. In control animals, locomotor activity 4-8 weeks after infection did not differ from baseline (activity measured prior to infection, Fig. A2-2A, C). In contrast, locomotor activity in AAV2-Cre-ZsGreen-infected animals progressively increased from 6-8 weeks post-infection (Fig. A2-2B, C). Two-way ANOVA revealed a significant main effect of virus ($F_{1, 140} = 58.7$, $p < 0.001$) and time ($F_{3, 140} = 16.3$, $p < 0.001$) and significant time x virus interaction ($F_{3, 140} = 20.3$, $p < 0.001$). Post-hoc analysis indicated a statistically significant increase in locomotor activity six and eight weeks post-infection for AAV2-Cre-ZsGreen ($p < 0.001$), but not AAV2-eGFP infected mice. To determine the role of DA in hyperactivity elicited by reduced Dicer expression in the VTA, we injected control and hyperactive VTA Cre-expressing Dicer$^{flox/flox}$ mice with the DA agonist, amphetamine (Fig. A2-2D, E, F). Two-way ANOVA indicated a significant drug treatment and virus interaction ($F_{1, 23} = 7.52$, $p < 0.05$). Control animals responded to amphetamine with increased locomotor activity compared to a saline injection (Fig. A2-2D, F). Interestingly, hyperactivity in VTA Cre-expressing animals was paradoxically reduced in response to amphetamine similar to what

is seen in models of attention deficit hyperactivity disorder ($p < 0.05$, Fig. A2-2E, F) (Gong et al., 2011, Won et al., 2011).

To test the hypothesis that reduction of Dicer expression was necessary for VTA DAergic neuron maintenance and survival, $Dicer^{flox/flox}$ mice were injected with AAV2-Cre-ZsGreen unilaterally into the VTA. Six weeks post-infection, brains were harvested, sliced, and labeled with the nuclear stain, DAPI, the neuronal specific nuclear stain, NeuN, and the TH antibody allowing for detection of total cells, total neurons, and DAergic neurons, respectively, in infected and control midbrain regions. The number of non-neuronal cells (DAPI positive, NeuN negative), DAergic (TH immunopositive), and non-DAergic neurons (NeuN positive, TH immunonegative) in the VTA were counted and compared to the non-infected side 6 weeks after injection (Fig. A2-3A, B). Two-way ANOVA indicated a significant effect of virus infection ($F_{1, 12} = 7.93$, $p < 0.05$), cell type ($F_{2, 12} = 623.6$, $p < 0.001$), and a significant virus x cell type interaction ($F_{2,12} = 20.6$, $p<0.001$). Post-hoc analysis revealed that reduction of Dicer expression significantly reduced the number of TH immunopositive neurons within the VTA compared to the non-infected side (Fig. A2-3B, $p < 0.001$) while increasing the number of non-neuronal cells ($p<0.05$), presumably glia which proliferate or migrate to the lesioned area (Maia, Arlicot et al. 2012). Although there was a trend for decreased non-TH immunopositive neurons with reduced Dicer expression compared to control, it was not statistically significant. In addition, TH staining was dramatically reduced in the nucleus accumbens (NAc) indicating

loss of DAergic neuron terminals (Fig. A2-3C). Reduction of TH staining was localized to the NAc; whereas dorsal striatum (DSt) was relatively unaffected consistent with loss of DAergic neurons specifically in the VTA. To further control for the specificity of our viral-mediated approach, we unilaterally infected the VTA of $Dicer^{flox/flox}$ mice with AAV2-eGFP and unilaterally infected the VTA of WT mice ($Dicer^{wt/wt}$) with AAV2-Cre-ZsGreen. The number of VTA DAergic neurons in the infected sides of both sets of control mice did not significantly differ compared to the number of VTA DAergic neurons in the non-infected sides (Fig. A2-4A).

To determine if reducing Dicer expression induced apoptosis as the mechanism of cell death in DAergic neurons within the VTA, we infected the VTA of a cohort of $Dicer^{flox/flox}$ mice with AAV2-Cre-ZsGreen and performed TUNEL staining at various time points post-infection including 2, 4, 6, and 8 weeks (Fig. A2-4B, C). One-way ANOVA indicated a main effect of time on TUNEL-positive cells ($F_{4, 32} = 49.6$, $p < 0.001$, Fig. A2-4C). Post-hoc analysis revealed a significant increase in neurons undergoing apoptosis at four and six weeks post-infection compared to two weeks post-infection ($p < 0.001$). Thus, TUNEL staining was detected as early as two weeks post-infection, but peaked at 4 weeks indicating reduced Dicer expression triggers apoptosis in adult VTA. Interestingly, the majority of TUNEL stained nuclei within the infected area did not co-localize with Zs-Green expression. As TUNEL stained slices are processed at fixed time intervals, this is likely due to loss of Zs-Green expression in dying/dead neurons or diffusion of fluorophore in apoptotic neurons with compromised membrane integrity.

To determine the effect of Dicer deletion in SNpc, adult Dicer$^{flox/flox}$ mice were infected with AAV2-Cre-ZsGreen bilaterally in SNpc. Locomotor activity was monitored weekly post-infection (Fig. A2-5). Locomotor activity was not affected by reduced Dicer expression in the SNpc as locomotor activity did not differ from baseline up to 8 weeks post-Cre expression (Fig. A2-5A, B, C). Because DA is critical for motor coordination learning in addition to voluntary movement (Beeler, Cao et al. 2010), we compared rotarod performance of AAV2-Cre-ZsGreen-infected animals at 4- and 8-weeks post-infection to control-infected animals (Fig. A2-5D). Two-way ANOVA indicated a significant main effect of trial ($F_{6, 162} = 13.3$, $p < 0.001$) and virus ($F_{2, 27} = 5.05$, $p < 0.05$) but not a significant interaction. Over seven successive trials on the accelerating rotarod, control mice significantly increased their latency to fall of the apparatus indicating motor coordination learning. Post-hoc analysis revealed that AAV2-Cre-ZsGreen-infected animals exhibited poorer performance at 8- but not 4-weeks post-infection, compared to controls as reflected in decreased latency to fall on trials 3-7 compared to AAV2-eGFP infected mice ($p<0.05$). As with the VTA, the number of TH immunopositive neurons in the SNpc of AAV2-Cre-ZsGreen-infected animals was significantly reduced compared to control indicating Dicer expression is necessary for DAergic neuron survival in adult animals (Fig. A2-6A, B). This was also confirmed by decreased TH labeling in DSt of infected animals (Fig. A2- 6C).

A1.D. Discussion

Here we show that Dicer expression is critical for survival and maintenance of adult DAergic midbrain neurons in C57BL/6J mice. Genetic deletion of Dicer specifically in midbrain elicited a progressive loss of both VTA and SNpc DAergic neurons through an apoptotic mechanism. The present data extend previous studies (Kim, Inoue et al. 2007) and indicate that Dicer expression is necessary for survival of DAergic neurons even in adulthood. The progressive loss of DAergic neurons over time in the VTA resulted in hyperactivity and this hyperactivity was, paradoxically, reduced by amphetamine. These data are consistent with previous VTA lesioning studies in rats, which also induced amphetamine-sensitive hyperactivity (Galey, Simon et al. 1977, Le Moal, Stinus et al. 1977, Stinus, Gaffori et al. 1977). Interestingly, Dicer loss in SNpc did not affect locomotor activity but did impair rotarod performance cogent with prior work implicating a role for striatal DA in acquisition of motor learning (Beeler, Cao et al. 2010). Our results also support recent data indicating that, at least in mice, skilled motor learning is more sensitive to the effects of partial DAergic neuron depletion compared to simple motor activity (Chagniel, Robitaille et al. 2012).

A previous study examined Dicer deletion under control of the DAT promoter and found that animals that develop without Dicer expression in DAT-expressing neurons exhibit significant loss of neurons by three weeks of age and a 90 % loss by 8 weeks (Kim, Inoue et al. 2007). Neuronal loss occurred via apoptosis.

Similarly, our study indicates knockout of Dicer in adult DAergic neuron-rich midbrain areas also induces apoptosis. Apoptosis peaked 4 weeks post-infection returning to baseline after 8 weeks matching the progressive severity of the measured motor behavioral phenotype in these animals and also mirroring the peak time of Cre-expression using AAV2-mediated gene delivery.

The criticality of Dicer expression and Dicer-processed miRNA function in the CNS differs between brain regions, is developmentally-dependent, and depends on neuronal sub-type. For example, genetic deletion of Dicer in cells that express calmodulin kinase II (CAMKII), a marker for glutamatergic neurons in cortex and hippocampus, has different phenotypes in mice depending on the developmental period when the deletion occurs. Crossing $Dicer^{flox/flox}$ mice with a-R1AG-5 CAMKII-Cre mice results in Dicer deletion at embryonic day 15.5 (e15.5) (Davis, Cuellar et al. 2008). The resulting phenotype included microcephaly, significant increase in early post-natal apoptosis, and death by 20 days of age. Deleting Dicer in CamKII-expressing neurons beginning at P18 using a different Cre line also induces neurodegeneration with abnormal tau hyperphosphorylation (Hebert, Papadopoulou et al. 2010). In contrast, inducing Dicer deletion in CaMKII-expressing neurons during adulthood using a tamoxifen-inducible promoter enhances learning and memory in mice without dramatic neurodegeration for up to 14 weeks post-deletion (Konopka, Kiryk et al. 2010). Similarly, Dicer deletion in adult amygdala or in striatal dopaminoceptive medium spiny neurons does not induce apoptosis or neurodegeneration in these brain areas (Cuellar, Davis et al.

2008, Haramati, Navon et al. 2011). Interestingly, deletion of Dicer in Purkinje neurons of the cerebellum elicits a relatively slow neurodegenerative process whereby these neurons appear normal up to 10 weeks of age but begin to degenerate over the next several weeks of life (Schaefer, O'Carroll et al. 2007). In contrast, our data indicate that in the absence of Dicer expression, DAergic neurons degenerate rapidly; whereas non-DAergic (presumably GABAergic) neurons within the VTA were more resistant to cell death similar to striatal medium spiny neurons and Purkinje neurons which are also GABAergic (Schaefer, O'Carroll et al. 2007, Cuellar, Davis et al. 2008).

Interestingly, Kim et. al. identified a specific miRNA, miR-133b, that is enriched in DAergic neurons and depleted in Parkinson's disease brains, regulates DAergic neuron differentiation (Kim, Inoue et al. 2007). While the precise role of miRNA-133b in DAergic neuron maintenance is unclear (Heyer, Pani et al. 2012), it raises the intriguing possibility that a specific set of miRNAs may be critical for DAergic neuron integrity throughout their lifespan. Identification of miRNAs integral for DAergic neuron health could lead to new strategies for treatment of DAergic neuron degenerative diseases such as Parkinson's disease.

In summary, our data indicate that Dicer expression and Dicer-dependent miRNAs appear to be necessary for adult DAergic neuron maintenance and survival. Combined with previous studies, Dicer expression is critical for DAergic neuron integrity from early post-natal periods throughout adulthood.

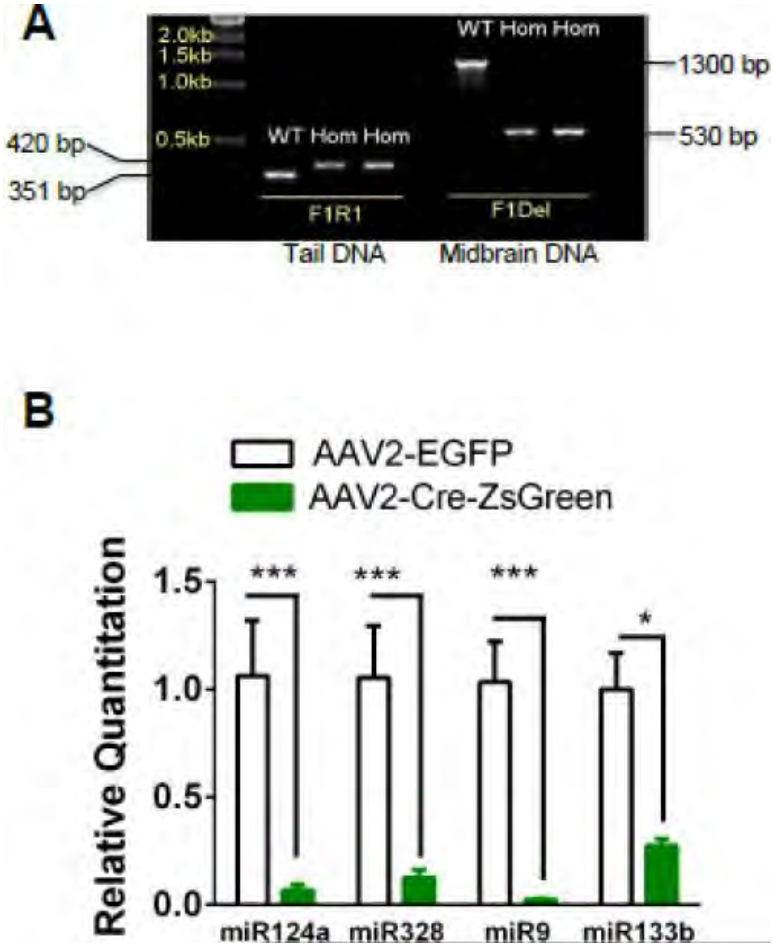

Figure A2-1. Verification of conditional Dicer knock-out.

A. DNA agarose gel illustrating amplified DNA fragments from genomic DNA of WT and homozygous Dicer$^{flox/flox}$ mice using Dicer F1 and Dicer R1 primers (left). Right, amplified fragments from midbrain DNA of WT and Dicer$^{flox/flox}$ infected with AAV2-Cre-ZsGreen using the Dicer F1 and Dicer Del primers.

B. Midbrain miRNA expression from Dicer$^{flox/flox}$ mice infected with AAV2-eGFP (white bars) or AAV2-Cre-ZsGreen (green bars). *$p < 0.05$, *** $p < 0.001$, Student's t-test (n =3 mice/treatment).

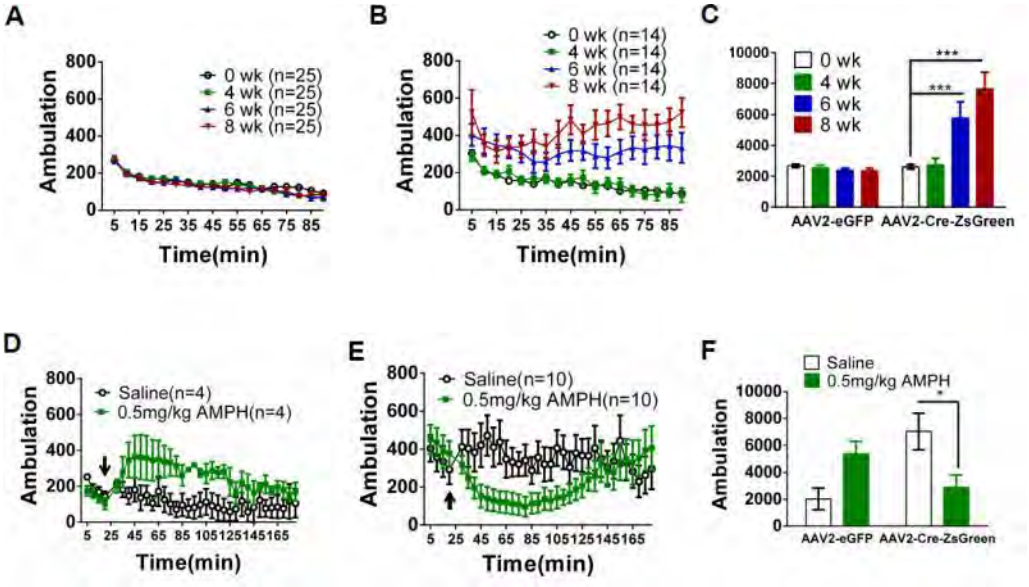

Figure A2-2. Dicer loss in adult VTA elicits locomotor hyperactivity.

A. Ambulation in Dicer$^{flox/flox}$ mice infected with AAV2-eGFP in the VTA. Ambulation at baseline (prior to injection) and 4, 6, and 8 weeks (wk) post-infection over 90 min are shown. Each data point represents summed ambulation during 5 min intervals (the VTA was correctly targeted in 25/26 mice).

B. Ambulation in Dicer$^{flox/flox}$ mice infected with AAV2-Cre-ZsGreen in the VTA. Ambulation at baseline and 4, 6, and 8 weeks post-infection are shown (the VTA was correctly targeted in 14/16 mice).

C. Summed total ambulation over 90 min in each group at each time point post-infection.

D. Ambulatory response to saline (i.p., open circles) or 0.5 mg/kg amphetamine (AMPH, i.p., green squares) in Dicer$^{flox/flox}$ mice expressing eGFP in VTA (the

VTA was correctly targeted in 4/4 mice). Time of injection is indicated by the arrow.

E. Ambulatory response to saline or AMPH in Dicer$^{flox/flox}$ mice expressing Cre in VTA (the VTA was correctly targeted in 10/12 mice).

F. Summed total ambulation over 90 min post-saline or -AMPH injection in each group. Two-way ANOVA, Bonferroni post-hoc, * $p < 0.05$, ***$p < 0.001$.

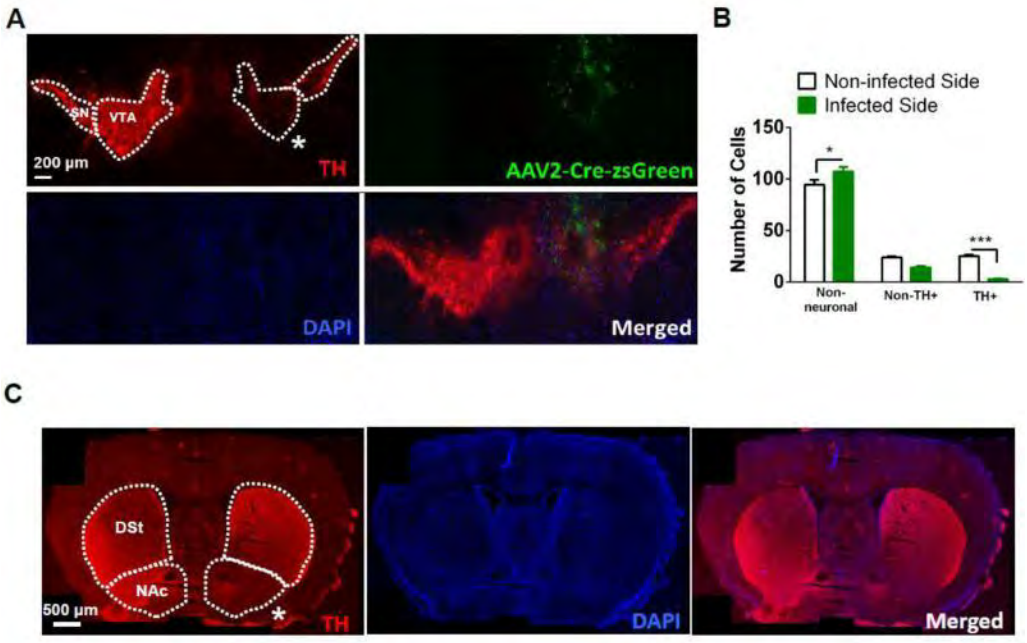

Figure A2-3. Dicer expression is necessary for DAergic neuron survival in the adult VTA.

A. Representative photomicrograph from a Dicer$^{flox/flox}$ mouse infected with AAV2-Cre-ZsGreen unilaterally. Dicer loss leads to significant reduction of TH immunopositive neurons (stained red, top left panel) on the infected side (indicated by the white asterisk). Photomicrograph of virus infected area (green, top right panel) is shown. DAPI-labeled cells are depicted in blue (bottom left panel). Merged image is illustrated in the bottom right panel.

B. Average total number of non-neuronal cells, TH-immunonegative (non-TH+) neurons and TH-immunopositive (TH+) neurons in the VTA of AAV2-Cre-ZsGreen-infected (infected compare to the non-infected side). Cell counts were calculated 8 weeks after virus injection (n = 15-42 slices from 3 mice/treatment).

C. Representative photomicrograph illustrating loss of TH expression in the NAc. Twoway ANOVA, Bonferroni post-hoc, *p < 0.05, *** p < 0.001.

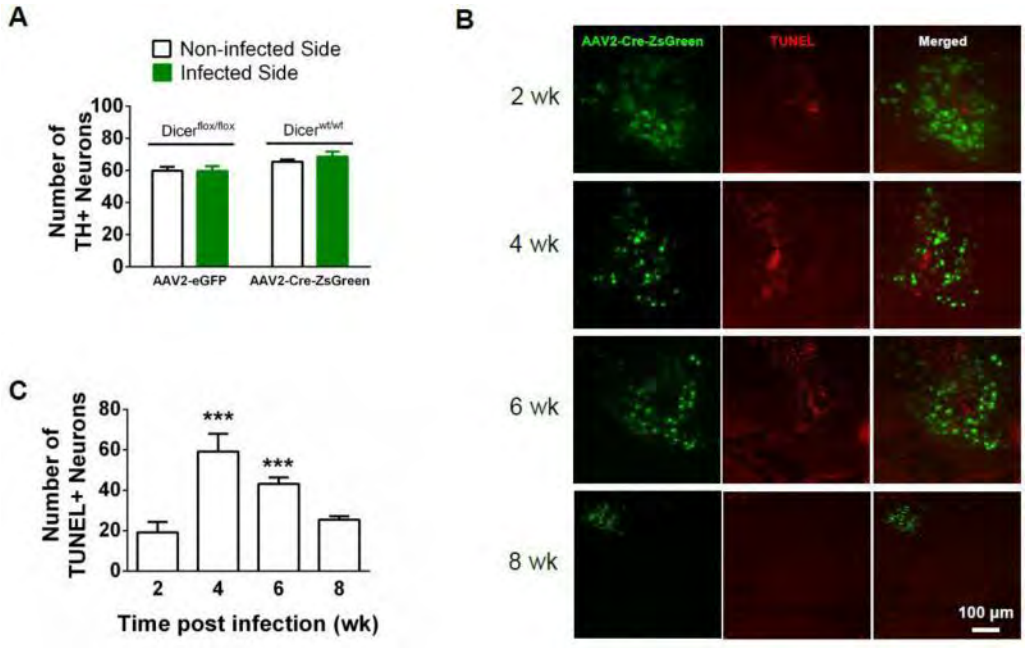

Figure A2-4. Loss of adult VTA DAergic neurons with reduced Dicer expression is specific and triggered by apoptosis.

A. Averaged sum of TH immunopositive VTA neurons in Dicer$^{flox/flox}$mice infected with AAV2-eGFP and Dicer$^{wt/wt}$ mice infected with AAV2-Cre-ZsGreen. TH immunopositive neurons are compared between the infected and control, non-infected side.

B. Representative photomicrographs illustrating AAV2-Cre-ZsGreen expression in the VTA (green, left), TUNEL stained neurons (red, middle) and merged images (right) at different time points after virus injection in Dicer$^{flox/flox}$ mice.

C. Number of TUNEL-positive neurons in infected Dicer$^{flox/flox}$ mice at different time points. One-way ANOVA, Bonferroni post-hoc, *** $p < 0.001$.

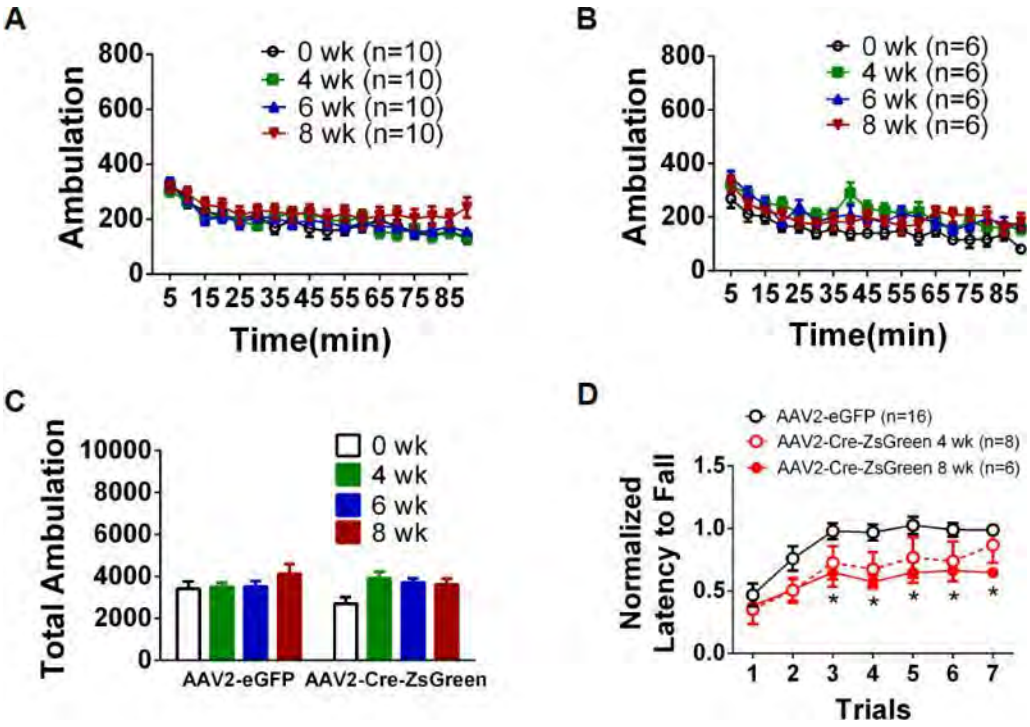

Figure A2-5. Loss of Dicer expression in SNpc impairs motor-learning.

Ambulation in Dicer$^{flox/flox}$ mice infected with (A) AAV2-eGFP or (B) AAV2-Cre-ZsGreen in the SNpc at baseline (prior to injection) and 4, 6, and 8 weeks post-infection over 90 min are shown (the SNpc was correctly targeted in A) 10/10 and 6/7 mice, respectively).

C. Summed total ambulation from (A) and (B).

D. Normalized latency to fall off an accelerating rotarod on 7 consecutive trials in Dicer$^{flox/flox}$ mice infected with AAV2-eGFP or AAV2-Cre-ZsGreen (4- or 8-weeks post-infection) in the SNpc. Each trial was normalized to the average latency of trials 5-7 in control, AAV2-eGFP-infected animals (i.e. when rotarod performance reached a stable baseline). Two-way ANOVA, Bonferroni Post-hoc, * $p < 0.05$.

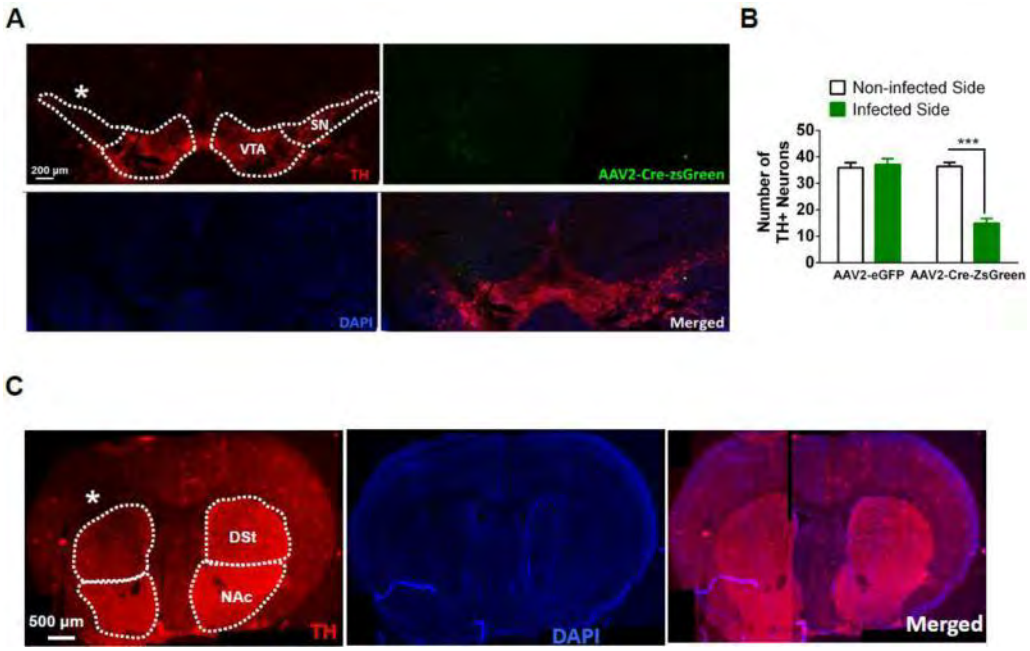

Figure A2-6. Dicer expression is necessary for DAergic neuron survival in the adult SNpc.

A. Representative photomicrographs illustrating TH expression (red, top left panel), AAV2-Cre-ZsGreen-infected area (green, top right panel), DAPI staining (blue, bottom left panel) and merged signals (bottom right panel). The infected side is denoted by a white asterisk.

B. Average total number of TH-immunopositive neurons in the SNpc of AAV2-eGFP (control) and AAV2-Cre-ZsGreen infected mice. Neurons were quantified 8 weeks after virus injection (n = 18-20 slices from 4 mice/treatment).

C. Representative photomicrograph illustrating loss of TH expression in the DSt.

References:

Adhikari, A. (2014). "Distributed circuits underlying anxiety." Front Behav Neurosci **8**: 112.
Agetsuma, M., H. Aizawa, T. Aoki, R. Nakayama, M. Takahoko, M. Goto, T. Sassa, R. Amo, T. Shiraki, K. Kawakami, T. Hosoya, S. Higashijima and H. Okamoto (2010). "The habenula is crucial for experience-dependent modification of fear responses in zebrafish." Nat Neurosci **13**(11): 1354-1356.
Aizawa, H., M. Kobayashi, S. Tanaka, T. Fukai and H. Okamoto (2012). "Molecular characterization of the subnuclei in rat habenula." J Comp Neurol **520**(18): 4051-4066.
Akabas, M. H., C. Kaufmann, P. Archdeacon and A. Karlin (1994). "Identification of acetylcholine receptor channel-lining residues in the entire M2 segment of the alpha subunit." Neuron **13**(4): 919-927.
Albuquerque, E. X., E. F. Pereira, M. Alkondon and S. W. Rogers (2009). "Mammalian nicotinic acetylcholine receptors: from structure to function." Physiol Rev **89**(1): 73-120.
Amat, J., P. D. Sparks, P. Matus-Amat, J. Griggs, L. R. Watkins and S. F. Maier (2001). "The role of the habenular complex in the elevation of dorsal raphe nucleus serotonin and the changes in the behavioral responses produced by uncontrollable stress." Brain Res **917**(1): 118-126.
Ambros, V. (2004). "The functions of animal microRNAs." Nature **431**(7006): 350-355.
Anderson, S. M. and D. H. Brunzell (2012). "Low dose nicotine and antagonism of beta2 subunit containing nicotinic acetylcholine receptors have similar effects on affective behavior in mice." PLoS One **7**(11): e48665.
Anderson, S. M. and D. H. Brunzell (2015). "Anxiolytic-like and anxiogenic-like effects of nicotine are regulated via diverse action at beta2*nicotinic acetylcholine receptors." Br J Pharmacol **172**(11): 2864-2877.
Antolin-Fontes, B., J. L. Ables, A. Gorlich and I. Ibanez-Tallon (2014). "The habenulo-interpeduncular pathway in nicotine aversion and withdrawal." Neuropharmacology.
Baenziger, J. E., K. W. Miller, M. P. McCarthy and K. J. Rothschild (1992). "Probing conformational changes in the nicotinic acetylcholine receptor by Fourier transform infrared difference spectroscopy." Biophys J **62**(1): 64-66.
Balcita-Pedicino, J. J., N. Omelchenko, R. Bell and S. R. Sesack (2011). "The inhibitory influence of the lateral habenula on midbrain dopamine cells: ultrastructural evidence for indirect mediation via the rostromedial mesopontine tegmental nucleus." J Comp Neurol **519**(6): 1143-1164.
Baldwin, P. R., R. Alanis and R. Salas (2011). "The Role of the Habenula in Nicotine Addiction." J Addict Res Ther **S1**(2).
Barlow, D. H. D., V. Mark (2009). Abnormal Psychology: An Integrative Approach (Fifth ed.), Belmont, CA: Wadsworth Cengage Learning.
Bartel, D. P. (2004). "MicroRNAs: genomics, biogenesis, mechanism, and function." Cell **116**(2): 281-297.
Beeler, J. A., Z. F. Cao, M. A. Kheirbek, Y. Ding, J. Koranda, M. Murakami, U. J. Kang and X. Zhuang (2010). "Dopamine-dependent motor learning: insight into levodopa's long-duration response." Ann Neurol **67**(5): 639-647.
Benowitz, N. L. (2008). "Neurobiology of nicotine addiction: implications for smoking cessation treatment." Am J Med **121**(4 Suppl 1): S3-10.

Benwell, M. E., D. J. Balfour and J. M. Anderson (1988). "Evidence that tobacco smoking increases the density of (-)-[3H]nicotine binding sites in human brain." J Neurochem **50**(4): 1243-1247.
Berrettini, W., X. Yuan, F. Tozzi, K. Song, C. Francks, H. Chilcoat, D. Waterworth, P. Muglia and V. Mooser (2008). "Alpha-5/alpha-3 nicotinic receptor subunit alleles increase risk for heavy smoking." Mol Psychiatry **13**(4): 368-373.
Bicker, S. and G. Schratt (2008). "microRNAs: tiny regulators of synapse function in development and disease." J Cell Mol Med **12**(5a): 1466-1476.
Bikadi, Z. and M. Simonyi (2003). "Muscarinic and nicotinic cholinergic agonists: structural analogies and discrepancies." Curr Med Chem **10**(23): 2611-2620.
Bischoff, S., S. Leonhard, N. Reymann, V. Schuler, R. Shigemoto, K. Kaupmann and B. Bettler (1999). "Spatial distribution of GABA(B)R1 receptor mRNA and binding sites in the rat brain." J Comp Neurol **412**(1): 1-16.
Boehme, S., V. Ritter, S. Tefikow, U. Stangier, B. Strauss, W. H. Miltner and T. Straube (2014). "Brain activation during anticipatory anxiety in social anxiety disorder." Soc Cogn Affect Neurosci **9**(9): 1413-1418.
Brattelid, T., E. K. Aarnes, E. Helgeland, S. Guvaag, H. Eichele and A. K. Jonassen (2011). "Normalization strategy is critical for the outcome of miRNA expression analyses in the rat heart." Physiol Genomics **43**(10): 604-610.
Brody, A. L., M. A. Mandelkern, M. E. Jarvik, G. S. Lee, E. C. Smith, J. C. Huang, R. G. Bota, G. Bartzokis and E. D. London (2004). "Differences between smokers and nonsmokers in regional gray matter volumes and densities." Biol Psychiatry **55**(1): 77-84.
Buccafusco, J. J., L. C. Shuster and A. V. Terry, Jr. (2007). "Disconnection between activation and desensitization of autonomic nicotinic receptors by nicotine and cotinine." Neurosci Lett **413**(1): 68-71.
Butler, R. K., L. C. White, D. Frederick-Duus, K. F. Kaigler, J. R. Fadel and M. A. Wilson (2012). "Comparison of the activation of somatostatin- and neuropeptide Y-containing neuronal populations of the rat amygdala following two different anxiogenic stressors." Exp Neurol **238**(1): 52-63.
Cao, X., G. Yeo, A. R. Muotri, T. Kuwabara and F. H. Gage (2006). "Noncoding RNAs in the mammalian central nervous system." Annu Rev Neurosci **29**: 77-103.
Carboni, L., R. Carletti, S. Tacconi, C. Corti and F. Ferraguti (1998). "Differential expression of SAPK isoforms in the rat brain. An in situ hybridisation study in the adult rat brain and during post-natal development." Brain Res Mol Brain Res **60**(1): 57-68.
Carlson, J., K. Noguchi and G. Ellison (2001). "Nicotine produces selective degeneration in the medial habenula and fasciculus retroflexus." Brain Res **906**(1-2): 127-134.
Carvalho, M. C., C. M. Moreira, J. M. Zanoveli and M. L. Brandao (2012). "Central, but not basolateral, amygdala involvement in the anxiolytic-like effects of midazolam in rats in the elevated plus maze." J Psychopharmacol **26**(4): 543-554.
Chagniel, L., C. Robitaille, C. Lacharite-Mueller, G. Bureau and M. Cyr (2012). "Partial dopamine depletion in MPTP-treated mice differentially altered motor skill learning and action control." Behav Brain Res **228**(1): 9-15.
Champtiaux, N. and J. P. Changeux (2002). "Knock-out and knock-in mice to investigate the role of nicotinic receptors in the central nervous system." Curr Drug Targets CNS Neurol Disord **1**(4): 319-330.

Champtiaux, N., C. Gotti, M. Cordero-Erausquin, D. J. David, C. Przybylski, C. Lena, F. Clementi, M. Moretti, F. M. Rossi, N. Le Novere, J. M. McIntosh, A. M. Gardier and J. P. Changeux (2003). "Subunit composition of functional nicotinic receptors in dopaminergic neurons investigated with knock-out mice." J Neurosci **23**(21): 7820-7829.
Champtiaux, N., Z. Y. Han, A. Bessis, F. M. Rossi, M. Zoli, L. Marubio, J. M. McIntosh and J. P. Changeux (2002). "Distribution and pharmacology of alpha 6-containing nicotinic acetylcholine receptors analyzed with mutant mice." J Neurosci **22**(4): 1208-1217.
Charles, K. J., M. L. Evans, M. J. Robbins, A. R. Calver, R. A. Leslie and M. N. Pangalos (2001). "Comparative immunohistochemical localisation of GABA(B1a), GABA(B1b) and GABA(B2) subunits in rat brain, spinal cord and dorsal root ganglion." Neuroscience **106**(3): 447-467.
Cheeta, S., S. Tucci and S. E. File (2001). "Antagonism of the anxiolytic effect of nicotine in the dorsal raphe nucleus by dihydro-beta-erythroidine." Pharmacol Biochem Behav **70**(4): 491-496.
Cockcroft, V. B., D. J. Osguthorpe, E. A. Barnard and G. G. Lunt (1990). "Modeling of agonist binding to the ligand-gated ion channel superfamily of receptors." Proteins **8**(4): 386-397.
Cole, A. J., D. W. Saffen, J. M. Baraban and P. F. Worley (1989). "Rapid increase of an immediate early gene messenger RNA in hippocampal neurons by synaptic NMDA receptor activation." Nature **340**(6233): 474-476.
Contestabile, A. and B. A. Flumerfelt (1981). "Afferent connections of the interpeduncular nucleus and the topographic organization of the habenulo-interpeduncular pathway: an HRP study in the rat." J Comp Neurol **196**(2): 253-270.
Contestabile, A. and F. Fonnum (1983). "Cholinergic and GABAergic forebrain projections to the habenula and nucleus interpeduncularis: surgical and kainic acid lesions." Brain Res **275**(2): 287-297.
Contestabile, A., L. Villani, A. Fasolo, M. F. Franzoni, L. Gribaudo, O. Oktedalen and F. Fonnum (1987). "Topography of cholinergic and substance P pathways in the habenulo-interpeduncular system of the rat. An immunocytochemical and microchemical approach." Neuroscience **21**(1): 253-270.
Cosgrove, K. P. (2010). "Imaging receptor changes in human drug abusers." Curr Top Behav Neurosci **3**: 199-217.
Couturier, S., D. Bertrand, J. M. Matter, M. C. Hernandez, S. Bertrand, N. Millar, S. Valera, T. Barkas and M. Ballivet (1990). "A neuronal nicotinic acetylcholine receptor subunit (alpha 7) is developmentally regulated and forms a homo-oligomeric channel blocked by alpha-BTX." Neuron **5**(6): 847-856.
Cuellar, T. L., T. H. Davis, P. T. Nelson, G. B. Loeb, B. D. Harfe, E. Ullian and M. T. McManus (2008). "Dicer loss in striatal neurons produces behavioral and neuroanatomical phenotypes in the absence of neurodegeneration." Proc Natl Acad Sci U S A **105**(14): 5614-5619.
Cuello, A. C., P. C. Emson, G. Paxinos and T. Jessell (1978). "Substance P containing and cholinergic projections from the habenula." Brain Res **149**(2): 413-429.
Damaj, M. I., W. Kao and B. R. Martin (2003). "Characterization of spontaneous and precipitated nicotine withdrawal in the mouse." J Pharmacol Exp Ther **307**(2): 526-534.
Dani, J. A. and D. Bertrand (2007). "Nicotinic acetylcholine receptors and nicotinic cholinergic mechanisms of the central nervous system." Annu Rev Pharmacol Toxicol **47**: 699-729.
Dani, J. A. and M. De Biasi (2013). "Mesolimbic dopamine and habenulo-interpeduncular pathways in nicotine withdrawal." Cold Spring Harb Perspect Med **3**(6).

Davis, T. H., T. L. Cuellar, S. M. Koch, A. J. Barker, B. D. Harfe, M. T. McManus and E. M. Ullian (2008). "Conditional loss of Dicer disrupts cellular and tissue morphogenesis in the cortex and hippocampus." J Neurosci **28**(17): 4322-4330.
Dawson, G. R. and M. D. Tricklebank (1995). "Use of the elevated plus maze in the search for novel anxiolytic agents." Trends Pharmacol Sci **16**(2): 33-36.
De Pietri Tonelli, D., J. N. Pulvers, C. Haffner, E. P. Murchison, G. J. Hannon and W. B. Huttner (2008). "miRNAs are essential for survival and differentiation of newborn neurons but not for expansion of neural progenitors during early neurogenesis in the mouse embryonic neocortex." Development **135**(23): 3911-3921.
Dinopoulos, A., G. C. Papadopoulos, J. G. Parnavelas, J. Antonopoulos and A. N. Karamanlidis (1989). "Basal forebrain projections to the lower brain stem in the rat." Exp Neurol **105**(3): 316-319.
Drenan, R. M., R. Nashmi, P. Imoukhuede, H. Just, S. McKinney and H. A. Lester (2008). "Subcellular trafficking, pentameric assembly, and subunit stoichiometry of neuronal nicotinic acetylcholine receptors containing fluorescently labeled alpha6 and beta3 subunits." Mol Pharmacol **73**(1): 27-41.
Durkin, M. M., C. A. Gunwaldsen, B. Borowsky, K. A. Jones and T. A. Branchek (1999). "An in situ hybridization study of the distribution of the GABA(B2) protein mRNA in the rat CNS." Brain Res Mol Brain Res **71**(2): 185-200.
Duvarci, S., E. P. Bauer and D. Pare (2009). "The bed nucleus of the stria terminalis mediates inter-individual variations in anxiety and fear." J Neurosci **29**(33): 10357-10361.
Edelstein, S. J., O. Schaad, E. Henry, D. Bertrand and J. P. Changeux (1996). "A kinetic mechanism for nicotinic acetylcholine receptors based on multiple allosteric transitions." Biol Cybern **75**(5): 361-379.
Elgoyhen, A. B., D. E. Vetter, E. Katz, C. V. Rothlin, S. F. Heinemann and J. Boulter (2001). "alpha10: a determinant of nicotinic cholinergic receptor function in mammalian vestibular and cochlear mechanosensory hair cells." Proc Natl Acad Sci U S A **98**(6): 3501-3506.
Farb, D. H. and M. H. Ratner (2014). "Targeting the modulation of neural circuitry for the treatment of anxiety disorders." Pharmacol Rev **66**(4): 1002-1032.
Fenno, L., O. Yizhar and K. Deisseroth (2011). "The development and application of optogenetics." Annu Rev Neurosci **34**: 389-412.
Fenster, C. P., M. F. Rains, B. Noerager, M. W. Quick and R. A. Lester (1997). "Influence of subunit composition on desensitization of neuronal acetylcholine receptors at low concentrations of nicotine." J Neurosci **17**(15): 5747-5759.
File, S. E., P. J. Kenny and A. M. Ouagazzal (1998). "Bimodal modulation by nicotine of anxiety in the social interaction test: role of the dorsal hippocampus." Behav Neurosci **112**(6): 1423-1429.
File, S. E., H. Zangrossi, Jr., F. L. Sanders and P. S. Mabbutt (1994). "Raised corticosterone in the rat after exposure to the elevated plus-maze." Psychopharmacology (Berl) **113**(3-4): 543-546.
Fiore, R., G. Siegel and G. Schratt (2008). "MicroRNA function in neuronal development, plasticity and disease." Biochim Biophys Acta **1779**(8): 471-478.
Fonck, C., B. N. Cohen, R. Nashmi, P. Whiteaker, D. A. Wagenaar, N. Rodrigues-Pinguet, P. Deshpande, S. McKinney, S. Kwoh, J. Munoz, C. Labarca, A. C. Collins, M. J. Marks and H. A. Lester (2005). "Novel seizure phenotype and sleep disruptions in knock-in mice with hypersensitive alpha 4* nicotinic receptors." J Neurosci **25**(49): 11396-11411.

Fonck, C., R. Nashmi, R. Salas, C. Zhou, Q. Huang, M. De Biasi, R. A. Lester and H. A. Lester (2009). "Demonstration of functional alpha4-containing nicotinic receptors in the medial habenula." Neuropharmacology **56**(1): 247-253.
Fowler, C. D. and P. J. Kenny (2012). "Utility of genetically modified mice for understanding the neurobiology of substance use disorders." Hum Genet **131**(6): 941-957.
Fowler, C. D., Q. Lu, P. M. Johnson, M. J. Marks and P. J. Kenny (2011). "Habenular alpha5 nicotinic receptor subunit signalling controls nicotine intake." Nature **471**(7340): 597-601.
Frahm, S., M. A. Slimak, L. Ferrarese, J. Santos-Torres, B. Antolin-Fontes, S. Auer, S. Filkin, S. Pons, J. F. Fontaine, V. Tsetlin, U. Maskos and I. Ibanez-Tallon (2011). "Aversion to nicotine is regulated by the balanced activity of beta4 and alpha5 nicotinic receptor subunits in the medial habenula." Neuron **70**(3): 522-535.
Galey, D., H. Simon and M. Le Moal (1977). "Behavioral effects of lesions in the A10 dopaminergic area of the rat." Brain Res **124**(1): 83-97.
Gangitano, D., R. Salas, Y. Teng, E. Perez and M. De Biasi (2009). "Progesterone modulation of alpha5 nAChR subunits influences anxiety-related behavior during estrus cycle." Genes Brain Behav **8**(4): 398-406.
Gerzanich, V., R. Anand and J. Lindstrom (1994). "Homomers of alpha 8 and alpha 7 subunits of nicotinic receptors exhibit similar channel but contrasting binding site properties." Mol Pharmacol **45**(2): 212-220.
Gorlich, A., B. Antolin-Fontes, J. L. Ables, S. Frahm, M. A. Slimak, J. D. Dougherty and I. Ibanez-Tallon (2013). "Reexposure to nicotine during withdrawal increases the pacemaking activity of cholinergic habenular neurons." Proc Natl Acad Sci U S A **110**(42): 17077-17082.
Gorne-Tschelnokow, U., A. Strecker, C. Kaduk, D. Naumann and F. Hucho (1994). "The transmembrane domains of the nicotinic acetylcholine receptor contain alpha-helical and beta structures." Embo j **13**(2): 338-341.
Gottesfeld, Z. (1983). "Origin and distribution of noradrenergic innervation in the habenula: a neurochemical study." Brain Res **275**(2): 299-304.
Gotti, C. and F. Clementi (2004). "Neuronal nicotinic receptors: from structure to pathology." Prog Neurobiol **74**(6): 363-396.
Gotti, C., F. Clementi, A. Fornari, A. Gaimarri, S. Guiducci, I. Manfredi, M. Moretti, P. Pedrazzi, L. Pucci and M. Zoli (2009). "Structural and functional diversity of native brain neuronal nicotinic receptors." Biochem Pharmacol **78**(7): 703-711.
Gotti, C., S. Guiducci, V. Tedesco, S. Corbioli, L. Zanetti, M. Moretti, A. Zanardi, R. Rimondini, M. Mugnaini, F. Clementi, C. Chiamulera and M. Zoli (2010). "Nicotinic acetylcholine receptors in the mesolimbic pathway: primary role of ventral tegmental area alpha6beta2* receptors in mediating systemic nicotine effects on dopamine release, locomotion, and reinforcement." J Neurosci **30**(15): 5311-5325.
Gotti, C., W. Hanke, K. Maury, M. Moretti, M. Ballivet, F. Clementi and D. Bertrand (1994). "Pharmacology and biophysical properties of alpha 7 and alpha 7-alpha 8 alpha-bungarotoxin receptor subtypes immunopurified from the chick optic lobe." Eur J Neurosci **6**(8): 1281-1291.
Govind, A. P., P. Vezina and W. N. Green (2009). "Nicotine-induced upregulation of nicotinic receptors: underlying mechanisms and relevance to nicotine addiction." Biochem Pharmacol **78**(7): 756-765.

Grabus, S. D., B. R. Martin, A. M. Batman, R. F. Tyndale, E. Sellers and M. I. Damaj (2005). "Nicotine physical dependence and tolerance in the mouse following chronic oral administration." Psychopharmacology (Berl) **178**(2-3): 183-192.
Gradinaru, V., K. R. Thompson and K. Deisseroth (2008). "eNpHR: a Natronomonas halorhodopsin enhanced for optogenetic applications." Brain Cell Biol **36**(1-4): 129-139.
Grady, S. R., M. Moretti, M. Zoli, M. J. Marks, A. Zanardi, L. Pucci, F. Clementi and C. Gotti (2009). "Rodent habenulo-interpeduncular pathway expresses a large variety of uncommon nAChR subtypes, but only the alpha3beta4* and alpha3beta3beta4* subtypes mediate acetylcholine release." J Neurosci **29**(7): 2272-2282.
Grady, S. R., O. Salminen, D. C. Laverty, P. Whiteaker, J. M. McIntosh, A. C. Collins and M. J. Marks (2007). "The subtypes of nicotinic acetylcholine receptors on dopaminergic terminals of mouse striatum." Biochem Pharmacol **74**(8): 1235-1246.
Grant, B. F., F. S. Stinson, D. A. Dawson, S. P. Chou, M. C. Dufour, W. Compton, R. P. Pickering and K. Kaplan (2004). "Prevalence and co-occurrence of substance use disorders and independent mood and anxiety disorders: results from the National Epidemiologic Survey on Alcohol and Related Conditions." Arch Gen Psychiatry **61**(8): 807-816.
Guillem, K., B. Bloem, R. B. Poorthuis, M. Loos, A. B. Smit, U. Maskos, S. Spijker and H. D. Mansvelder (2011). "Nicotinic acetylcholine receptor beta2 subunits in the medial prefrontal cortex control attention." Science **333**(6044): 888-891.
Hamill, G. S. and B. Fass (1984). "Differential distribution of diagonal band afferents to subnuclei of the interpeduncular nucleus in rats." Neurosci Lett **48**(1): 43-48.
Hamill, G. S. and D. M. Jacobowitz (1984). "A study of afferent projections to the rat interpeduncular nucleus." Brain Res Bull **13**(4): 527-539.
Hamill, G. S. and N. J. Lenn (1984). "The subnuclear organization of the rat interpeduncular nucleus: a light and electron microscopic study." J Comp Neurol **222**(3): 396-408.
Hamill, G. S., J. A. Olschowka, N. J. Lenn and D. M. Jacobowitz (1984). "The subnuclear distribution of substance P, cholecystokinin, vasoactive intestinal peptide, somatostatin, leu-enkephalin, dopamine-beta-hydroxylase, and serotonin in the rat interpeduncular nucleus." J Comp Neurol **226**(4): 580-596.
Haramati, S., I. Navon, O. Issler, G. Ezra-Nevo, S. Gil, R. Zwang, E. Hornstein and A. Chen (2011). "MicroRNA as repressors of stress-induced anxiety: the case of amygdalar miR-34." J Neurosci **31**(40): 14191-14203.
Harfe, B. D., M. T. McManus, J. H. Mansfield, E. Hornstein and C. J. Tabin (2005). "The RNaseIII enzyme Dicer is required for morphogenesis but not patterning of the vertebrate limb." Proc Natl Acad Sci U S A **102**(31): 10898-10903.
Harvey, S. C., F. N. Maddox and C. W. Luetje (1996). "Multiple determinants of dihydro-beta-erythroidine sensitivity on rat neuronal nicotinic receptor alpha subunits." J Neurochem **67**(5): 1953-1959.
Haun, F., T. C. Eckenrode and M. Murray (1992). "Habenula and thalamus cell transplants restore normal sleep behaviors disrupted by denervation of the interpeduncular nucleus." J Neurosci **12**(8): 3282-3290.
Hebert, S. S., A. S. Papadopoulou, P. Smith, M. C. Galas, E. Planel, A. N. Silahtaroglu, N. Sergeant, L. Buee and B. De Strooper (2010). "Genetic ablation of Dicer in adult forebrain neurons results in abnormal tau hyperphosphorylation and neurodegeneration." Hum Mol Genet **19**(20): 3959-3969.

Henderson, B. J., R. Srinivasan, W. A. Nichols, C. N. Dilworth, D. F. Gutierrez, E. D. Mackey, S. McKinney, R. M. Drenan, C. I. Richards and H. A. Lester (2014). "Nicotine exploits a COPI-mediated process for chaperone-mediated up-regulation of its receptors." J Gen Physiol **143**(1): 51-66.
Herkenham, M. (1981). "Anesthetics and the habenulo-interpeduncular system: selective sparing of metabolic activity." Brain Res **210**(1-2): 461-466.
Herkenham, M. and W. J. Nauta (1977). "Afferent connections of the habenular nuclei in the rat. A horseradish peroxidase study, with a note on the fiber-of-passage problem." J Comp Neurol **173**(1): 123-146.
Herkenham, M. and W. J. Nauta (1979). "Efferent connections of the habenular nuclei in the rat." J Comp Neurol **187**(1): 19-47.
Heyer, M. P., A. K. Pani, R. J. Smeyne, P. J. Kenny and G. Feng (2012). "Normal midbrain dopaminergic neuron development and function in miR-133b mutant mice." J Neurosci **32**(32): 10887-10894.
Hikosaka, O. (2010). "The habenula: from stress evasion to value-based decision-making." Nat Rev Neurosci **11**(7): 503-513.
Hira, R., F. Ohkubo, Y. R. Tanaka, Y. Masamizu, G. J. Augustine, H. Kasai and M. Matsuzaki (2013). "In vivo optogenetic tracing of functional corticocortical connections between motor forelimb areas." Front Neural Circuits **7**: 55.
Hong, S., T. C. Jhou, M. Smith, K. S. Saleem and O. Hikosaka (2011). "Negative reward signals from the lateral habenula to dopamine neurons are mediated by rostromedial tegmental nucleus in primates." J Neurosci **31**(32): 11457-11471.
Huang, T., Y. Liu, M. Huang, X. Zhao and L. Cheng (2010). "Wnt1-cre-mediated conditional loss of Dicer results in malformation of the midbrain and cerebellum and failure of neural crest and dopaminergic differentiation in mice." J Mol Cell Biol **2**(3): 152-163.
Huang, W. and M. D. Li (2009). "Differential allelic expression of dopamine D1 receptor gene (DRD1) is modulated by microRNA miR-504." Biol Psychiatry **65**(8): 702-705.
Hunt, S. P., A. Pini and G. Evan (1987). "Induction of c-fos-like protein in spinal cord neurons following sensory stimulation." Nature **328**(6131): 632-634.
Huppi, K., S. E. Martin and N. J. Caplen (2005). "Defining and assaying RNAi in mammalian cells." Mol Cell **17**(1): 1-10.
Improgo, M. R., N. A. Schlichting, R. Y. Cortes, R. Zhao-Shea, A. R. Tapper and P. D. Gardner (2010). "ASCL1 regulates the expression of the CHRNA5/A3/B4 lung cancer susceptibility locus." Mol Cancer Res **8**(2): 194-203.
Improgo, M. R., M. D. Scofield, A. R. Tapper and P. D. Gardner (2010). "The nicotinic acetylcholine receptor CHRNA5/A3/B4 gene cluster: dual role in nicotine addiction and lung cancer." Prog Neurobiol **92**(2): 212-226.
Improgo, M. R., A. R. Tapper and P. D. Gardner (2011). "Nicotinic acetylcholine receptor-mediated mechanisms in lung cancer." Biochem Pharmacol **82**(8): 1015-1021.
Jackson, K. J., B. R. Martin, J. P. Changeux and M. I. Damaj (2008). "Differential role of nicotinic acetylcholine receptor subunits in physical and affective nicotine withdrawal signs." J Pharmacol Exp Ther **325**(1): 302-312.
Jennings, J. H., D. R. Sparta, A. M. Stamatakis, R. L. Ung, K. E. Pleil, T. L. Kash and G. D. Stuber (2013). "Distinct extended amygdala circuits for divergent motivational states." Nature **496**(7444): 224-228.

Kao, P. N. and A. Karlin (1986). "Acetylcholine receptor binding site contains a disulfide cross-link between adjacent half-cystinyl residues." J Biol Chem **261**(18): 8085-8088.
Karlin, A., R. N. Cox, M. Dipaola, E. Holtzman, P. N. Kao, P. Lobel, L. Wang and N. Yodh (1986). "Functional domains of the nicotinic acetylcholine receptor." Ann N Y Acad Sci **463**: 53-69.
Karr, J., V. Vagin, K. Chen, S. Ganesan, O. Olenkina, V. Gvozdev and D. E. Featherstone (2009). "Regulation of glutamate receptor subunit availability by microRNAs." J Cell Biol **185**(4): 685-697.
Kaufling, J., P. Veinante, S. A. Pawlowski, M. J. Freund-Mercier and M. Barrot (2009). "Afferents to the GABAergic tail of the ventral tegmental area in the rat." J Comp Neurol **513**(6): 597-621.
Kenny, P. J. and A. Markou (2001). "Neurobiology of the nicotine withdrawal syndrome." Pharmacol Biochem Behav **70**(4): 531-549.
Kessler, R. C., W. T. Chiu, O. Demler, K. R. Merikangas and E. E. Walters (2005). "Prevalence, severity, and comorbidity of 12-month DSM-IV disorders in the National Comorbidity Survey Replication." Arch Gen Psychiatry **62**(6): 617-627.
Kim, J., K. Inoue, J. Ishii, W. B. Vanti, S. V. Voronov, E. Murchison, G. Hannon and A. Abeliovich (2007). "A MicroRNA feedback circuit in midbrain dopamine neurons." Science **317**(5842): 1220-1224.
Kim, J. S. and E. D. Levin (1996). "Nicotinic, muscarinic and dopaminergic actions in the ventral hippocampus and the nucleus accumbens: effects on spatial working memory in rats." Brain Res **725**(2): 231-240.
Kim, S. Y., A. Adhikari, S. Y. Lee, J. H. Marshel, C. K. Kim, C. S. Mallory, M. Lo, S. Pak, J. Mattis, B. K. Lim, R. C. Malenka, M. R. Warden, R. Neve, K. M. Tye and K. Deisseroth (2013). "Diverging neural pathways assemble a behavioural state from separable features in anxiety." Nature **496**(7444): 219-223.
Kim, U. and S. Y. Chang (2005). "Dendritic morphology, local circuitry, and intrinsic electrophysiology of neurons in the rat medial and lateral habenular nuclei of the epithalamus." J Comp Neurol **483**(2): 236-250.
Klemm, W. R. (2004). "Habenular and interpeduncularis nuclei: shared components in multiple-function networks." Med Sci Monit **10**(11): Ra261-273.
Kobayashi, Y., Y. Sano, E. Vannoni, H. Goto, H. Suzuki, A. Oba, H. Kawasaki, S. Kanba, H. P. Lipp, N. P. Murphy, D. P. Wolfer and S. Itohara (2013). "Genetic dissection of medial habenula-interpeduncular nucleus pathway function in mice." Front Behav Neurosci **7**: 17.
Konopka, W., A. Kiryk, M. Novak, M. Herwerth, J. R. Parkitna, M. Wawrzyniak, A. Kowarsch, P. Michaluk, J. Dzwonek, T. Arnsperger, G. Wilczynski, M. Merkenschlager, F. J. Theis, G. Kohr, L. Kaczmarek and G. Schutz (2010). "MicroRNA loss enhances learning and memory in mice." J Neurosci **30**(44): 14835-14842.
Kuryatov, A., V. Gerzanich, M. Nelson, F. Olale and J. Lindstrom (1997). "Mutation causing autosomal dominant nocturnal frontal lobe epilepsy alters Ca2+ permeability, conductance, and gating of human alpha4beta2 nicotinic acetylcholine receptors." J Neurosci **17**(23): 9035-9047.
Labarca, C., M. W. Nowak, H. Zhang, L. Tang, P. Deshpande and H. A. Lester (1995). "Channel gating governed symmetrically by conserved leucine residues in the M2 domain of nicotinic receptors." Nature **376**(6540): 514-516.
Labarca, C., J. Schwarz, P. Deshpande, S. Schwarz, M. W. Nowak, C. Fonck, R. Nashmi, P. Kofuji, H. Dang, W. Shi, M. Fidan, B. S. Khakh, Z. Chen, B. J. Bowers, J. Boulter, J. M. Wehner and H. A. Lester (2001). "Point mutant mice with hypersensitive alpha 4 nicotinic receptors show dopaminergic deficits and increased anxiety." Proc Natl Acad Sci U S A **98**(5): 2786-2791.

Lai, A., N. Parameswaran, M. Khwaja, P. Whiteaker, J. M. Lindstrom, H. Fan, J. M. McIntosh, S. R. Grady and M. Quik (2005). "Long-term nicotine treatment decreases striatal alpha 6* nicotinic acetylcholine receptor sites and function in mice." Mol Pharmacol **67**(5): 1639-1647.
Lammel, S., B. K. Lim and R. C. Malenka (2014). "Reward and aversion in a heterogeneous midbrain dopamine system." Neuropharmacology **76 Pt B**: 351-359.
Lansdell, S. J. and N. S. Millar (2000). "Cloning and heterologous expression of Dalpha4, a Drosophila neuronal nicotinic acetylcholine receptor subunit: identification of an alternative exon influencing the efficiency of subunit assembly." Neuropharmacology **39**(13): 2604-2614.
Le Moal, M., L. Stinus, H. Simon, J. P. Tassin, A. M. Thierry, G. Blanc, J. Glowinski and B. Cardo (1977). "Behavioral effects of a lesion in the ventral mesencephalic tegmentum: evidence for involvement of A10 dopaminergic neurons." Adv Biochem Psychopharmacol **16**: 237-245.
Le Novere, N. and J. P. Changeux (1995). "Molecular evolution of the nicotinic acetylcholine receptor: an example of multigene family in excitable cells." J Mol Evol **40**(2): 155-172.
Le Novere, N., M. Zoli and J. P. Changeux (1996). "Neuronal nicotinic receptor alpha 6 subunit mRNA is selectively concentrated in catecholaminergic nuclei of the rat brain." Eur J Neurosci **8**(11): 2428-2439.
Lecca, S., M. Melis, A. Luchicchi, M. G. Ennas, M. P. Castelli, A. L. Muntoni and M. Pistis (2011). "Effects of drugs of abuse on putative rostromedial tegmental neurons, inhibitory afferents to midbrain dopamine cells." Neuropsychopharmacology **36**(3): 589-602.
Lecourtier, L. and P. H. Kelly (2007). "A conductor hidden in the orchestra? Role of the habenular complex in monoamine transmission and cognition." Neurosci Biobehav Rev **31**(5): 658-672.
Lecourtier, L., H. C. Neijt and P. H. Kelly (2004). "Habenula lesions cause impaired cognitive performance in rats: implications for schizophrenia." Eur J Neurosci **19**(9): 2551-2560.
Lee, A., A. S. Mathuru, C. Teh, C. Kibat, V. Korzh, T. B. Penney and S. Jesuthasan (2010). "The habenula prevents helpless behavior in larval zebrafish." Curr Biol **20**(24): 2211-2216.
Lenn, N. J. (1976). "Synapses in the interpeduncular nucleus: electron microscopy of normal and habenula lesioned rats." J Comp Neurol **166**(1): 77-99.
Leslie, F. M., C. Y. Mojica and D. D. Reynaga (2013). "Nicotinic receptors in addiction pathways." Mol Pharmacol **83**(4): 753-758.
Lester, H. A., C. Fonck, A. R. Tapper, S. McKinney, M. I. Damaj, S. Balogh, J. Owens, J. M. Wehner, A. C. Collins and C. Labarca (2003). "Hypersensitive knockin mouse strains identify receptors and pathways for nicotine action." Curr Opin Drug Discov Devel **6**(5): 633-639.
Lester, R. A. and J. A. Dani (1995). "Acetylcholine receptor desensitization induced by nicotine in rat medial habenula neurons." J Neurophysiol **74**(1): 195-206.
Levin, E. D., S. J. Briggs, N. C. Christopher and J. T. Auman (1994). "Working memory performance and cholinergic effects in the ventral tegmental area and substantia nigra." Brain Res **657**(1-2): 165-170.
Li, Q., S. Bian, J. Hong, Y. Kawase-Koga, E. Zhu, Y. Zheng, L. Yang and T. Sun (2011). "Timing specific requirement of microRNA function is essential for embryonic and postnatal hippocampal development." PLoS One **6**(10): e26000.
Liang, Y., R. Salas, L. Marubio, D. Bercovich, M. De Biasi, A. L. Beaudet and J. A. Dani (2005). "Functional polymorphisms in the human beta4 subunit of nicotinic acetylcholine receptors." Neurogenetics **6**(1): 37-44.
Lin, J. Y. (2011). "A user's guide to channelrhodopsin variants: features, limitations and future developments." Exp Physiol **96**(1): 19-25.

Lin, J. Y., M. Z. Lin, P. Steinbach and R. Y. Tsien (2009). "Characterization of engineered channelrhodopsin variants with improved properties and kinetics." Biophys J **96**(5): 1803-1814.
Liu, L., L. M. Hendrickson, M. J. Guildford, R. Zhao-Shea, P. D. Gardner and A. R. Tapper (2013). "Nicotinic acetylcholine receptors containing the alpha4 subunit modulate alcohol reward." Biol Psychiatry **73**(8): 738-746.
Liu, L., R. Zhao-Shea, J. M. McIntosh, P. D. Gardner and A. R. Tapper (2012). "Nicotine persistently activates ventral tegmental area dopaminergic neurons via nicotinic acetylcholine receptors containing alpha4 and alpha6 subunits." Mol Pharmacol **81**(4): 541-548.
Lukas, R. J., J. P. Changeux, N. Le Novere, E. X. Albuquerque, D. J. Balfour, D. K. Berg, D. Bertrand, V. A. Chiappinelli, P. B. Clarke, A. C. Collins, J. A. Dani, S. R. Grady, K. J. Kellar, J. M. Lindstrom, M. J. Marks, M. Quik, P. W. Taylor and S. Wonnacott (1999). "International Union of Pharmacology. XX. Current status of the nomenclature for nicotinic acetylcholine receptors and their subunits." Pharmacol Rev **51**(2): 397-401.
MacDermott, A. B., L. W. Role and S. A. Siegelbaum (1999). "Presynaptic ionotropic receptors and the control of transmitter release." Annu Rev Neurosci **22**: 443-485.
Machado-de-Sousa, J. P., L. Osorio Fde, A. P. Jackowski, R. A. Bressan, M. H. Chagas, N. Torro-Alves, A. L. Depaula, J. A. Crippa and J. E. Hallak (2014). "Increased amygdalar and hippocampal volumes in young adults with social anxiety." PLoS One **9**(2): e88523.
Maia, S., N. Arlicot, E. Vierron, S. Bodard, J. Vergote, D. Guilloteau and S. Chalon (2012). "Longitudinal and parallel monitoring of neuroinflammation and neurodegeneration in a 6-hydroxydopamine rat model of Parkinson's disease." Synapse **66**(7): 573-583.
Mansvelder, H. D., J. R. Keath and D. S. McGehee (2002). "Synaptic mechanisms underlie nicotine-induced excitability of brain reward areas." Neuron **33**(6): 905-919.
Mansvelder, H. D. and D. S. McGehee (2000). "Long-term potentiation of excitatory inputs to brain reward areas by nicotine." Neuron **27**(2): 349-357.
Mao, D., D. C. Perry, R. P. Yasuda, B. B. Wolfe and K. J. Kellar (2008). "The alpha4beta2alpha5 nicotinic cholinergic receptor in rat brain is resistant to up-regulation by nicotine in vivo." J Neurochem **104**(2): 446-456.
Marks, M. J., J. B. Burch and A. C. Collins (1983). "Effects of chronic nicotine infusion on tolerance development and nicotinic receptors." J Pharmacol Exp Ther **226**(3): 817-825.
Marks, M. J., J. R. Pauly, S. D. Gross, E. S. Deneris, I. Hermans-Borgmeyer, S. F. Heinemann and A. C. Collins (1992). "Nicotine binding and nicotinic receptor subunit RNA after chronic nicotine treatment." J Neurosci **12**(7): 2765-2784.
Marks, M. J., P. P. Rowell, J. Z. Cao, S. R. Grady, S. E. McCallum and A. C. Collins (2004). "Subsets of acetylcholine-stimulated 86Rb+ efflux and [125I]-epibatidine binding sites in C57BL/6 mouse brain are differentially affected by chronic nicotine treatment." Neuropharmacology **46**(8): 1141-1157.
Marks, M. J., K. W. Smith and A. C. Collins (1998). "Differential agonist inhibition identifies multiple epibatidine binding sites in mouse brain." J Pharmacol Exp Ther **285**(1): 377-386.
Martin, S. E. and N. J. Caplen (2006). "Mismatched siRNAs downregulate mRNAs as a function of target site location." FEBS Lett **580**(15): 3694-3698.
Marubio, L. M., M. del Mar Arroyo-Jimenez, M. Cordero-Erausquin, C. Lena, N. Le Novere, A. de Kerchove d'Exaerde, M. Huchet, M. I. Damaj and J. P. Changeux (1999). "Reduced antinociception in mice lacking neuronal nicotinic receptor subunits." Nature **398**(6730): 805-810.

Masand, P. S. and S. Gupta (2003). "The safety of SSRIs in generalised anxiety disorder: any reason to be anxious?" Expert Opin Drug Saf **2**(5): 485-493.
Mathuru, A. S. and S. Jesuthasan (2013). "The medial habenula as a regulator of anxiety in adult zebrafish." Front Neural Circuits **7**: 99.
McCallum, S. E., N. Parameswaran, T. Bordia, H. Fan, R. F. Tyndale, J. W. Langston, J. M. McIntosh and M. Quik (2006). "Increases in alpha4* but not alpha3*/alpha6* nicotinic receptor sites and function in the primate striatum following chronic oral nicotine treatment." J Neurochem **96**(4): 1028-1041.
McClernon, F. J., R. V. Kozink and J. E. Rose (2008). "Individual differences in nicotine dependence, withdrawal symptoms, and sex predict transient fMRI-BOLD responses to smoking cues." Neuropsychopharmacology **33**(9): 2148-2157.
McGranahan, T. M., N. E. Patzlaff, S. R. Grady, S. F. Heinemann and T. K. Booker (2011). "alpha4beta2 nicotinic acetylcholine receptors on dopaminergic neurons mediate nicotine reward and anxiety relief." J Neurosci **31**(30): 10891-10902.
McIntosh, J. M., L. Azam, S. Staheli, C. Dowell, J. M. Lindstrom, A. Kuryatov, J. E. Garrett, M. J. Marks and P. Whiteaker (2004). "Analogs of alpha-conotoxin MII are selective for alpha6-containing nicotinic acetylcholine receptors." Mol Pharmacol **65**(4): 944-952.
McLoughlin, H. S., S. K. Fineberg, L. L. Ghosh, L. Tecedor and B. L. Davidson (2012). "Dicer is required for proliferation, viability, migration and differentiation in corticoneurogenesis." Neuroscience **223**: 285-295.
Michl, T., M. Jocic, A. Heinemann, R. Schuligoi and P. Holzer (2001). "Vagal afferent signaling of a gastric mucosal acid insult to medullary, pontine, thalamic, hypothalamic and limbic, but not cortical, nuclei of the rat brain." Pain **92**(1-2): 19-27.
Millar, N. S. and C. Gotti (2009). "Diversity of vertebrate nicotinic acetylcholine receptors." Neuropharmacology **56**(1): 237-246.
Mishina, M., T. Takai, K. Imoto, M. Noda, T. Takahashi, S. Numa, C. Methfessel and B. Sakmann (1986). "Molecular distinction between fetal and adult forms of muscle acetylcholine receptor." Nature **321**(6068): 406-411.
Moller, C., L. Wiklund, W. Sommer, A. Thorsell and M. Heilig (1997). "Decreased experimental anxiety and voluntary ethanol consumption in rats following central but not basolateral amygdala lesions." Brain Res **760**(1-2): 94-101.
Montgomery, K. C. (1955). "The relation between fear induced by novel stimulation and exploratory behavior." J Comp Physiol Psychol **48**(4): 254-260.
Moreira, C. M., S. Masson, M. C. Carvalho and M. L. Brandao (2007). "Exploratory behaviour of rats in the elevated plus-maze is differentially sensitive to inactivation of the basolateral and central amygdaloid nuclei." Brain Res Bull **71**(5): 466-474.
Morel, C., L. Fattore, S. Pons, Y. A. Hay, F. Marti, B. Lambolez, M. De Biasi, M. Lathrop, W. Fratta, U. Maskos and P. Faure (2014). "Nicotine consumption is regulated by a human polymorphism in dopamine neurons." Mol Psychiatry **19**(8): 930-936.
Morley, B. J. (1986). "The interpeduncular nucleus." Int Rev Neurobiol **28**: 157-182.
Morris, J. S., K. A. Smith, P. J. Cowen, K. J. Friston and R. J. Dolan (1999). "Covariation of activity in habenula and dorsal raphe nuclei following tryptophan depletion." Neuroimage **10**(2): 163-172.
Morrison, F. G. and K. J. Ressler (2014). "From the neurobiology of extinction to improved clinical treatments." Depress Anxiety **31**(4): 279-290.

Mugnaini, M., M. Tessari, G. Tarter, E. Merlo Pich, C. Chiamulera and B. Bunnemann (2002). "Upregulation of [3H]methyllycaconitine binding sites following continuous infusion of nicotine, without changes of alpha7 or alpha6 subunit mRNA: an autoradiography and in situ hybridization study in rat brain." Eur J Neurosci **16**(9): 1633-1646.
Mukhin, A. G., A. S. Kimes, S. I. Chefer, J. A. Matochik, C. S. Contoreggi, A. G. Horti, D. B. Vaupel, O. Pavlova and E. A. Stein (2008). "Greater nicotinic acetylcholine receptor density in smokers than in nonsmokers: a PET study with 2-18F-FA-85380." J Nucl Med **49**(10): 1628-1635.
Nashmi, R., M. E. Dickinson, S. McKinney, M. Jareb, C. Labarca, S. E. Fraser and H. A. Lester (2003). "Assembly of alpha4beta2 nicotinic acetylcholine receptors assessed with functional fluorescently labeled subunits: effects of localization, trafficking, and nicotine-induced upregulation in clonal mammalian cells and in cultured midbrain neurons." J Neurosci **23**(37): 11554-11567.
Nashmi, R., C. Xiao, P. Deshpande, S. McKinney, S. R. Grady, P. Whiteaker, Q. Huang, T. McClure-Begley, J. M. Lindstrom, C. Labarca, A. C. Collins, M. J. Marks and H. A. Lester (2007). "Chronic nicotine cell specifically upregulates functional alpha 4* nicotinic receptors: basis for both tolerance in midbrain and enhanced long-term potentiation in perforant path." J Neurosci **27**(31): 8202-8218.
National Research Council Institute for Laboratory Animal, R. (1996). Guide for the Care and Use of Laboratory Animals. Washington (DC), National Academies Press (US)

Copyright 1996 by the National Academy of Sciences. All rights reserved.
Nef, P., C. Oneyser, C. Alliod, S. Couturier and M. Ballivet (1988). "Genes expressed in the brain define three distinct neuronal nicotinic acetylcholine receptors." Embo j **7**(3): 595-601.
Neugebauer, N. M., E. B. Einstein, M. B. Lopez, T. D. McClure-Begley, Y. S. Mineur and M. R. Picciotto (2013). "Morphine dependence and withdrawal induced changes in cholinergic signaling." Pharmacol Biochem Behav **109**: 77-83.
Nguyen, H. N., B. A. Rasmussen and D. C. Perry (2003). "Subtype-selective up-regulation by chronic nicotine of high-affinity nicotinic receptors in rat brain demonstrated by receptor autoradiography." J Pharmacol Exp Ther **307**(3): 1090-1097.
O'Neill, A. B. and J. D. Brioni (1994). "Benzodiazepine receptor mediation of the anxiolytic-like effect of (-)-nicotine in mice." Pharmacol Biochem Behav **49**(3): 755-757.
Olausson, P., P. Akesson, J. A. Engel and B. Soderpalm (2001). "Effects of 5-HT1A and 5-HT2 receptor agonists on the behavioral and neurochemical consequences of repeated nicotine treatment." Eur J Pharmacol **420**(1): 45-54.
Orr-Urtreger, A., F. M. Goldner, M. Saeki, I. Lorenzo, L. Goldberg, M. De Biasi, J. A. Dani, J. W. Patrick and A. L. Beaudet (1997). "Mice deficient in the alpha7 neuronal nicotinic acetylcholine receptor lack alpha-bungarotoxin binding sites and hippocampal fast nicotinic currents." J Neurosci **17**(23): 9165-9171.
Ouagazzal, A. M., P. J. Kenny and S. E. File (1999). "Modulation of behaviour on trials 1 and 2 in the elevated plus-maze test of anxiety after systemic and hippocampal administration of nicotine." Psychopharmacology (Berl) **144**(1): 54-60.
Page C, M. C., Sutter M, Walker M, Hoffman BB (2002). " Integrated Pharmacology (2nd ed.)."
Parker, S. L., Y. Fu, K. McAllen, J. Luo, J. M. McIntosh, J. M. Lindstrom and B. M. Sharp (2004). "Up-regulation of brain nicotinic acetylcholine receptors in the rat during long-term self-

administration of nicotine: disproportionate increase of the alpha6 subunit." Mol Pharmacol **65**(3): 611-622.
Paylor, R., M. Nguyen, J. N. Crawley, J. Patrick, A. Beaudet and A. Orr-Urtreger (1998). "Alpha7 nicotinic receptor subunits are not necessary for hippocampal-dependent learning or sensorimotor gating: a behavioral characterization of Acra7-deficient mice." Learn Mem **5**(4-5): 302-316.
Perry, D. C., M. I. Davila-Garcia, C. A. Stockmeier and K. J. Kellar (1999). "Increased nicotinic receptors in brains from smokers: membrane binding and autoradiography studies." J Pharmacol Exp Ther **289**(3): 1545-1552.
Perry, D. C., D. Mao, A. B. Gold, J. M. McIntosh, J. C. Pezzullo and K. J. Kellar (2007). "Chronic nicotine differentially regulates alpha6- and beta3-containing nicotinic cholinergic receptors in rat brain." J Pharmacol Exp Ther **322**(1): 306-315.
Phillipson, O. T. and C. J. Pycock (1982). "Dopamine neurones of the ventral tegmentum project to both medial and lateral habenula. Some implications for habenular function." Exp Brain Res **45**(1-2): 89-94.
Picciotto, M. R., D. H. Brunzell and B. J. Caldarone (2002). "Effect of nicotine and nicotinic receptors on anxiety and depression." Neuroreport **13**(9): 1097-1106.
Picciotto, M. R. and P. J. Kenny (2013). "Molecular mechanisms underlying behaviors related to nicotine addiction." Cold Spring Harb Perspect Med **3**(1): a012112.
Picciotto, M. R., M. Zoli, C. Lena, A. Bessis, Y. Lallemand, N. Le Novere, P. Vincent, E. M. Pich, P. Brulet and J. P. Changeux (1995). "Abnormal avoidance learning in mice lacking functional high-affinity nicotine receptor in the brain." Nature **374**(6517): 65-67.
Picciotto, M. R., M. Zoli, V. Zachariou and J. P. Changeux (1997). "Contribution of nicotinic acetylcholine receptors containing the beta 2-subunit to the behavioural effects of nicotine." Biochem Soc Trans **25**(3): 824-829.
Pidoplichko, V. I., M. DeBiasi, J. T. Williams and J. A. Dani (1997). "Nicotine activates and desensitizes midbrain dopamine neurons." Nature **390**(6658): 401-404.
Pietrzykowski, A. Z., R. M. Friesen, G. E. Martin, S. I. Puig, C. L. Nowak, P. M. Wynne, H. T. Siegelmann and S. N. Treistman (2008). "Posttranscriptional regulation of BK channel splice variant stability by miR-9 underlies neuroadaptation to alcohol." Neuron **59**(2): 274-287.
Plenge, P., E. T. Mellerup and G. Wortwein (2002). "Characterization of epibatidine binding to medial habenula: potential role in analgesia." J Pharmacol Exp Ther **302**(2): 759-765.
Politz, J. C., E. M. Hogan and T. Pederson (2009). "MicroRNAs with a nucleolar location." Rna **15**(9): 1705-1715.
Qin, C. and M. Luo (2009). "Neurochemical phenotypes of the afferent and efferent projections of the mouse medial habenula." Neuroscience **161**(3): 827-837.
Qin, S., C. B. Young, X. Duan, T. Chen, K. Supekar and V. Menon (2014). "Amygdala subregional structure and intrinsic functional connectivity predicts individual differences in anxiety during early childhood." Biol Psychiatry **75**(11): 892-900.
Raybuck, J. D. and T. J. Gould (2010). "The role of nicotinic acetylcholine receptors in the medial prefrontal cortex and hippocampus in trace fear conditioning." Neurobiol Learn Mem **94**(3): 353-363.
Ren, J., C. Qin, F. Hu, J. Tan, L. Qiu, S. Zhao, G. Feng and M. Luo (2011). "Habenula "cholinergic" neurons co-release glutamate and acetylcholine and activate postsynaptic neurons via distinct transmission modes." Neuron **69**(3): 445-452.

Rodgers, R. J., J. Haller, A. Holmes, J. Halasz, T. J. Walton and P. F. Brain (1999). "Corticosterone response to the plus-maze: high correlation with risk assessment in rats and mice." Physiol Behav **68**(1-2): 47-53.
Romanelli, M. N., P. Gratteri, L. Guandalini, E. Martini, C. Bonaccini and F. Gualtieri (2007). "Central nicotinic receptors: structure, function, ligands, and therapeutic potential." ChemMedChem **2**(6): 746-767.
Ronnekleiv, O. K. and M. Moller (1979). "Brain-pineal nervous connections in the rat: an ultrastructure study following habenular lesion." Exp Brain Res **37**(3): 551-562.
Ross, S. A., J. Y. Wong, J. J. Clifford, A. Kinsella, J. S. Massalas, M. K. Horne, I. E. Scheffer, I. Kola, J. L. Waddington, S. F. Berkovic and J. Drago (2000). "Phenotypic characterization of an alpha 4 neuronal nicotinic acetylcholine receptor subunit knock-out mouse." J Neurosci **20**(17): 6431-6441.
Rossi, J., N. Balthasar, D. Olson, M. Scott, E. Berglund, C. E. Lee, M. J. Choi, D. Lauzon, B. B. Lowell and J. K. Elmquist (2011). "Melanocortin-4 receptors expressed by cholinergic neurons regulate energy balance and glucose homeostasis." Cell Metab **13**(2): 195-204.
Rubio, A., M. Perez and J. Avila (2006). "Acetylcholine receptors and tau phosphorylation." Curr Mol Med **6**(4): 423-428.
Russo, S. J., J. W. Murrough, M. H. Han, D. S. Charney and E. J. Nestler (2012). "Neurobiology of resilience." Nat Neurosci **15**(11): 1475-1484.
Sah, P., E. S. Faber, M. Lopez De Armentia and J. Power (2003). "The amygdaloid complex: anatomy and physiology." Physiol Rev **83**(3): 803-834.
Saito, Y. C., N. Tsujino, E. Hasegawa, K. Akashi, M. Abe, M. Mieda, K. Sakimura and T. Sakurai (2013). "GABAergic neurons in the preoptic area send direct inhibitory projections to orexin neurons." Front Neural Circuits **7**: 192.
Salamone, J. D. and M. Correa (2012). "The mysterious motivational functions of mesolimbic dopamine." Neuron **76**(3): 470-485.
Salas, R., K. D. Cook, L. Bassetto and M. De Biasi (2004). "The alpha3 and beta4 nicotinic acetylcholine receptor subunits are necessary for nicotine-induced seizures and hypolocomotion in mice." Neuropharmacology **47**(3): 401-407.
Salas, R., R. Sturm, J. Boulter and M. De Biasi (2009). "Nicotinic receptors in the habenulo-interpeduncular system are necessary for nicotine withdrawal in mice." J Neurosci **29**(10): 3014-3018.
Sandyk, R. (1991). "Relevance of the habenular complex to neuropsychiatry: a review and hypothesis." Int J Neurosci **61**(3-4): 189-219.
Schaefer, A., D. O'Carroll, C. L. Tan, D. Hillman, M. Sugimori, R. Llinas and P. Greengard (2007). "Cerebellar neurodegeneration in the absence of microRNAs." J Exp Med **204**(7): 1553-1558.
Sgard, F., E. Charpantier, S. Bertrand, N. Walker, D. Caput, D. Graham, D. Bertrand and F. Besnard (2002). "A novel human nicotinic receptor subunit, alpha10, that confers functionality to the alpha9-subunit." Mol Pharmacol **61**(1): 150-159.
Sheffield, E. B., M. W. Quick and R. A. Lester (2000). "Nicotinic acetylcholine receptor subunit mRNA expression and channel function in medial habenula neurons." Neuropharmacology **39**(13): 2591-2603.
Shibata, H., T. Suzuki and M. Matsushita (1986). "Afferent projections to the interpeduncular nucleus in the rat, as studied by retrograde and anterograde transport of wheat germ agglutinin conjugated to horseradish peroxidase." J Comp Neurol **248**(2): 272-284.

Shih, P. Y., S. E. Engle, G. Oh, P. Deshpande, N. L. Puskar, H. A. Lester and R. M. Drenan (2014). "Differential expression and function of nicotinic acetylcholine receptors in subdivisions of medial habenula." J Neurosci **34**(29): 9789-9802.
Shimano, T., B. Fyk-Kolodziej, N. Mirza, M. Asako, K. Tomoda, S. Bledsoe, Z. H. Pan, S. Molitor and A. G. Holt (2013). "Assessment of the AAV-mediated expression of channelrhodopsin-2 and halorhodopsin in brainstem neurons mediating auditory signaling." Brain Res **1511**: 138-152.
Shumake, J., E. Edwards and F. Gonzalez-Lima (2003). "Opposite metabolic changes in the habenula and ventral tegmental area of a genetic model of helpless behavior." Brain Res **963**(1-2): 274-281.
Silveira, M. C., G. Sandner and F. G. Graeff (1993). "Induction of Fos immunoreactivity in the brain by exposure to the elevated plus-maze." Behav Brain Res **56**(1): 115-118.
Slimak, M. A., J. L. Ables, S. Frahm, B. Antolin-Fontes, J. Santos-Torres, M. Moretti, C. Gotti and I. Ibanez-Tallon (2014). "Habenular expression of rare missense variants of the beta4 nicotinic receptor subunit alters nicotine consumption." Front Hum Neurosci **8**: 12.
Somerville, L. H., P. J. Whalen and W. M. Kelley (2010). "Human bed nucleus of the stria terminalis indexes hypervigilant threat monitoring." Biol Psychiatry **68**(5): 416-424.
Steinbach, J. H. (1989). "Structural and functional diversity in vertebrate skeletal muscle nicotinic acetylcholine receptors." Annu Rev Physiol **51**: 353-365.
Stern, W. C., A. Johnson, J. D. Bronzino and P. J. Morgane (1981). "Neuropharmacology of the afferent projections from the lateral habenula and substantia nigra to the anterior raphe in the rat." Neuropharmacology **20**(10): 979-989.
Stinus, L., O. Gaffori, H. Simon and M. Le Moal (1977). "Small doses of apomorphine and chronic administration of d-amphetamine reduce locomotor hyperactivity produced by radiofrequency lesions of dopaminergic A10 neurons area." Biol Psychiatry **12**(6): 719-732.
Sugama, S., B. P. Cho, H. Baker, T. H. Joh, J. Lucero and B. Conti (2002). "Neurons of the superior nucleus of the medial habenula and ependymal cells express IL-18 in rat CNS." Brain Res **958**(1): 1-9.
Sulzer, D. and D. J. Surmeier (2013). "Neuronal vulnerability, pathogenesis, and Parkinson's disease." Mov Disord **28**(1): 41-50.
Sutherland, R. J. (1982). "The dorsal diencephalic conduction system: a review of the anatomy and functions of the habenular complex." Neurosci Biobehav Rev **6**(1): 1-13.
Takagishi, M. and T. Chiba (1991). "Efferent projections of the infralimbic (area 25) region of the medial prefrontal cortex in the rat: an anterograde tracer PHA-L study." Brain Res **566**(1-2): 26-39.
Tapper, A. R., S. L. McKinney, R. Nashmi, J. Schwarz, P. Deshpande, C. Labarca, P. Whiteaker, M. J. Marks, A. C. Collins and H. A. Lester (2004). "Nicotine activation of alpha4* receptors: sufficient for reward, tolerance, and sensitization." Science **306**(5698): 1029-1032.
Thornton, E. W. and G. E. Bradbury (1989). "Effort and stress influence the effect of lesion of the habenula complex in one-way active avoidance learning." Physiol Behav **45**(5): 929-935.
Threlfell, S., T. Lalic, N. J. Platt, K. A. Jennings, K. Deisseroth and S. J. Cragg (2012). "Striatal dopamine release is triggered by synchronized activity in cholinergic interneurons." Neuron **75**(1): 58-64.
Treit, D., J. Menard and C. Royan (1993). "Anxiogenic stimuli in the elevated plus-maze." Pharmacol Biochem Behav **44**(2): 463-469.

Tsai, H. C., F. Zhang, A. Adamantidis, G. D. Stuber, A. Bonci, L. de Lecea and K. Deisseroth (2009). "Phasic firing in dopaminergic neurons is sufficient for behavioral conditioning." Science **324**(5930): 1080-1084.
Tsetlin, V., D. Kuzmin and I. Kasheverov (2011). "Assembly of nicotinic and other Cys-loop receptors." J Neurochem **116**(5): 734-741.
Turner, J. R., L. M. Castellano and J. A. Blendy (2010). "Nicotinic partial agonists varenicline and sazetidine-A have differential effects on affective behavior." J Pharmacol Exp Ther **334**(2): 665-672.
Tye, K. M., R. Prakash, S. Y. Kim, L. E. Fenno, L. Grosenick, H. Zarabi, K. R. Thompson, V. Gradinaru, C. Ramakrishnan and K. Deisseroth (2011). "Amygdala circuitry mediating reversible and bidirectional control of anxiety." Nature **471**(7338): 358-362.
Ullsperger, M. and D. Y. von Cramon (2003). "Error monitoring using external feedback: specific roles of the habenular complex, the reward system, and the cingulate motor area revealed by functional magnetic resonance imaging." J Neurosci **23**(10): 4308-4314.
Valjakka, A., J. Vartiainen, L. Tuomisto, J. T. Tuomisto, H. Olkkonen and M. M. Airaksinen (1998). "The fasciculus retroflexus controls the integrity of REM sleep by supporting the generation of hippocampal theta rhythm and rapid eye movements in rats." Brain Res Bull **47**(2): 171-184.
Varani, A. P., L. M. Moutinho, B. Bettler and G. N. Balerio (2012). "Acute behavioural responses to nicotine and nicotine withdrawal syndrome are modified in GABA(B1) knockout mice." Neuropharmacology **63**(5): 863-872.
Vasudevan, S., Y. Tong and J. A. Steitz (2007). "Switching from repression to activation: microRNAs can up-regulate translation." Science **318**(5858): 1931-1934.
Vertes, R. P. and B. Fass (1988). "Projections between the interpeduncular nucleus and basal forebrain in the rat as demonstrated by the anterograde and retrograde transport of WGA-HRP." Exp Brain Res **73**(1): 23-31.
Viswanath, H., A. Q. Carter, P. R. Baldwin, D. L. Molfese and R. Salas (2013). "The medial habenula: still neglected." Front Hum Neurosci **7**: 931.
Walker, D. L. and M. Davis (1997). "Double dissociation between the involvement of the bed nucleus of the stria terminalis and the central nucleus of the amygdala in startle increases produced by conditioned versus unconditioned fear." J Neurosci **17**(23): 9375-9383.
Wang, D. G., N. Gong, B. Luo and T. L. Xu (2006). "Absence of GABA type A signaling in adult medial habenular neurons." Neuroscience **141**(1): 133-141.
Ware, J. J., M. B. van den Bree and M. R. Munafo (2011). "Association of the CHRNA5-A3-B4 gene cluster with heaviness of smoking: a meta-analysis." Nicotine Tob Res **13**(12): 1167-1175.
Wickham, R., W. Solecki, L. Rathbun, J. M. McIntosh and N. A. Addy (2013). "Ventral tegmental area alpha6beta2 nicotinic acetylcholine receptors modulate phasic dopamine release in the nucleus accumbens core." Psychopharmacology (Berl) **229**(1): 73-82.
Wilcox, K. S., G. R. Christoph, B. A. Double and R. J. Leonzio (1986). "Kainate and electrolytic lesions of the lateral habenula: effect on avoidance responses." Physiol Behav **36**(3): 413-417.
Wilson, G. G. and A. Karlin (1998). "The location of the gate in the acetylcholine receptor channel." Neuron **20**(6): 1269-1281.
Wonnacott, S. (1997). "Presynaptic nicotinic ACh receptors." Trends Neurosci **20**(2): 92-98.
Woolf, N. J. and L. L. Butcher (1985). "Cholinergic systems in the rat brain: II. Projections to the interpeduncular nucleus." Brain Res Bull **14**(1): 63-83.

Xu, W., S. Gelber, A. Orr-Urtreger, D. Armstrong, R. A. Lewis, C. N. Ou, J. Patrick, L. Role, M. De Biasi and A. L. Beaudet (1999). "Megacystis, mydriasis, and ion channel defect in mice lacking the alpha3 neuronal nicotinic acetylcholine receptor." Proc Natl Acad Sci U S A **96**(10): 5746-5751.
Yamaguchi, T., T. Danjo, I. Pastan, T. Hikida and S. Nakanishi (2013). "Distinct roles of segregated transmission of the septo-habenular pathway in anxiety and fear." Neuron **78**(3): 537-544.
Yassa, M. A., R. L. Hazlett, C. E. Stark and R. Hoehn-Saric (2012). "Functional MRI of the amygdala and bed nucleus of the stria terminalis during conditions of uncertainty in generalized anxiety disorder." J Psychiatr Res **46**(8): 1045-1052.
Zamore, P. D. and B. Haley (2005). "Ribo-gnome: the big world of small RNAs." Science **309**(5740): 1519-1524.
Zarrindast, M. R., H. Homayoun, A. Babaie, A. Etminani and B. Gharib (2000). "Involvement of adrenergic and cholinergic systems in nicotine-induced anxiogenesis in mice." Eur J Pharmacol **407**(1-2): 145-158.
Zaveri, N., F. Jiang, C. Olsen, W. Polgar and L. Toll (2010). "Novel alpha3beta4 nicotinic acetylcholine receptor-selective ligands. Discovery, structure-activity studies, and pharmacological evaluation." J Med Chem **53**(22): 8187-8191.
Zhao-Shea, R., S. R. DeGroot, L. Liu, M. Vallaster, X. Pang, Q. Su, G. Gao, O. J. Rando, G. E. Martin, O. George, P. D. Gardner and A. R. Tapper (2015). "Increased CRF signalling in a ventral tegmental area-interpeduncular nucleus-medial habenula circuit induces anxiety during nicotine withdrawal." Nat Commun **6**: 6770.
Zhao-Shea, R., L. Liu, X. Pang, P. D. Gardner and A. R. Tapper (2013). "Activation of GABAergic neurons in the interpeduncular nucleus triggers physical nicotine withdrawal symptoms." Curr Biol **23**(23): 2327-2335.
Zhao-Shea, R., L. Liu, L. G. Soll, M. R. Improgo, E. E. Meyers, J. M. McIntosh, S. R. Grady, M. J. Marks, P. D. Gardner and A. R. Tapper (2011). "Nicotine-mediated activation of dopaminergic neurons in distinct regions of the ventral tegmental area." Neuropsychopharmacology **36**(5): 1021-1032.
Zhao, H. and B. Rusak (2005). "Circadian firing-rate rhythms and light responses of rat habenular nucleus neurons in vivo and in vitro." Neuroscience **132**(2): 519-528.
Zoli, M., F. Pistillo and C. Gotti (2014). "Diversity of native nicotinic receptor subtypes in mammalian brain." Neuropharmacology.